INVESTIGATION OF MUSIC ALGORITHM BASED AND WD-PCA METHOD BASED ELECTROMAGNETIC TARGET CLASSIFICATION TECHNIQUES FOR THEIR NOISE PERFORMANCES

A THESIS SUBMITTED TO
THE GRADUATE SCHOOL OF NATURAL AND APPLIED SCIENCES
OF
MIDDLE EAST TECHNICAL UNIVERSITY

BY

EMRE ERGİN

IN PARTIAL FULFILLMENT OF THE REQUIREMENTS
FOR
THE DEGREE OF MASTER OF SCIENCE
IN
ELECTRICAL AND ELECTRONICS ENGINEERING

OCTOBER 2009

Approval of the thesis:

INVESTIGATION OF MUSIC ALGORITHM BASED AND WD-PCA METHOD BASED ELECTROMAGNETIC TARGET CLASSIFICATION TECHNIQUES FOR THEIR NOISE PERFORMANCES

submitted by **EMRE ERGİN** in partial fulfillment of the requirements for the degree of **Master of Science in Electrical and Electronics Engineering Department, Middle East Technical University** by,

Prof. Dr. Canan Özgen
Dean, Graduate School of **Natural and Applied Sciences** _____

Prof. Dr. İsmet Erkmen
Head of Department, **Electrical and Electronics Engineering** _____

Prof. Dr. Gönül Turhan Sayan
Supervisor, **Electrical and Electronics Eng. Dept., METU** _____

Examining Committee Members:

Prof. Dr. Mustafa Kuzuoğlu
Electrical and Electronics Engineering Dept., METU _____

Prof. Dr. Gönül Turhan Sayan
Electrical and Electronics Engineering Dept., METU _____

Prof. Dr. Gülbin Dural
Electrical and Electronics Engineering Dept., METU _____

Prof. Dr. Kemal Leblebicioğlu
Electrical and Electronics Engineering Dept., METU _____

Dr. Mustafa Seçmen
MEMS Araştırma ve Uygulama Merkezi _____

Date: 22.10.2009

I hereby declare that all information in this document has been obtained and presented in accordance with academic rules and ethical conduct. I also declare that, as required by these rules and conduct, I have fully cited referenced all material and results that are not original to this work.

Name, Last name: Emre ERGİN

Signature :

ABSTRACT

INVESTIGATION OF MUSIC ALGORITHM BASED AND WD-PCA METHOD BASED ELECTROMAGNETIC TARGET CLASSIFICATION TECHNIQUES FOR THEIR NOISE PERFORMANCES

Ergin, Emre

M.S., Department of Electrical and Electronics Engineering

Supervisor :Prof. Dr. Gönül Turhan Sayan

October 2009, 125 pages

Multiple Signal Classification (MUSIC) Algorithm based and Wigner Distribution-Principal Component Analysis (WD-PCA) based classification techniques are very recently suggested resonance region approaches for electromagnetic target classification. In this thesis, performances of these two techniques will be compared concerning their robustness for noise and their capacity to handle large number of candidate targets. In this context, classifier design simulations will be demonstrated for target libraries containing conducting and dielectric spheres and for dielectric coated conducting spheres. Small scale aircraft targets modeled by thin conducting wires will also be used in classifier design demonstrations.

Keywords: Electromagnetic target classification, MUSIC algorithm, Wigner-Ville distribution, principal component analysis, feature extraction.

ÖZ

MUSIC ALGORİTMASINA VE WD-PCA METODUNA DAYALI ELEKTROMANYETİK HEDEF SINIFLANDIRMA TEKNİKLERİNİN GÜRÜLTÜ PERFORMANSLARININ İNCELENMESİ

Ergin, Emre
Y. Lisans, Elektrik ve Elektronik Mühendisliği Bölümü
Tez Yöneticisi : Prof. Dr. Gönül Turhan Sayan

Ekim 2009, 125 sayfa

Çoklu İşaret Sınıflandırma (MUSIC) Algoritması ve Wigner Dağılımı-Esas Bileşenler Analizi (WD-PCA) metodlarına dayalı sınıflandırma teknikleri, resonans bölgesinde son zamanlarda önerilmiş elektromanyetik hedef sınıflandırma yaklaşımlarıdır. Bu tezde, bu iki farklı tekniğin gürültüye dayanıklılık ve çok sayıda aday hedefi ayırdedebilme konusundaki performansları karşılaştırılacaktır. Bu bağlamda gerçekleştirilecek olan sınıflandırıcı tasarım benzetimlerinde iletken ve yalıtkan küreler ile yalıtkan kaplı iletken küreleri içeren hedef kümeleri kullanılacaktır. İnce iletken tellerle modellenmiş küçük ölçekli bir uçak hedef kümesi için de sınıflandırıcı tasarım benzetimleri yapılacaktır.

Anahtar sözcükler: Elektromanyetik hedef sınıflandırma, MUSIC algoritması, Wigner-Ville dağılımı, esas bileşenler analizi, öznitelik çıkarımı.

To My Family

ACKNOWLEDGEMENTS

I would like to express my deepest gratitude to my supervisor Prof. Dr. Gönül TURHAN SAYAN for her guidance, advices, and encouragements, insight throughout this thesis study. I would like to thank also for giving me the opportunity to work on this issue.

My special thanks go to my fiancée Medine ATAY. It would be very difficult for me to complete this study without her support.

Lastly, I would like to express my gratitude to my parents, Mehmet and Nermin Ergin and my sister, Özlem Ergin for their encouragement and support.

TABLE OF CONTENTS

LIST OF TABLES

LIST OF FIGURES

CHAPTER 1

INTRODUCTION

Recognition of targets from their electromagnetic scattered signals is a complicated problem as such data are highly frequency, aspect and polarization dependent. These dependencies make classification of targets almost impossible without using an effective feature extraction process that would provide aspect and polarization independent target features. Also, the extracted features must be highly sensitive to geometrical and material properties such as size, shape and electrical parameters (permittivity, permeability, conductivity) of individual targets to discriminate similar objects from each other. Another complication in target recognition is the unavoidable presence of noise contaminating the scattered signals and causing additional ambiguity to this challenging problem. Therefore, feature extraction techniques used in electromagnetic target classifier design must be tested for robustness under practically low signal-to-noise ratio (SNR) conditions.

There are various techniques suggested for target classification in the area of electromagnetic target recognition. Most of these techniques are based on the use of natural resonance concept within the framework of linear system modeling. Possibility of representing a finite size electromagnetic scatterer by a linear time-invariant system model was first suggested by Kennaugh and

Cosgriff [1] in 1958 and studied further by Kennaugh and Moffatt [2] in 1965. Their work implied that poles of the system function of a given target could be used to describe the natural component of the target response. Marin investigated the natural mode representation of transient scattering from rotationally symmetric bodies in his 1974 paper [3]. Later, in mid 1970s, Baum formalized the Singularity Expansion Method (SEM) to establish a mathematical expression for the natural response of a target in terms of target poles and the associated residue functions [4]. The residues of this expansion are known to be strong functions of aspect and polarization while the poles are invariant with respect to such excitation and observation conditions. The SEM is meaningful in the resonance region with the condition that the ratio between a target's largest line-of-sight dimension and the wavelength of operation remains roughly in the range from 0.1 to 10. In other words, the wavelength of electromagnetic excitation needs to be comparable to the overall size of the scattering object. Therefore, the target recognition methods inspired by the SEM during the last three decades are essentially resonance region methods.

Most of the target recognition techniques in resonance region utilize system poles of targets either directly or indirectly because the complete set of system poles identifies a given scattering object uniquely in an aspect and polarization invariant manner. In the direct approach, a subset of target poles which are excited over the bandwidth of operation can be extracted as features from late-time scattered signals of a given target as demonstrated in references [5, 6] but this process is known to be quite vulnerable to the SNR level. Therefore, extraction of alternative target feature sets which are less sensitive to noise while still being related to a subset of the complex natural resonance (CNR) frequencies (i.e. system poles) of the target turns out to be an indirect but more feasible approach in classifier design. Introduction of the K-pulse concept by Kennaugh in 1981 [7] to be used for target

recognition was a very significant and novel attempt in this direction. As defined by Kennaugh, the time-limited K-pulse signal of a target was nothing but an aspect and polarization invariant target feature such that the Laplace spectrum zeros of this feature signal were the same as the target's system poles. Inspired by Kennaugh's K-pulse idea and by Baum's SEM, various target recognition schemes have been suggested in the resonance region literature in 1980s such as the K-pulse based methods [8-11] and E-pulse based methods [12-13]. Most of the electromagnetic target recognition studies published in 1990s and 2000s combined the natural resonance based target recognition approach with advanced pattern recognition and signal processing techniques such as time-frequency representations [14-18], neural networks [19-21, 24], global optimization techniques [22-23] and statistical techniques [18, 24-26].

The main objective of this thesis is to investigate the target discrimination performances of two recently suggested electromagnetic classification techniques which are the Multiple Signal Classification (MUSIC) algorithm based technique introduced very recently by Secmen and Turhan-Sayan in 2008 [25-26] and the Wigner Distribution-Principal Component Analysis (WD-PCA) based technique introduced for the first time by Turhan-Sayan in 2005 [18]. Both of these resonance region techniques make use of the natural resonance mechanism for feature extraction from a properly selected late-time portion of scattered electromagnetic signals at multiple aspects. The extracted target features are indirectly related to target poles in both techniques. In this thesis, these two target classification techniques will be compared regarding their robustness under excessive noise and their capacity to discriminate highly similar objects as the number of library targets gets larger. For this purpose, various classifiers will be designed for separate libraries of conducting spheres, dielectric spheres and dielectric coated conducting spheres. Another classifier will also be designed for a mixed

target library containing a large number of spheres from all these three subclasses. Scattered signal databases at various SNR levels will be used to design and test target classifiers realized by both classifier design techniques (the MUSIC based technique and the WD-PCA technique) to evaluate and compare their noise performances. Similar classifier design simulations will also be done for a target library containing small scale aircraft targets modeled by thin perfectly conducting wires for further performance analysis. Advantages of using slightly or moderately noisy scattered data in classifier design phase will also be demonstrated for both techniques.

The organization of the rest of the thesis is as follows:

Chapter 2 gives the theory and design steps of the MUSIC algorithm based and the WD-PCA based electromagnetic target recognition techniques together with their feature extraction methods.

Chapter 3 presents the classifier design simulations by both techniques for various target libraries composed of only spherical objects. Classifiers designed under difference noise conditions will be tested at various SNR levels to evaluate and to compare the noise performances of the MUSIC algorithm based and WD-PCA based classifier design techniques.

Classifier design simulations realized for small-scale aircraft models will be presented in Chapter 4. Noise performances of both the MUSIC algorithm based design technique and the WD-PCA based design technique will be evaluated and compared using scattered data of different SNR levels both in the classifier design phase and in the test phase.

Finally, the concluding remarks and suggestions for future study will be outlined in Chapter 5.

There is also an Appendix containing a sample MATLAB code written for real-time decision testing as a part of the MUSIC algorithm based classifier design.

CHAPTER II

THEORETICAL BACKGROUND

In this chapter, theoretical background and basic design steps for the MUSIC algorithm based and the WD-PCA based electromagnetic classifier design techniques are outlined.

2.1. MUSIC Algorithm Based Classifier Design Technique

As mentioned in the Introduction section, one of the electromagnetic target recognition methods investigated in this thesis is based on the use of MUSIC algorithm together with the utilization of natural resonance mechanism to extract target features over a sufficiently late-time interval of the target's scattered response. In general, the MUSIC algorithm is used to extract the parameters of damped sinusoidal signal components of a given transient signal in the presence of additive Gaussian noise. It is widely used in the areas of biomedical, telecommunication, signal processing and electromagnetics in applications such as the estimation of direction-of-arrival due to its high resolution [27-29]. In this thesis, the MUSIC algorithm is used to extract a target feature called Music Spectrum Matrix (MSM) from the late-time portion of a given scattered response at a given aspect. The MSM features extracted for a given target at several reference aspects are finally

superposed to obtain a single target feature called Fused Music Spectrum Matrix (FMSM) to characterize the target in the classifier's feature database.

2.1.1. Target Feature Extraction Using the MUSIC Algorithm

The MUSIC algorithm is a parametric method for spectral estimation based on the fact that the sinusoidal signal components and the additive Gaussian noise component of a given signal are uncorrelated. $x(n)$ is the superposition of (L/2) cosine signals sampled at N discrete time points and corrupted by an additive Gaussian noise signal $w(n)$. The resulting noisy signal $z(n)$ can be expressed as

$$z(n) = x(n) + w(n) = \sum_{i=1}^{L/2} b_i(\emptyset, \theta) e^{\alpha_i n} \cos(w_i n + \delta_i) + w(n) \qquad (2.1.a)$$

The same signal can also be expressed in terms of complex exponentials as

$$z(n) = \sum_{i=1}^{L} c_i(\emptyset, \theta) e^{s_i n} + w(n), \;\; n = 1, \dots, N \qquad (2.1.b)$$

where $s_i = \alpha_i + jw_i$ and $c_i(\emptyset, \theta) = b_i(\emptyset, \theta) e^{j\delta_i}$

The noise-free signal component $x(n)$ expressed in Equation (2.1) can be interpreted as the natural response of an electromagnetic scatterer over a chosen late-time interval, sampled at N discrete time points. The system function of this scatterer has L/2 pairs of system poles $s_i = \alpha_i \pm jw_i$ excited over the bandwith of the scattered signals. In other words, a given target of concern is represented by a linear, time invariant, causal system and the

natural part of its scattered response $x(n)$ is expanded according to the SEM in Equation 2.1 at an arbitrary aspect $(\emptyset, \theta)$.

For an integer m that satisfies the condition $L < m < N$, we can form the vector $\bar{y}(n)$ of length m as

$$\bar{y}(n) = [z(n)\ \ z(n-1)\ \ldots\ \ z(n-m+1)]^T \tag{2.2}$$

where the symbol T stands for the transpose operation.

As the signal and noise components of $z(n)$ in Equation (2.1) are uncorrelated, the correlation matrix IR can be expressed as

$$\begin{aligned} IR = E\left\{\overline{(y(n))}\ \overline{(y(n))}^H\right\} &= E\{\overline{x(n)}\ \overline{x(n)}^H\} + E\{\overline{w(n)}\ \overline{w(n)}^H\} \\ &= AE\{cc^H\}A^H + \sigma^2 I_{mxm} = ACA^H + \sigma^2 I_{mxm} \end{aligned} \tag{2.3}$$

where E is the expected value operator, the superscript H stands for the complex conjugate transpose, σ^2 is the variance of Gaussian noise and I is the unit matrix. The matrix A, defined in Equation (2.4), is a Vandermonde matrix whose dimensions and rank are mXL and L, respectively and the matrix C, which is defined in Equation (2.5), is an LXL matrix with rank L.

$$A = [a(s_1)\ a(s_2)\ \ldots\ \ a(s_L)]\ \ with\ a(s) = \frac{[1\ \ e^{-s}\ \ \ldots\ \ e^{-s(m-1)}]^T}{norm[1\ \ e^{-s}\ \ \ldots\ \ e^{-s(m-1)}]^T} \tag{2.4}$$

with $s = \alpha + jw$ being the complex frequency where $w = 2\pi f$.

$$C = E\{cc^H\} = E\left\{\begin{bmatrix} c_1 e^{s_1 n} \\ c_2 e^{s_2 n} \\ \vdots \\ c_L e^{s_L n} \end{bmatrix} \begin{bmatrix} c_1^* e^{s_1^* n} & c_2^* e^{s_2^* n} & \dots & c_L^* e^{s_L^* n} \end{bmatrix}\right\}$$
$$= \begin{bmatrix} m_1 & 0 & \dots & 0 \\ 0 & m_2 & \dots & \vdots \\ \vdots & \vdots & \ddots & \vdots \\ 0 & \dots & \dots & m_L \end{bmatrix} \quad (2.5)$$

In Equation (2.5), elements of the matrix C are zero except for the diagonal elements since

$$E\{c_l e^{s_l n} c_k^* e^{s_k^* n}\} = E\{b_l(\emptyset,\theta) e^{j\delta_l} e^{s_l n} b_k(\emptyset,\theta) e^{-j\delta_k} e^{s_k^* n}\}$$
$$= b_l(\emptyset,\theta) e^{s_l n} b_k(\emptyset,\theta) e^{s_k^* n} E\{e^{j(\delta_l - \delta_k)}\} = \begin{cases} m_l \ if \ k = l \\ 0 \ if \ k \neq l \end{cases} \quad (2.6)$$

In Equation (2.5) and (2.6), the phases of c_i's are assumed to be random phases having uniform distribution in the interval [-π, π].

Let $\lambda_1 \geq \lambda_2 \geq \dots \geq \lambda_m$ be the eigenvalues of the correlation matrix IR, ordered from the largest to the lowest, and let $S = [e_1\ e_2 \dots\dots e_L]$ be the subset of orthonormal eigenvectors associated with the first L eigenvalues $[\lambda_1\ \lambda_2 \dots\dots \lambda_L]$. Also, let $G = [e_{L+1} \dots . e_m]$ be the set of orthonormal eigenvectors associated with the remaining eigenvalues $[\lambda_{L+1} \dots\dots \lambda_m]$. For m >L, the matrix ACA^H is singular; it has a rank equal to L. So, ACA^H has L strictly positive eigenvalues while the remaining $m-L$ eigenvalues are all being equal to zero. Hence, the eigenvalues of IR for $i = L+1,\dots,m$ should be equal to σ^2. Therefore, we can write

$$IRG = \sigma^2 G \quad (2.7.a)$$

Also, by multiplying both sides of equation 2.3 by the matrix G from right, one can get

$$IRG = ACA^H G + \sigma^2 G \qquad (2.7.b)$$

These last two expressions imply that

$$ACA^H G = 0 \qquad (2.7.c)$$

In this equation, AC should be nonzero because this matrix has full column rank. Since the null space dimension of AC is equal to zero, $A^H G = 0$ should follow. In other words, $\{\bar{m}_i\}_{i=L+1}^{m}$ span both range space of G and null space of A^H. Then, the true complex frequency values, $\{\bar{s}_i\}_{i=1}^{n}$, which means the target poles, are the only solutions of the equation

$$a^H(s)GG^H a(s) = 0 \qquad (for\ any\ m > L) \qquad (2.8)$$

The values of m and L are important parameters in classifier design using the MUSIC algorithm. The parameter m may be chosen as large as possible for good resolution, but not too close to N, to still allow a reliable estimation of the covariance matrix. In some applications, the largest possible value that may be selected for m may also be limited by computational complexity considerations [30]. However, it is usually advised to choose $m = N/2$ to obtain the best performance [31]. Another important design parameter is L which should be an even number by definition such that half of which denotes the number of estimated damped sinusoidal signals in the reference data. Based on past experience with the MUSIC algorithm [26], L can be chosen as $m/2$. The overestimation of L does not cause a serious problem but reduces the accuracy rate of the classifier very slightly. However, the

underestimation of this parameter may cause serious deterioration in the classifier performance.

The “MUSIC spectrum function” can be defined as

$$P(s) = \frac{1}{a^H(s)\, GG^H a(s)} \tag{2.9}$$

where $s = \alpha + j\omega$ is the complex frequency. It can be seen from the equation (2.8) that the function $P(s)$ has peak values in the spectrum at $s = s_i$ values. The discretized and normalized version of $P(s)$ can be used to construct the normalized MUSIC Spectrum Matrix (MSM) $[P(u,v)]$ with elements

$$P(u,v) = \frac{P_{unnorm}(u,v)}{\|P_{unnorm}(u,v)\|} \tag{2.10}$$

where

$$P_{unnorm}(u,v) = \frac{1}{a^H(\alpha_u + j\omega_v)\, GG^H a(\alpha_u + j\omega_v)} \tag{2.11}$$

and

$$\|P_{unnorm}(u,v)\| = \sqrt{\sum_{v=1}^{k_2}\sum_{u=1}^{k_1}(P_{unnorm}(u,v))^2} \tag{2.12}$$

with $u = 1,\ldots,k_1$ and $v = 1,\ldots,k_2$ being the row and column indices of the MUSIC spectrum matrix. An MSM is an aspect dependent target feature matrix and gives us a natural-resonance related power distribution map of a given target over the complex frequency plane.

To extract MSM features from a given scattered natural response $z(n)$, the vector $\bar{y}(n)$ is constructed first using Equation (2.2). Then, the correlation matrix for this $\bar{y}(n)$ is computed as shown below

$$\tilde{IR} = \frac{1}{N}\sum_{n=m}^{N} \bar{y}(n)\ \bar{y}(n)^{H} \tag{2.13}$$

where N is the total number of time samples of $z(n)$ and m=N/2 for best noise performance. Afterwards, the eigenvalues and the eigenvectors of the correlation matrix $\widetilde{IR}$ are computed to construct the matrix G. Then, the associated MSM feature is computed using equations (2.4) and (2.9) through (2.12) for the provided scattered target signal.

2.1.2. Design Steps of the MUSIC Algorithm Based Classifier

An electromagnetic classifier will be designed for K_T targets using scattered target responses at K_A different aspect angles. These design aspects will be referred as reference aspects from now on. The common time span of the scattered signals is divided into certain overlapping subintervals. The MUSIC spectrum matrices (MSMs) are constructed over each subinterval for each target at each reference aspect angle by using the procedure outlined in section 2.1.1. Afterwards, the MSMs which belong to a given target at different reference aspects but over the same late-time subinterval are superposed and then normalized as shown in Equation 2.14 to form the

fused MUSIC spectrum matrix (FMSM) for the purpose of enhancing the captured pole information and reducing the aspect dependency.

$$FMSM_i(u,v) = \frac{P_{sum,i}(u,v)}{\|P_{sum,i}(u,v)\|} \quad for\ \forall i = 1,..,K_T \qquad (2.14)$$

where

$$P_{sum,i}(u,v) = \sum_{j=1}^{K_A} P_{i,j}(u,v)$$

Here, $FMSM_i$ refers to the FMSM of the ith target and $P_{i,j}$ refers to the MSM of target i at the reference aspect j.

This process is repeated for each late-time subinterval to be used next to determine the optimal time interval of classifier design.

One of the most critical steps of the classifier design is the selection of a proper late-time design interval. All FMSMs and the individual MSMs computed for all targets at all reference aspect angles over all designated subintervals are used at this design step. Over the optimal late-time interval, summation of correlation coefficients between the MSMs and their matched FMSMs should be maximum. Also, summation of correlation coefficients between the MSMs and the mismatched FMSMs should be minimum. In other words, for each library target the MSMs constructed over the optimal late-time interval should be highly correlated only to the FMSM of this target. Selection of the optimal late-time interval for classification can be determined as follows [26]:

$$Index\left[Optimal\ late-time\ interval\right] = p^* \quad if\ \ r_{total}(p^*) \geq r_{total}(p) \quad \forall\, p = 1,..,P$$

where P is the number of candidate subintervals and

$$r_{total}(p) = \frac{1}{K_T K_A} \sum_{i=1}^{K_T} r_{i,match} - \frac{1}{K_T (K_T - 1) K_A} \sum_{i=1}^{K_T} r_{i,mismatch} \tag{2.15}$$

with

$$r_{i,match} = \sum_{j=1}^{K_A} \sum_{v=1}^{k_2} \sum_{u=1}^{k_1} FMSM_i(u,v) P_{i,j}(u,v)$$

and

$$r_{i,mismatch} = \sum_{\substack{k=1 \\ k \neq i}}^{K_T} \sum_{j=1}^{K_A} \sum_{v=1}^{k_2} \sum_{u=1}^{k_1} FMSM_i(u,v) P_{k,j}(u,v)$$

After the optimal late-time interval is selected, the feature database of the classifier is formed as the collection of Fused MSM (FMSM) features computed over this late-time interval for each library target. The optimal design interval may shift depending upon the SNR level of the scattered data used in classifier design.

2.2. WD-PCA Based Classifier Design Technique

As mentioned in the Introduction section, WD-PCA Based Classifier Design method is the second method to be investigated in this study. This method makes use of a well known time-frequency representation, the Wigner distribution (WD), and the principle component analysis (PCA) technique for feature extraction and for feature fusion as to be outlined in the next subsection.

2.2.1. Target Feature Extraction Using Wigner Distribution

In the first step of the WD-PCA based classifier design, the Wigner-Ville distribution (WD) is computed for each transient design signal belonging to each library target at each reference aspect. The total energy of each given scattered signal is normalized to unity at the beginning of the feature extraction process for gain invariant classification. The Wigner-Ville distribution is a real-valued, quadratic time–frequency representation preserving time shifts and frequency shifts of the signal and its output represents an approximate energy density function over the joint time-frequency plane. The auto-WD of a given time domain signal $x(t)$ is expressed as:

$$W_x(t, f) = \int_{\tau} x(t + \frac{\tau}{2}) x^*(t - \frac{\tau}{2}) e^{-j2\pi f\tau} d\tau \tag{2.16}$$

where the superscript (*) shows complex conjugation. WD satisfies marginal properties

$$\int_f W_x(t, f) df = p_x(t) = |x(t)|^2 \tag{2.17}$$

$$\int_t W_x(t, f) dt = P_x(f) = |X(f)|^2 \tag{2.18}$$

where $p_x(t)$ is the instantaneous power and $P_x(f)$ is the spectral energy density of the signal. Also, X(f) is the Fourier transform of the signal x(t). The WD output does not give an exact time-frequency energy density function defined at every point in the time-frequency plane. As explained by the uncertainty principle, it is not possible to have infinite resolution in both time and frequency simultaneously [33]. Accordingly, the WD outputs contain very

strong and highly oscillatory interference terms that may seriously deteriorate the identification capability of the classifier. Due to these oscillatory interference terms, the WD outputs may have negative values which cannot be interpreted as energy density terms. Therefore, these non-physical negative values in the WD output matrix are simply replaced by zeros to obtain a modified WD output as

$$\tilde{W}_x(t, f) = \frac{W_x(t, f) + abs(W_x(t, f))}{2} \tag{2.19}$$

as suggested in [17].

The modified auto WD output is further processed to obtain a partitioned energy density vector which is indirectly related to target poles. In obtaining this target feature for a given target at a given aspect, the total time span T_0 of the scattered target signal is divided into Q time bands (each having equal lengths of T_0/Q seconds) as the first step. The amount of signal energy contained in the time band q at a sample frequency f_m is given [18] as

$$E_q(f_m) = \int_{(q-1)\Delta}^{q\Delta} W_x(t, f_m) dt \quad \text{for q=1,2,3,.....Q} \tag{2.20}$$

where $\Delta = T_0$/Q , m =1,2,....,N/2 and $f_m = (m-1)/(T_0)$.

As all the scattered signals $x(t)$ are real-valued, the WD output matrix has even symmetry with respect to frequency. Therefore, it is enough to process only half of the WD output matrix for non-zero frequency samples, i.e. for m=1,2,…,N/2.

Then, the spectral energy density vector for the interval q is given as:

$$\overline{E}_q = [E_q(f_1) \quad E_q(f_2) ..... E_q(f_{N/2})] \tag{2.21}$$

Because there are Q non-overlapping time bands altogether, the partitioned energy density vector $\overline{E}$ is formed as

$$\overline{E} = [\overline{E}_1 \quad \overline{E}_2 ..... \overline{E}_Q] \tag{2.22}$$

having the length of (N/2) x Q.

If we choose two successive time bands (q and q+1) for feature vector construction to include $\bar{E}_q$ and $\bar{E}_{q+1}$, the resulting energy feature vector contains information also about the real parts of the natural resonance frequencies. So, the classifier performance can be enhanced significantly as discussed in [18]. The resulting 2-band aspect dependent feature vectors are called Late-Time Feature Vectors (LTFV). As mentioned before, one of the most important steps of the classifier design is the selection of the optimal late-time interval for classification design. In other words, we need to determine the late-time interval index q* which corresponds to the combination of two successive time bands (q and q+1). The value of q* can be determined by maximizing the Correct Classification Factor (CCF) given in Equation (2.23) for a pre-selected Q value [18]. The value of the parameters Q and q* of classifier design are decided by using scattered data only at the reference aspects.

$$CCF(q^*) = \frac{1}{M_{tar} K^2} \sum_{i,j} r_{i,j}^{matched} - \frac{1}{(M_{tar}{}^2 - M_{tar}) K^2} \sum_{i,j} r_{i,j}^{mismatched} \tag{2.23}$$

where M_{tar} is the number of targets and K is the number of reference aspects, $r_{i,j}^{matched}$ is the correlation coefficient between any two LTFVs which belong to

the same target at different aspects, $r_{i,j}^{mismatched}$ is the correlation coefficient between any two LTFVs which belong to different targets. The index q* is chosen from the possible values q*=1,2,…,Q-1. Then, the LTFVs are constructed over the optimum late time interval associated with the time band indices q and (q+1) for all library targets.

2.2.2. Feature Fusion Using the PCA Technique

As the last step of the WD-PCA classifier design, we use principal component analysis (PCA) to perform multiple aspect feature fusion. In this way, we can reduce aspect dependency of the resulting target features. Principal component analysis (PCA), which was first introduced by Pearson in 1901 [34], is used to identify common patterns in a given data set. This method is useful to analyze and compress different sets of data to highlight their similarities in general.

In the WD-PCA target classifier design method, a single characteristic feature vector, which can effectively represent the target over a broad range of aspects, is obtained by principal component analysis (PCA) as introduced by Turhan-Sayan in [18]. This single characteristic feature vector is called Fused Feature Vector (FFV) and the feature database of the classifier contains FFVs of all library targets. Later, during the real-time classification phase, the LTFV extracted from a received test signal over the optimal design interval is compared with the FFVs of this feature database. The target is identified based on the highest correlation coefficient computed.

PCA-based multi-aspect feature fusion technique is described as follows:
A feature matrix F of size K x N is constructed first for each library target. Rows of this matrix contain the LTFV of a given library target computed at K

different reference aspects. N is the length of each LTFV as discussed in section 2.2.1. Transpose of this feature matrix F is given in Equation (2.24).

$$F^T = [\bar{e}_1^T \quad \bar{e}_2^T \ldots\ldots\ldots\ldots \bar{e}_K^T] \tag{2.24}$$

The covariance matrix S_F of the feature matrix F is a symmetric positive-definite matrix of size K x K given as

$$S_F = \begin{bmatrix} s_1^2 & s_{12} & \ldots & s_{1K} \\ s_{21} & s_2^2 & \ldots & s_{2K} \\ . & . & & . \\ . & . & & . \\ . & . & & . \\ s_{K1} & s_{K2} & \ldots & s_K^2 \end{bmatrix} \tag{2.25}$$

where its off-diagonal entries $s_{ij} = s_{ji}$ denote covariance between feature vectors $\bar{e}_i$ and $\bar{e}_j$ and the diagonal entries s_i^2 represent the variance of feature vectors $\bar{e}_i$. We can write the correlation coefficient $r_{i,j}$ between the feature vectors $\bar{e}_i$ and $\bar{e}_j$ as

$$r_{i,j} = \frac{s_{i,j}}{\sqrt{s_i s_j}} \tag{2.26}$$

The covariance matrix S_F can be transformed into a diagonal matrix Λ using a similarity transformation as the covariance matrix is symmetric and positive-definite.

$$\Lambda = U^T S_F U \quad = \begin{bmatrix} \lambda_1 & 0 & \ldots & 0 \\ 0 & \lambda_2 & \ldots & 0 \\ . & . & & . \\ . & . & & . \\ . & . & & . \\ 0 & 0 & \ldots & \lambda_K \end{bmatrix} \tag{2.27}$$

where U is the modal matrix in the form

$$U = [u_1 \quad u_2 \ldots\ldots\ldots u_K] \tag{2.28}$$

with u_i's being the normalized eigenvectors corresponding to eigenvalues of the covariance matrix S_F. The eigenvalues λ_i are solved from

$$\det(S_F - \lambda I) = 0 \tag{2.29}$$

In equation (2.29), I is the identity matrix of size K x K. Then, λ_i (eigenvalues) are ordered from the largest to the smallest such that $\lambda_1 > \lambda_2 > \ldots > \lambda_K$. The corresponding eigenvectors t_i are solved from;

$$[S_F - \lambda_i I]t_i = 0 \qquad \text{i =1, 2,.....K} \tag{2.30}$$

Afterwards, these orthogonal eigenvectors are normalized to obtain the orthonormal eigenvectors,

$$u_i = \frac{t_i}{\sqrt{t_i t_i^T}} = \frac{t_i}{|t_i|} \tag{2.31}$$

to construct the matrix U that is used to transform the correlated feature vectors $\bar{e}_1, \bar{e}_2, \ldots, \bar{e}_k$ into a set of uncorrelated vectors, $z_1, z_2, \ldots, z_k$ by

$$Z = \begin{bmatrix} z_1 \\ z_2 \\ \vdots \\ z_K \end{bmatrix} = U^T \begin{bmatrix} \bar{e}_1 - mean(\bar{e}_1) I_N \\ \bar{e}_2 - mean(\bar{e}_2) I_N \\ \vdots \\ \bar{e}_K - mean(\bar{e}_K) I_N \end{bmatrix} \tag{2.32}$$

where I_N is a unity row vector (an all-ones row vector) of length N and the resulting matrix Z has a size of K x N which is the same as the size of feature

matrix F. z_i 's will be called the principal components (PCs) of feature matrix F. These z_i vectors (PCs) have zero-mean, and variance λ_i. This process must be repeated for all library targets. It can be shown that for each target the first principal component has the highest correlations with the original late-time feature vectors (LTFVs) extracted for that target since λ_1 has the highest percentage in the summation of λ_i for i=1,2,.....,K as shown in reference [18]. If this percentage is large enough, we may neglect the other principal components and use the first principal component as the fused feature vector (FFV) of the given target by itself. Otherwise, the other principal components can be linearly combined to construct the FFV of the target by proper weighting factors ($\overline{\lambda_i}$) as described in Equations (2.33) and (2.34) below;

$$FFV = \sum_{i=1}^{K} \overline{\lambda_i} z_i \qquad (2.33)$$

where

$$\overline{\lambda_i} = \frac{\lambda_i}{\sum_{j=1}^{K} \lambda_j} \qquad (2.34)$$

CHAPTER III

CLASSIFIER DESIGN APPLICATIONS AND RESULTS FOR SPHERICAL TARGETS

In this chapter, classifier design simulations and the associated performance results will be reported for various spherical target libraries. These libraries will contain perfectly conducting spheres of different sizes, dielectric spheres of exactly the same size but of slightly different permittivity values and dielectric coated perfectly conducting spheres of exactly the same external size but of different coating permittivity values and of different size for the inner conducting sphere. Moreover, a mixed target library which includes perfectly conducting spheres, dielectric spheres and also dielectric coated perfectly conducting spheres will be used for classifier design simulations. Both design techniques, the MUSIC algorithm based design technique and the WD-PCA based design technique, will be used to design classifiers for each specific target library. These classifiers will be tested extensively at various SNR levels to evaluate the robustness of these two different target classifier design techniques against noise in a comparative manner.

3.1 Description of Scattered Data Used in Classifier Design and Testing

In this chapter, all of our library targets are spheres. The impulse responses of these spherical targets are analytically synthesized in response to a plane

wave excitation that is linearly polarized in x-direction and propagates in z-direction as shown in Figure 3.1. The far field scattered responses are computed at the Φ= π / 2 plane for different values of the angle θ in the frequency domain over a bandwidth from zero to 19.1 GHz with frequency steps of Δf= for 37.3 MHz (i.e. at 512 frequency sample points) by using the analytical solutions provided in the reference [32]. These computations are performed at 12 different values of the bistatic aspect angle θb where θb = 180º – θ. The angle θ assumes the values θ = 15º, 30º, 45º, 60º, 75º, 90º, 105º, 120º, 135º, 150º, 165º and 179º. The corresponding time domain responses of spherical targets are computed by using the Inverse Fast Fourier Transformation (IFFT) of the windowed frequency-domain data with 1024 sample points over a total time span of T_o = 26.81 nanoseconds. In simulations, five reference aspects are used for classifier design purposes. These reference aspects are chosen to be θ = 15º, 45º, 90º, 135º, 179º. In other words, the feature database of each classifier is constructed using scattered data at only these reference aspects. The rest of the data at other aspects are used for performance testing only.

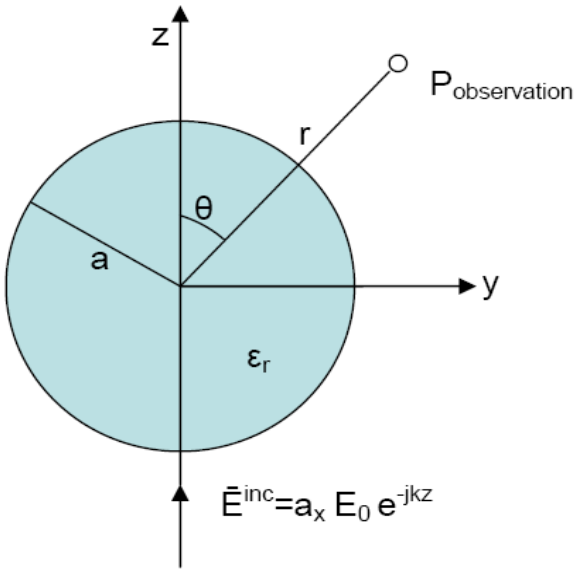

Figure 3.1 Problem geometry used to synthesize electromagnetic signals scattered from spherical targets.

3.2 Classifier Design for Perfectly Conducting Spheres

In this chapter, we will use a total of nine perfectly conducting spheres named as Tcon1, Tcon2, Tcon3, Tcon4, Tcon5, Tcon6, Tcon7, Tcon8 and Tcon9 having different radii of 8, 8.5, 9, 9.5, 10, 10.5, 11, 11.5 and 12 cm, respectively. Three different target libraries of conducting spheres called CLCON1, CLCON2 and CLCON3 containing three, five and nine targets, respectively, are constructed as shown in Table 3.1. Among these, the target library CLCON2 has been used to analyze and compare the noise performances of two different electromagnetic target classification techniques.

Table 3.1 Target library descriptions for perfectly conducting spheres

Target Library	Targets
CLCON1	Tcon1(r=8 cm), Tcon5(r=10 cm), Tcon9(r=12 cm)
CLCON2	Tcon1(r=8 cm), Tcon3(r=9 cm), Tcon5(r=10 cm), Tcon7(r=11 cm), Tcon9(r=12 cm)
CLCON3	Tcon1(r=8 cm), Tcon2(r=8.5 cm), Tcon3(r=9 cm), Tcon4(r=9.5 cm), Tcon5(r=10 cm), Tcon6(r=10.5 cm), Tcon7(r=11 cm), Tcon8(r=11.5 cm), Tcon9(r=12 cm)

3.2.1 Classifier Design Simulations for Conducting Spheres Using the MUSIC Algorithm Based Method

In this section, MUSIC algorithm based classifiers are designed for target libraries CLCON1, CLCON2 and CLCON3 using noise-free reference data and also another classifier is designed for the target library CLCON2 using a slightly noisy reference data set at 20 dB SNR level.

3.2.1.1 Classifier design with noise-free reference data

In the MUSIC algorithm based target classifier design method, firstly the total time span of scattered signals is divided into sixteen overlapping subintervals of length N=128. For each subinterval, the MUSIC spectrum matrices (MSMs) are computed at each different reference aspect angle θ = 15º, 45º, 90º, 135º, 179º. Then, these MSMs are superposed for each given target to obtain the fused MUSIC spectrum matrices (FMSMs) over each subinterval to determine the optimal late-time interval for classifier design.

While searching for the optimal late-time interval, the r_{total} values are computed for each subinterval using Equation (2.15). In other words, over the optimal late-time interval, summation of correlation coefficients between MSMs and their matched FMSM must be maximum and also summation of correlation coefficients between MSMs and mismatched FMSMs must be minimum. In this subsection, design parameters of the MUSIC algorithm are chosen to be N= 128, m= 64 and L= 32. The r_{total} values computed for each time subinterval during the classifier designs using noise-free reference data for target libraries CLCON2 and CLCON3 are shown in Figure 3.2.

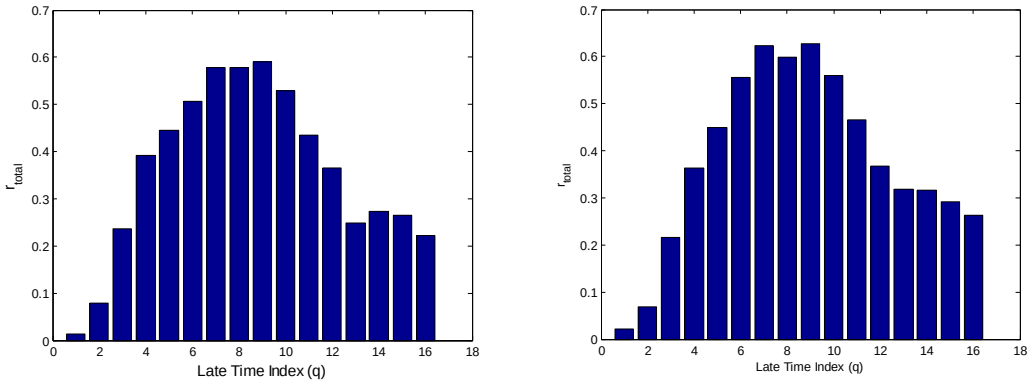

(a) (b)

Figure 3.2 The r_{total} values computed for the classifier designs for target libraries CLCON2 (a) and CLCON3 (b) in the noise free case.

The Correct classification factor (CCF) given by the r_{total} value is a statistical measure providing a good overall idea about the choice of design interval. However, we may still need fine tuning in individual design cases especially when there are several late-time intervals with very similarly high r_{total} values. Therefore, manual tests may also be useful to obtain the optimum late-time interval. For CLCON2 and CLCON3 target libraries (in noise-free design) the optimum late time interval is selected as the seventh time band which corresponds to [5.5, 8.8] nsec. Also, for the classifier for target library CLCON1 using noise-free data, the optimum late-time interval is obtained to be [4.8, 8.1] nsec. CCF values in the earlier time intervals are seen to be very

small in Figure 3.2 since these intervals contain forced scattered response components in addition to the superposition of damped sinusoidal natural response components. The presence of highly aspect dependent early-time scattered response components in data obviously causes deterioration in the aspect invariance and hence in the correct classification rate of the classifier. As we move into later time intervals, these forced response components vanish so we can obtain higher CCF values.

When we decide on the optimal design interval, the feature database composed of target FMSMs is also ready to make performance tests. As an example, in Figure 3.3 below, the MSM map of an unknown test signal (actually, the signal belongs to the conducting sphere Tcon5 (r=10 cm) at θ=30 degrees) is given together with all FMSMs maps belonging to three library targets of the CLCON1 library in the noise free case. The matched correlation coefficient between the MSM of this test target and the FMSM of Tcon5 is computed to be 0.5614 while the mismatched correlation coefficients turned out to be 0.0749 and 0.0862 for the library targets Tcon1(r=8 cm) and Tcon9(r=12 cm), respectively. Therefore, the test target is classified to be the sphere Tcon5(r=10 cm) with a very large safety margin. Accordingly, Figure 3.3 (b) and Figure 3.3 (d) are very similar to each other, as expected.

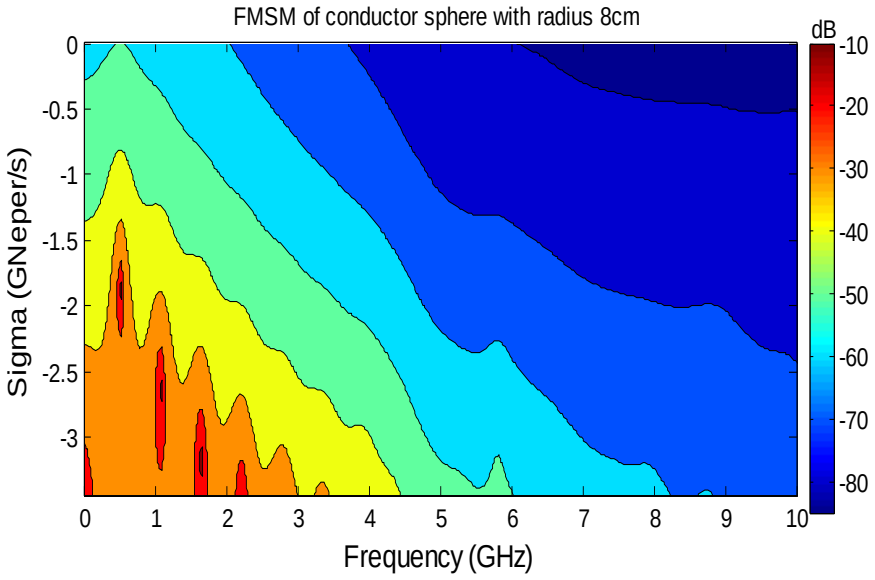
FMSM of conductor sphere with radius 8cm
dB
-10
-20
-30
-40
-50
-60
-70
-80
0
-0.5
-1
-1.5
-2
-2.5
-3
Sigma (GNeper/s)
0
1
2
3
4
5
6
7
8
9
10
Frequency (GHz)

(a)

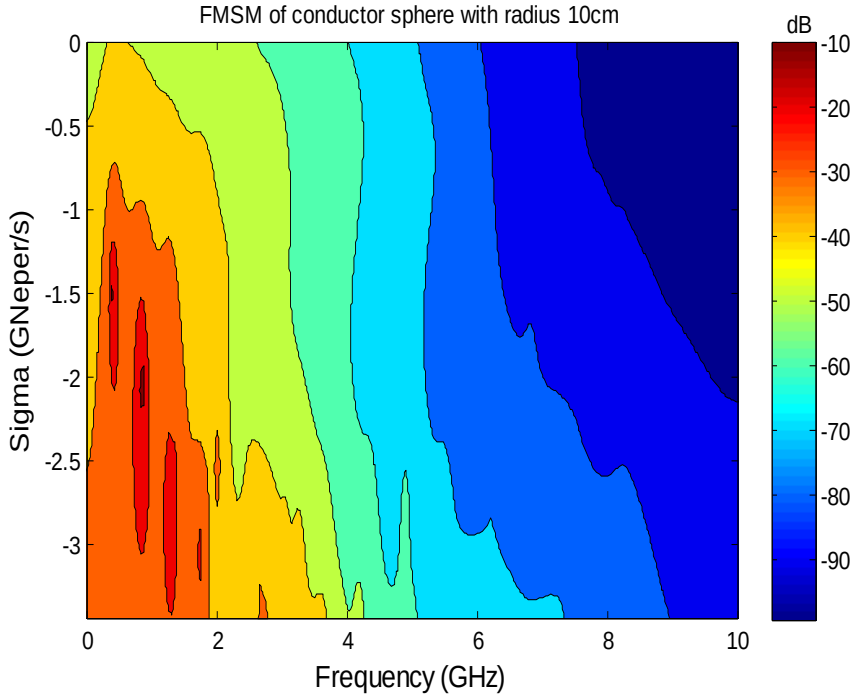
FMSM of conductor sphere with radius 10cm
dB
-10
-20
-30
-40
-50
-60
-70
-80
-90
0
-0.5
-1
-1.5
-2
-2.5
-3
Sigma (GNeper/s)
0
2
4
6
8
10
Frequency (GHz)

(b)

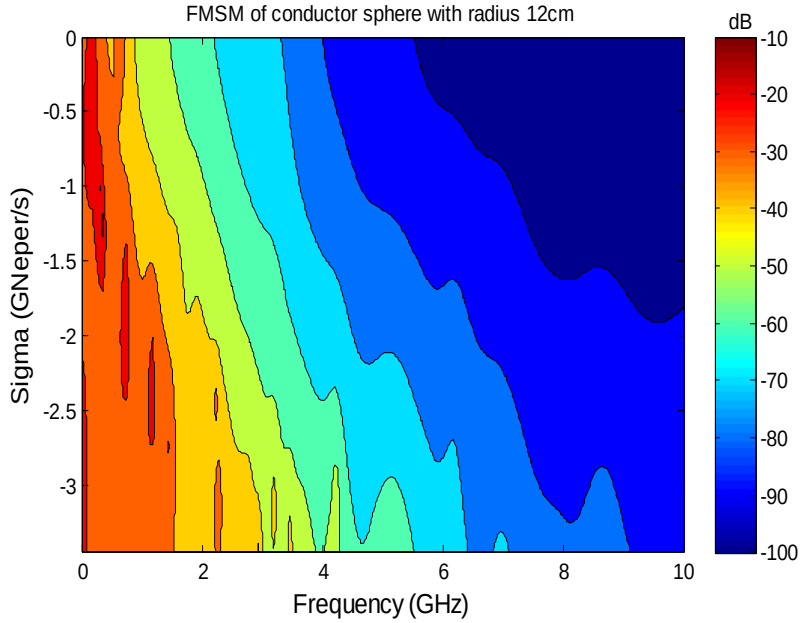

(c)

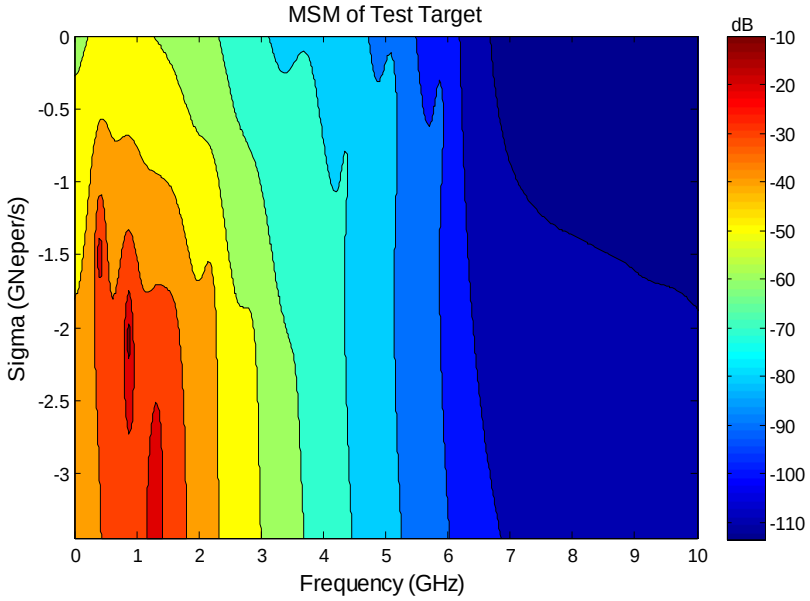

(d)

Figure 3.3 (a)-(c) The FMSM features of the perfectly conducting spheres with 8 cm, 10 cm and 12 cm radii of the CLCON1 library in the noise free case. (d) the MSM map of the test signal (belonging to the conducting sphere with radius of 10 cm at θ=30 degree aspect angle).

In the next example, correlation coefficients between the FMSMs of library targets (Tcon1, Tcon3, Tcon5, Tcon7 and Tcon9) and the MSMs of all available test signals are computed for the classifier designed for the library CLCON2 in noise free case. The results are plotted in Figure 3.4. In this figure, the first 12 indices refer to the test data belonging to the target Tcon1(r=8 cm) at 12 different aspect angles in the order θ = 15º, 30º, 45º, 60º, 75º, 90º, 105º, 120º, 135º, 150º, 165º and 179º. The next 12 indices from 13 to 24 belong to the second target Tcon3(r=9 cm) at the same aspects, and so on. For example, the blue curve gives us the correlation coefficients between the FMSM of the first library target (Tcon1) and the MSMs of all sixty test signals belonging to five library targets at 12 aspects. Here, first 12 data points on the blue curve show the matched correlation coefficients for the target Tcon1(r=8 cm). We can see in the Figure 3.4 that this classifier makes only one mistake in classification at index 47 which corresponds to the test of Tcon7(r=11 cm) at 165 degree aspect angle. The MSM feature extracted from this test signal over the optimal late-time interval [5.5, 8.8] nsec has the highest correlation with the FMSM of Tcon9. Therefore, this test target is incorrectly identified to be the sphere Tcon9 (r=12 cm) instead of Tcon7 (r=11 cm). The resulting correct classification rate (called also as accuracy rate) of this classifier (designed with the MUSIC algorithm based method at noise-free case) is computed to be 98.3% for 59 correct decision out of 60 tests.

Next, this classifier is tested at the SNR levels of 40 dB, 20 dB, 15 dB, 10 dB and 5 dB. Unfortunately, the accuracy rate of the classifier is found to drop sharply below 50% even at a very high SNR level of 40 dB. Accuracy rate was slightly above 20% at SNR=20 dB. These results are plotted in Figure 3.15 of section 3.2.3.

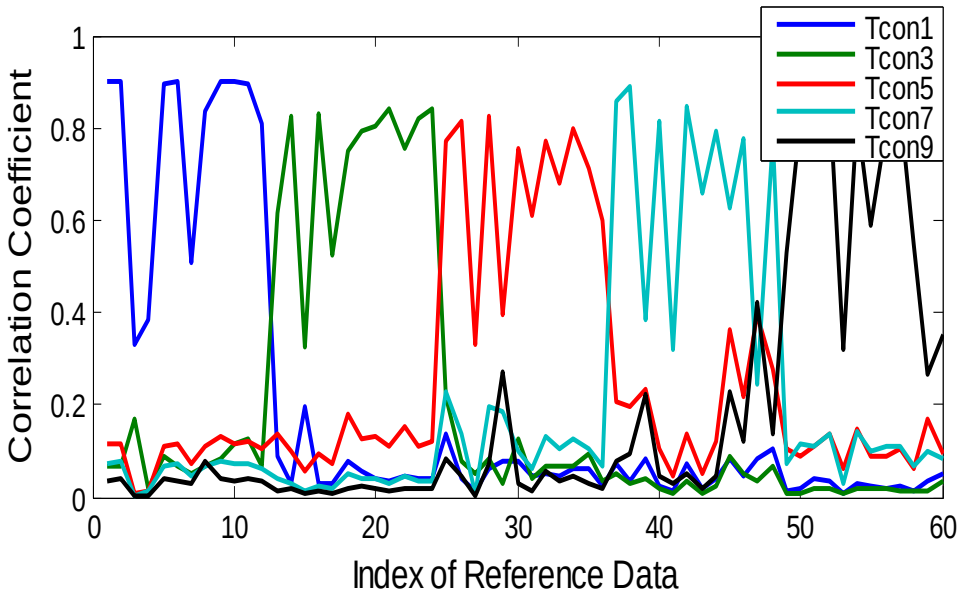

Figure 3.4 Correlation coefficients between the FMSMs of library targets and the MSMs of a total of 60 available test signals for the classifier designed for the target library CLCON2 in noise free case using the MUSIC based technique.

3.2.1.2 Classifier design with noisy reference data

In this subsection, a MUSIC algorithm based classifier is designed for the target library CLCON2 using a set of slightly noisy reference data at 20 dB SNR level. Again, the common time span of these noisy signals is divided into sixteen overlapping subintervals. Then, we create MSMs for each library target at all reference aspects over each subinterval. Afterwards, these MSMs are superposed for each given target to obtain the fused MUSIC spectrum matrices (FMSMs) of that target over all subintervals. To choose the optimum late time interval, again we compute r_{total} values for each subinterval and plot them as shown in Figure 3.5.

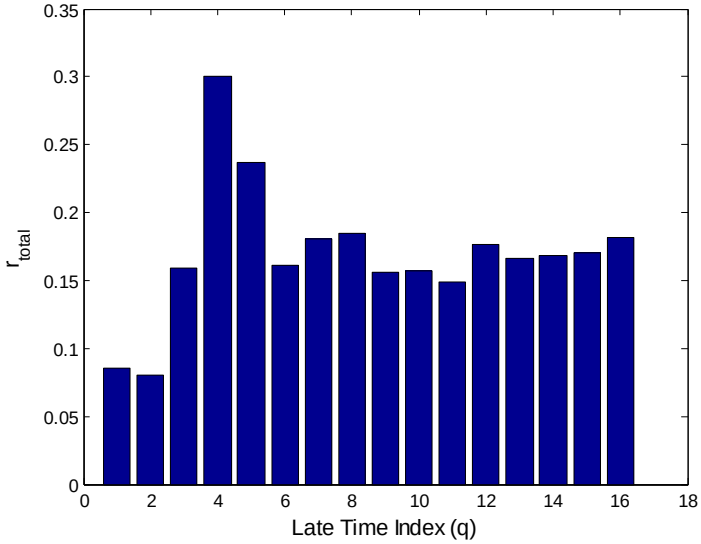

Figure 3.5 The r_{total} values computed for the classifier design for the library CLCON2 at 20 dB SNR level using the MUSIC based technique.

As it can be seen in Figure 3.5, r_{total} has a maximum at q = 4 for this noisy reference database with 20dB SNR. Therefore, we choose this time band as the optimum late time interval which is [3.0, 6.3] nsec. For, the classifier designed by using noise free reference data for the same target library, we selected [5.5, 8.8] nsec as the optimum late time design interval as mentioned in the subsection 3.2.1.1. Now, in this noisy case, we have to choose an earlier time band for design because perfectly conducting spheres are very low-Q targets with quickly decaying response signals. For such targets, the effective SNR of late-time scattered signals may become very low as the amplitudes of damped sinusoidal signals attenuate to very small values. As an example to this fact, two example test signals which are scattered responses of the target Tcon3(r=9) at θ=30 degrees aspect angle at SNR = 10 dB (blue line) and scattered response of the same target at the same aspect at noise free case (red line) are plotted in Figure 3.6 below.

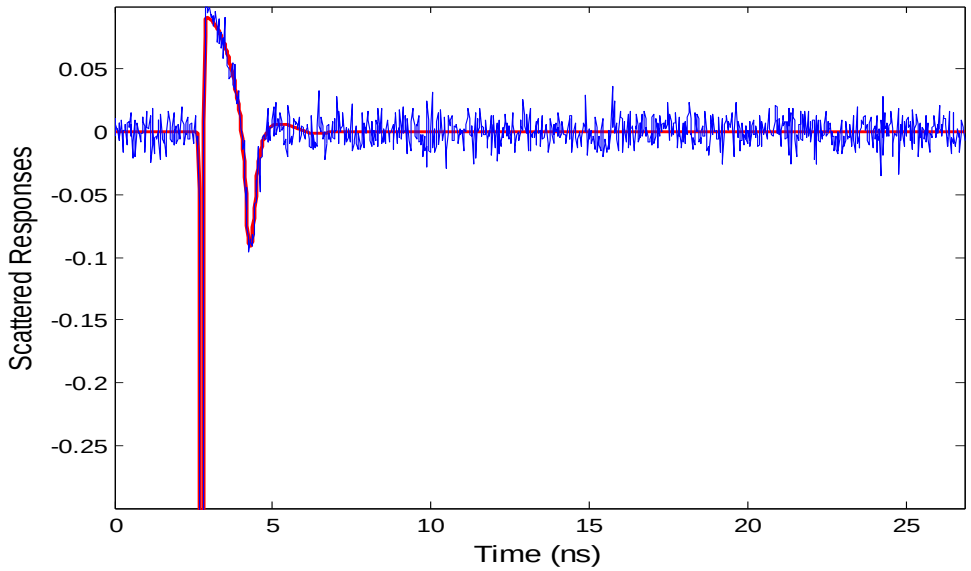

Figure 3.6 Scattered response of the target Tcon3(r=9) at 30 degrees aspect angle at SNR = 10 dB (blue line) and at noise free (red line) case.

Over the selected optimum late-time interval of [3.0-6.3] nseconds, all FMSMs computed for the library targets at 20 dB SNR level and the MSM feature of an arbitrarily selected test signal (belongs to Tcon1 at 90 degrees) at 10 dB SNR level are given in Figure 3.7. The correct classification rate of this classifier is computed against test data at various SNR levels (5dB, 10dB, 15dB, 20dB, 40dB and noise free cases) and results are plotted in Figure 3.15 of section 3.2.3. The accuracy rates is observed to be decaying from 80% to 50% as the overall SNR level decreases from infinity to 5dB as shown in that figure.

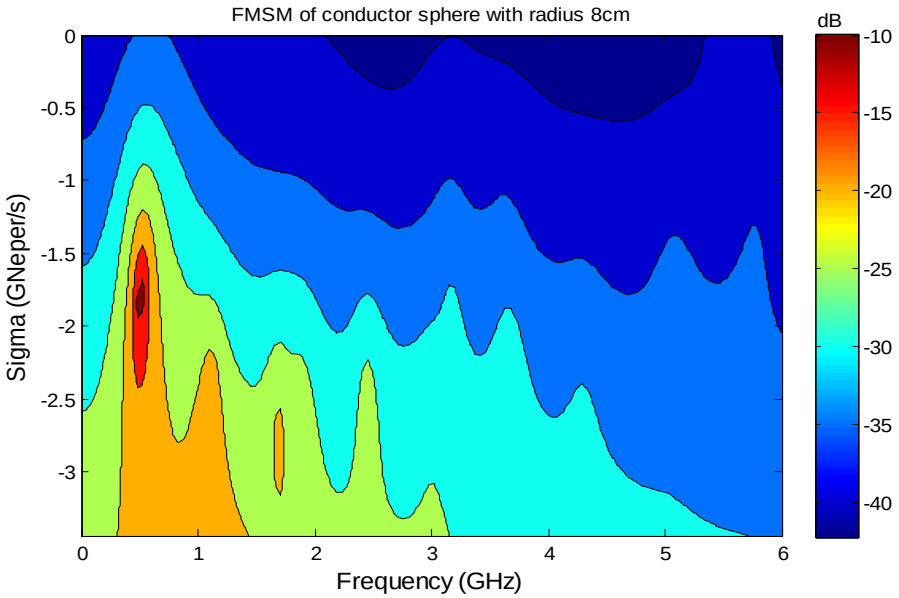
FMSM of conductor sphere with radius 8cm
dB
-10
-15
-20
-25
-30
-35
-40
0
-0.5
-1
-1.5
-2
-2.5
-3
Sigma (GNeper/s)
0
1
2
3
4
5
6
Frequency (GHz)

(a)

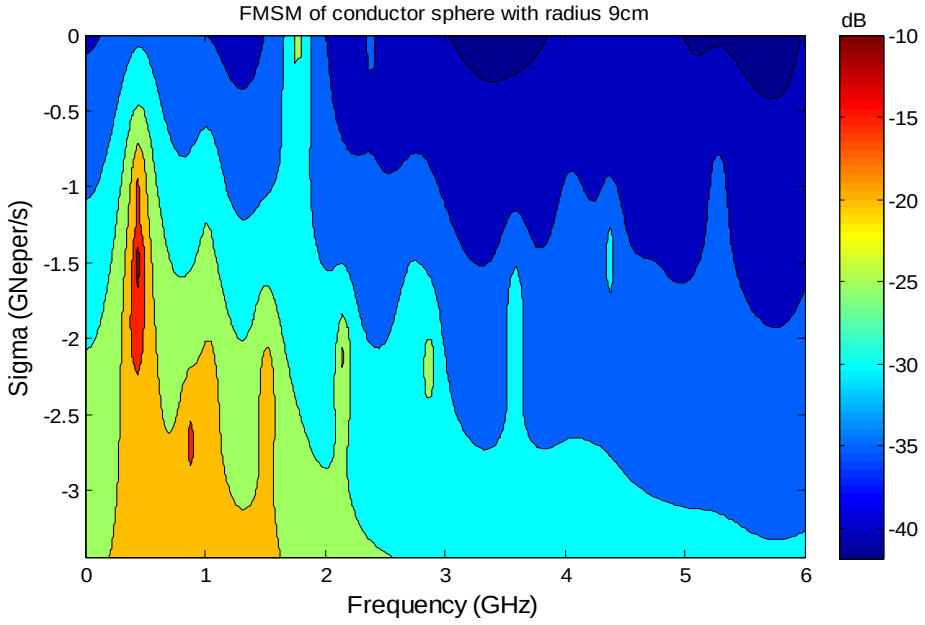
FMSM of conductor sphere with radius 9cm
dB
-10
-15
-20
-25
-30
-35
-40
0
-0.5
-1
-1.5
-2
-2.5
-3
Sigma (GNeper/s)
0
1
2
3
4
5
6
Frequency (GHz)

(b)

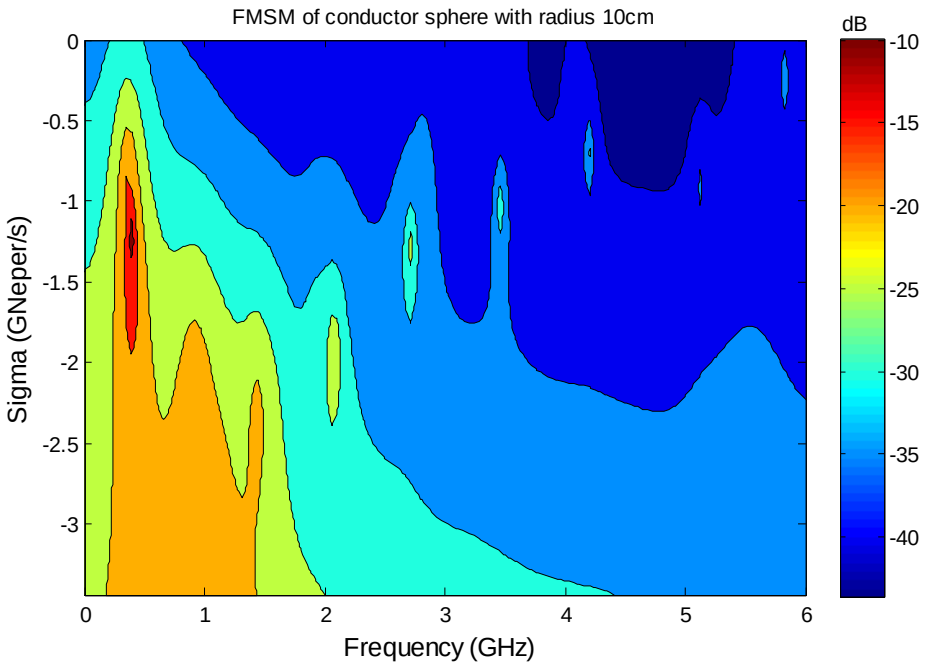
FMSM of conductor sphere with radius 10cm
dB
-10
-15
-20
-25
-30
-35
-40
Sigma (GNeper/s)
0
-0.5
-1
-1.5
-2
-2.5
-3
0
1
2
3
4
5
6
Frequency (GHz)

(c)

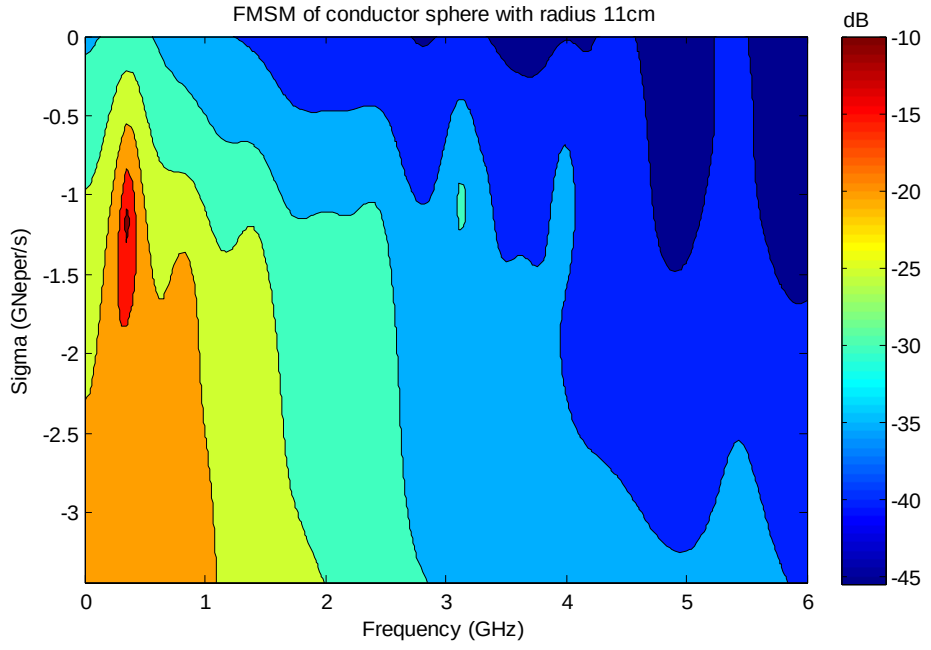
FMSM of conductor sphere with radius 11cm
dB
-10
-15
-20
-25
-30
-35
-40
-45
Sigma (GNeper/s)
0
-0.5
-1
-1.5
-2
-2.5
-3
0
1
2
3
4
5
6
Frequency (GHz)

(d)

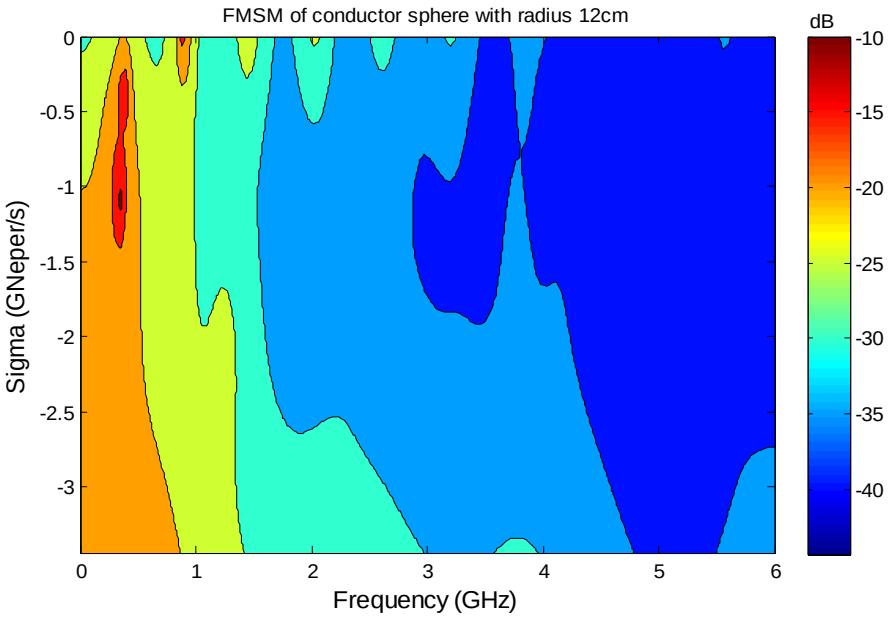

(e)

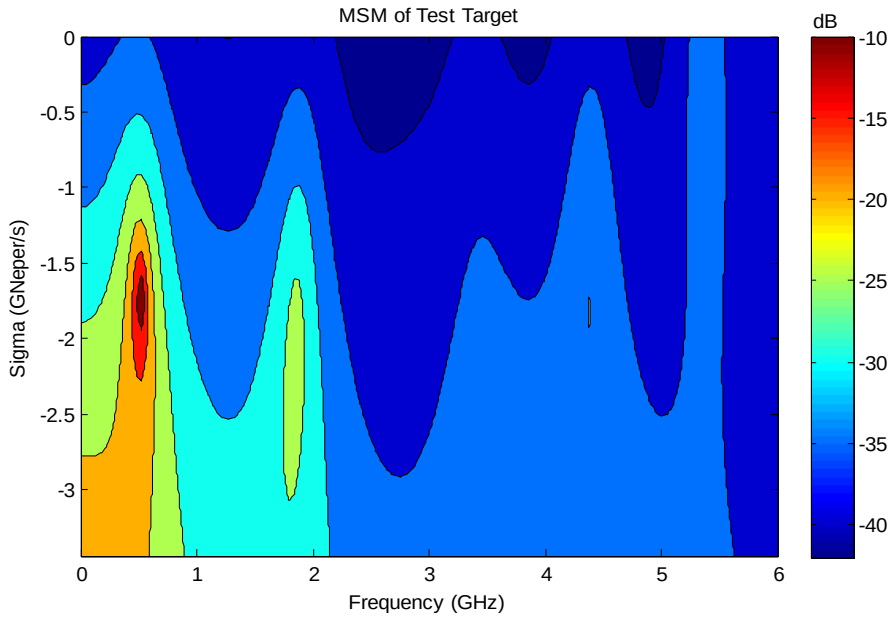

(f)

Figure 3.7 (a)-(e) The FMSM features of the perfectly conducting spheres with 8 cm, 9 cm, 10 cm, 11 cm and 12 cm radii at 20 dB SNR level for the classifier designed for the target library CLCON2 at 20 dB SNR level (f) the MSM map of the test signal (belonging to the conducting sphere with radius of 8 cm at 90 degree aspect angle at 10 dB SNR level)

3.2.2 Classifier Design Simulations for Conducting Spheres Using the WD-PCA Based Method

In this section, WD-PCA method based classifiers are designed for the target library CLCON2, firstly using noise-free reference data and then using slightly noisy reference data at 20 dB SNR level. Earlier, such target classifiers were designed by M. Ayar [35] for the target libraries CLCON1 and CLCON3 using noise free reference data. So, we will not repeat the same classifier designs but use his results for comparisons.

3.2.2.1 Classifier design with noise-free reference data

In this section, we design a classifier with noise-free reference signals for the target library CLCON2 using the WD-PCA based design technique. The resulting classifier is tested at various SNR levels of 40 dB, 20 dB, 15 dB, 10 dB and 5 dB in addition to the infinite SNR level.

As the first step of the classifier design, we compute the auto-WD matrix Wx of the discrete scattered signals x(t) with N=1024 sample points for all five reference aspects of all targets. Some contour plots of the auto-WD matrices for the target Tcon5 at 60º, 105º and 165º degrees aspect angles are given in Figure 3.8 as an example to show the behavior of these time-frequency domain images. Afterwards, energy density vectors are computed as described in Section 2.2.1 over Q=32 non-overlapping late-time intervals. Then, an optimal late-time interval for the classifier design is determined to construct the Late Time Features Vectors (LTFVs) for each library target at each reference aspect.

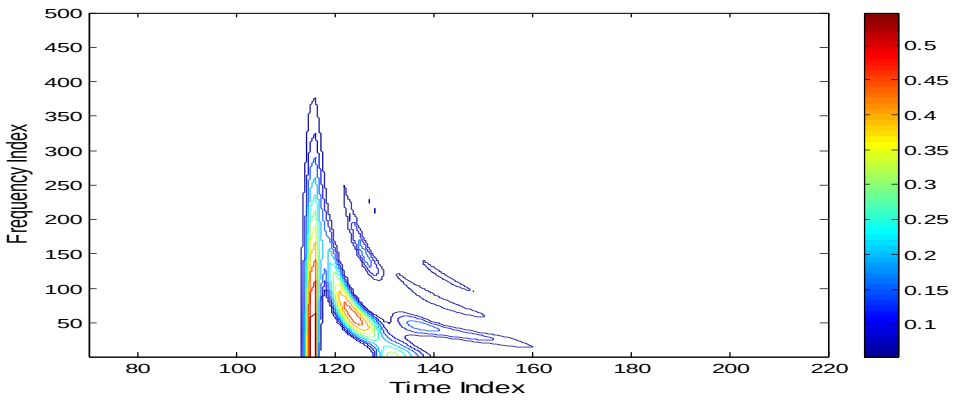

(a)

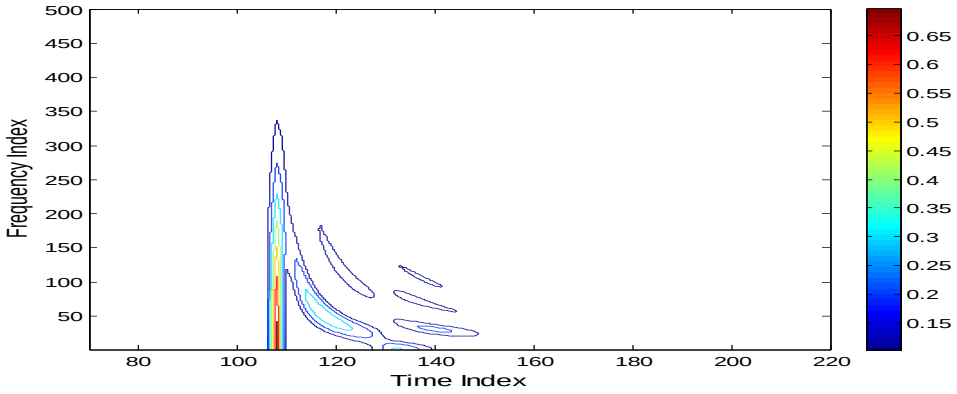

(b)

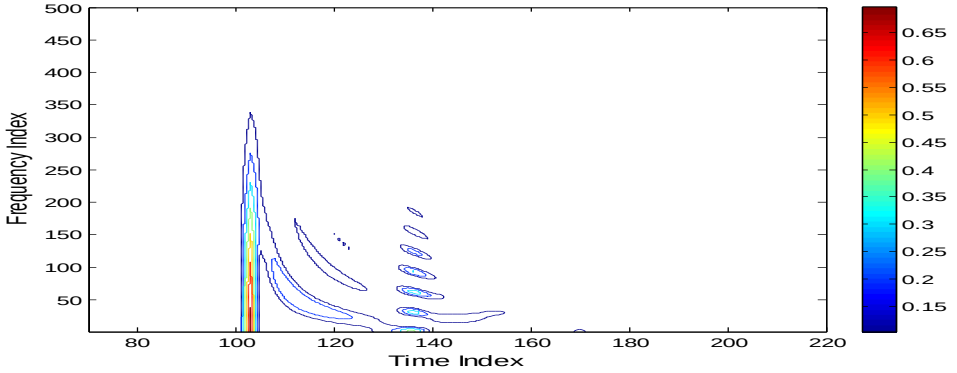

(c)

Figure 3.8 Contour plots of modified auto-Wigner distributions for the target Tcon5 at (a) 60º, (b) 105º, (c) 165º aspect angles.

The optimal late-time interval is determined by the help of Correct Classification Factor (CCF) which is computed over each the late-time interval q*. To obtain high CCF values, the first normalized summation in Equation 3.1 should be much larger than the second one for a satisfactory target classification performance. In other words the factor CCF must be as large as possible to satisfy our design objectives.

$$CCF(q^*) = \frac{1}{(M_{tar} K^2)} \sum_{i,j} r_{i,j}^{matched} - \frac{1}{(M_{tar}{}^2 - M_{tar}) K^2} \sum_{i,j} r_{i,j}^{mismatched} \quad (3.1)$$

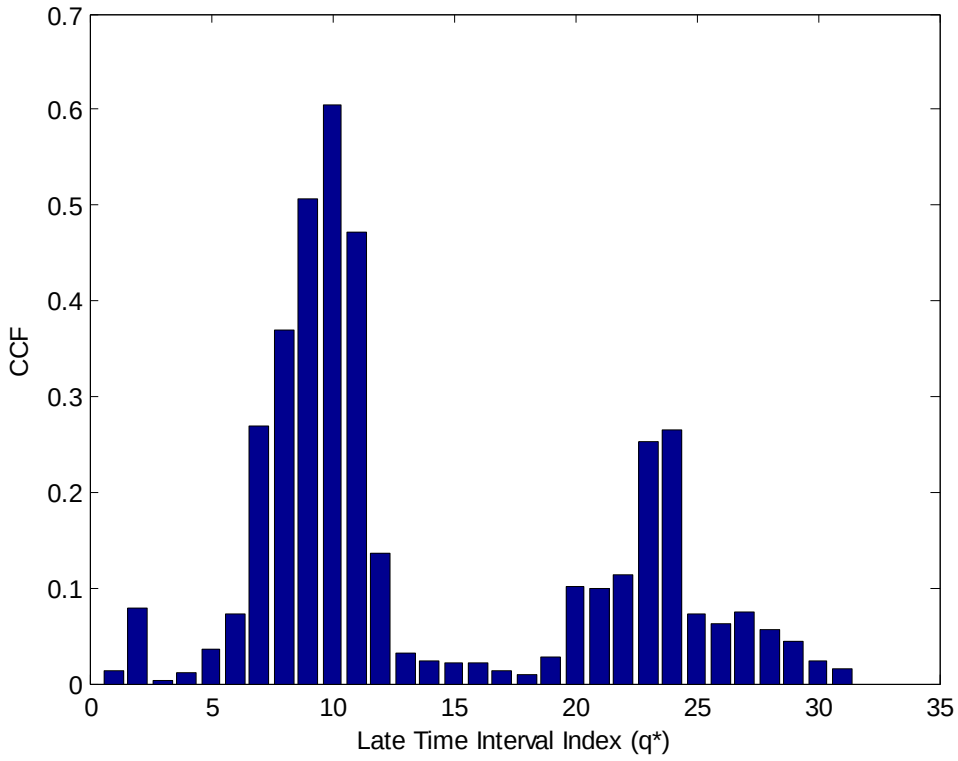

Figure 3.9 CCF plotted against q* to determine the optimal late-time design interval for the target set CLCON2 by using noise-free reference data

The CCF versus q* results for q*=1,…,31 are computed for the present design simulation and plotted in Figure 3.9. The values of CCF has a maximum at q* = 10 time window for noise-free reference data. So, we obtain the successive pair of bands with q=9 and q=10 as the optimum late-time design interval which is chosen to be [6.70, 8.38] ns for this noise-free classifier design.

Then, over this optimum late-time window, the late-time feature vectors (LTFV) are extracted for all targets at all aspect angles. LTFVs of the target Tcon1(r=8 cm), at the reference aspect angles θ = 15º, 45º, 90º, 135º, 179º for the noise free case are plotted in Figure 3.10 as an example.

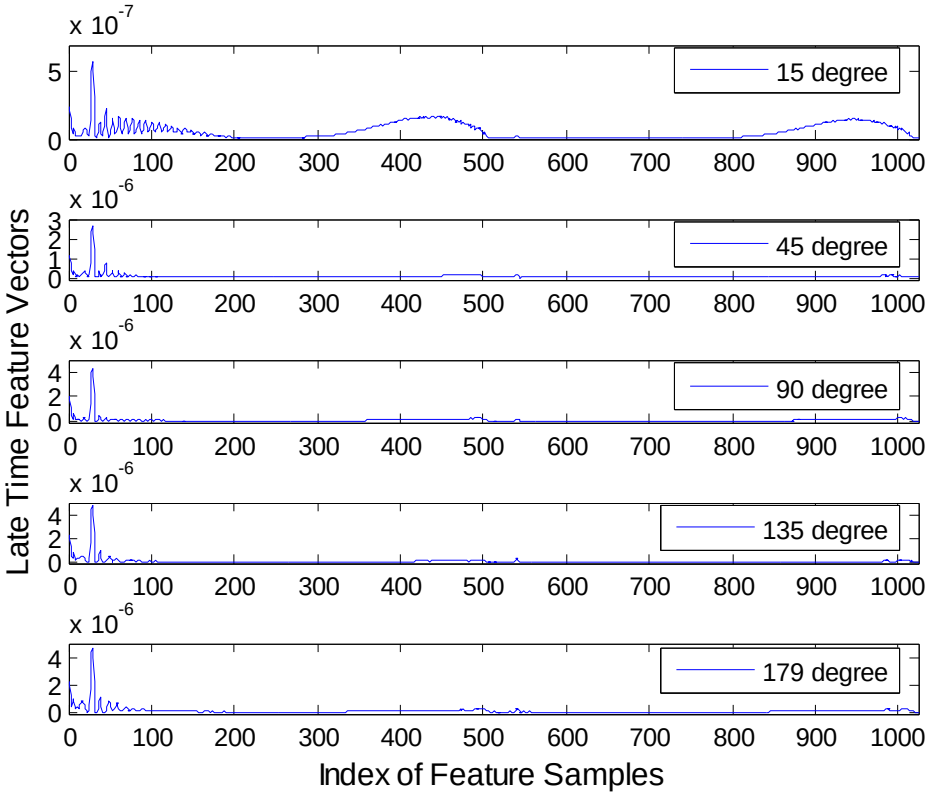

Figure 3.10 LTFVs of target Tcon1(r=8 cm) at the reference aspect angles θ = 15º, 45º, 90º, 135º, 179º for noise-free case

For each target, the principal component analysis (PCA) is applied to fuse associated LTFVs. The Fused Feature Vectors (FFVs) are constructed for each target and they are plotted in Figure 3.11 for noise-free design. These five fused feature vectors form the feature database of the designed classifier.

Next, the LTFVs of all test data are compared to FFVs of library targets to determine the correct classification rate of the resulting classifier. 100 percent accuracy is obtained against noise free test data as shown in Figure 3.15 of section 3.2.3. However, the accuracy rate shows a rapid decrease when the classifier is tested against noisy data even for the SNR level of 40 dB. In other words, both the MUSIC based classifier and the WD-PCA based classifier perform almost perfectly in noise-free testing but perform very poorly under noisy test conditions.

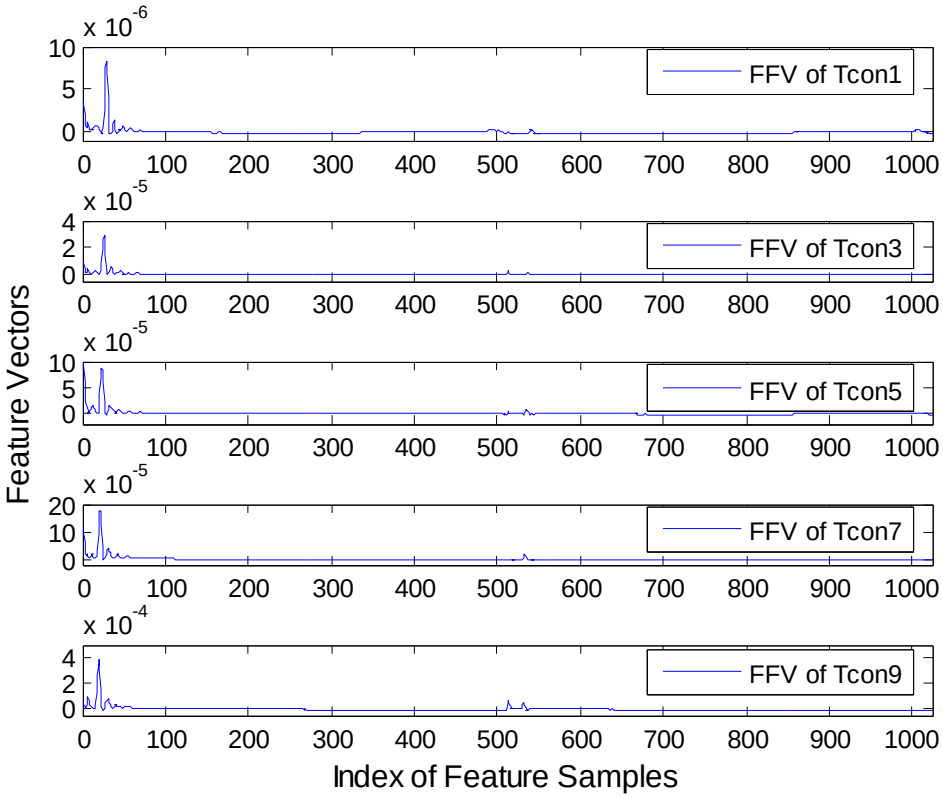

Figure 3.11 FFVs of all targets for CLCON2 at noise-free case

3.2.2.2 Classifier design with noisy reference data

In this section, we design another classifier for the target library CLCON2 using the WD-PCA based method, but this time, using reference data at 20 dB SNR level. All the design steps are the same as those outlined in section 3.2.2.1. Therefore, we are not repeating those here. The optimal late-time design interval for this simulation in decided based on the CCF plot given in Figure 3.12. This plot is constructed after computing the Wigner distribution matrices and the energy density vectors of library target responses at all reference aspects over 31 different late-time intervals.

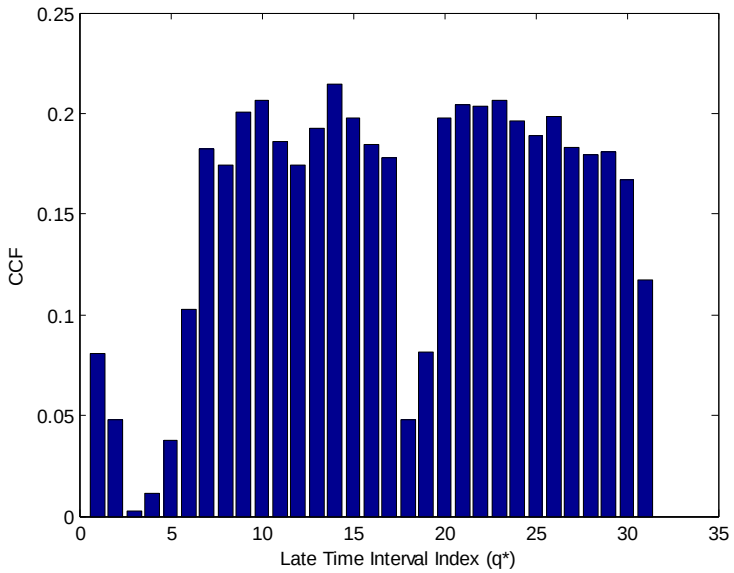

Figure 3.12 CCF plotted against q* to determine the optimal late-time design interval for the target set of CLCON2 by using noisy reference data with 20dB SNR level.

As mentioned before, perfectly conducting spheres are very low-Q targets and at very late time intervals, the signal decreases sharply and hence the effective SNR becomes very low. So we have to select earlier late-time bands whenever possible. For this 20 dB SNR level design, we choose the late-time bands q=6 and q=7 as the optimum late time interval after fine tuning. The optimal design interval turns out to be [4.19, 5.86] nsec.

As an example, the late-time feature vectors (LTFV) of the target Tcon5(r=10) extracted at the reference aspect angles θ = 15º, 45º, 90º, 135º, 179º with 20 dB SNR level over the selected optimum late-time interval are plotted in Figure 3.13.

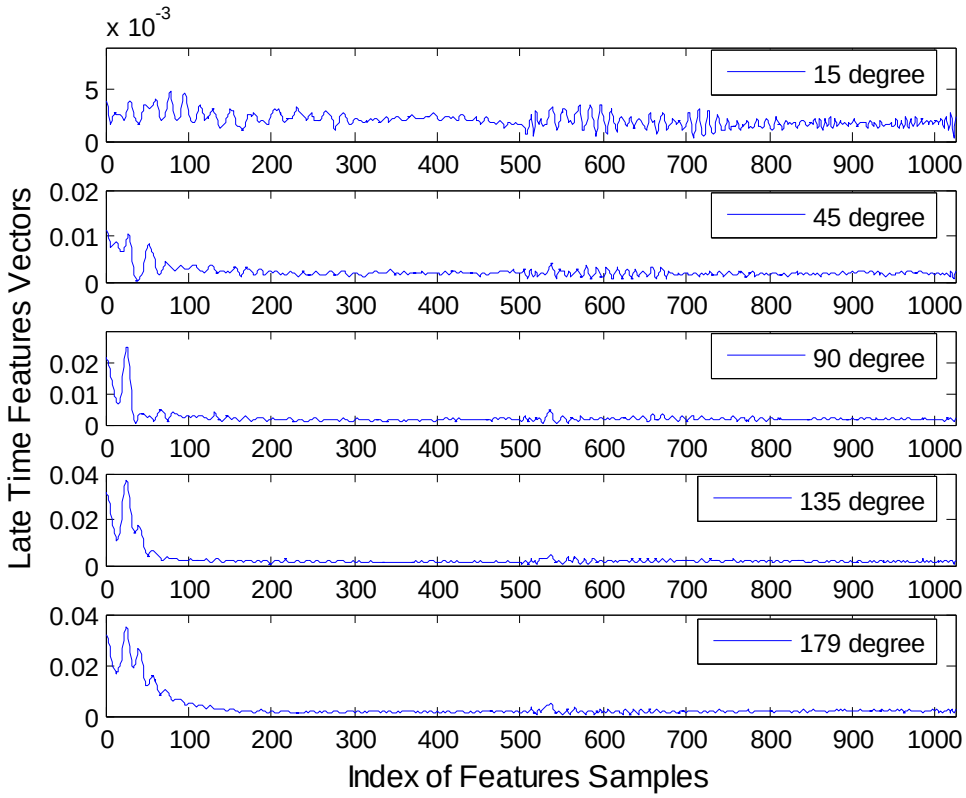

Figure 3.13 LTFVs of target Tcon5(r=10) at the reference aspect angles θ = 15º, 45º, 90º, 135º, 179º for 20 dB SNR level

For each target, the principal component analysis is applied to obtain its FFV from aspect dependent LTFVs. The eigenvalues obtained during the PCA process are listed in Table 3.2 for each library target. The resulting Fused Feature Vectors (FFVs) are plotted in Figure 3.14.

It can be seen in Table 3.2 that, for all targets, the largest eigenvalue (λ1) is much larger than the other eigenvalues λ2 through λ5. Hence, the leading principal component z1 is very dominant and can be used by itself as the FFV of the associated target as discussed in [18].

Table 3.2 Eigenvalues computed during the PCA process while designing the WD-PCA based classifier for the target library CLCON2 at 20 dB SNR level.

	Tcon1(r=8)	Tcon3(r=9)	Tcon5(r=10)	Tcon7(r=11)	Tcon9(r=12)
λ1	0.2366e-4	0.4295e-4	0.4984e-4	0.5295e-4	0.5821e-4
λ2	0.0145e-4	0.0214e-4	0.0230e-4	0.0269e-4	0.0309e-4
λ3	0.0061e-4	0.0082e-4	0.0100e-4	0.0114e-4	0.0100e-4
λ4	0.0045e-4	0.0034e-4	0.0032e-4	0.0043e-4	0.0036e-4
λ5	0.0024e-4	0.0029e-4	0.0029e-4	0.0027e-4	0.0023e-4

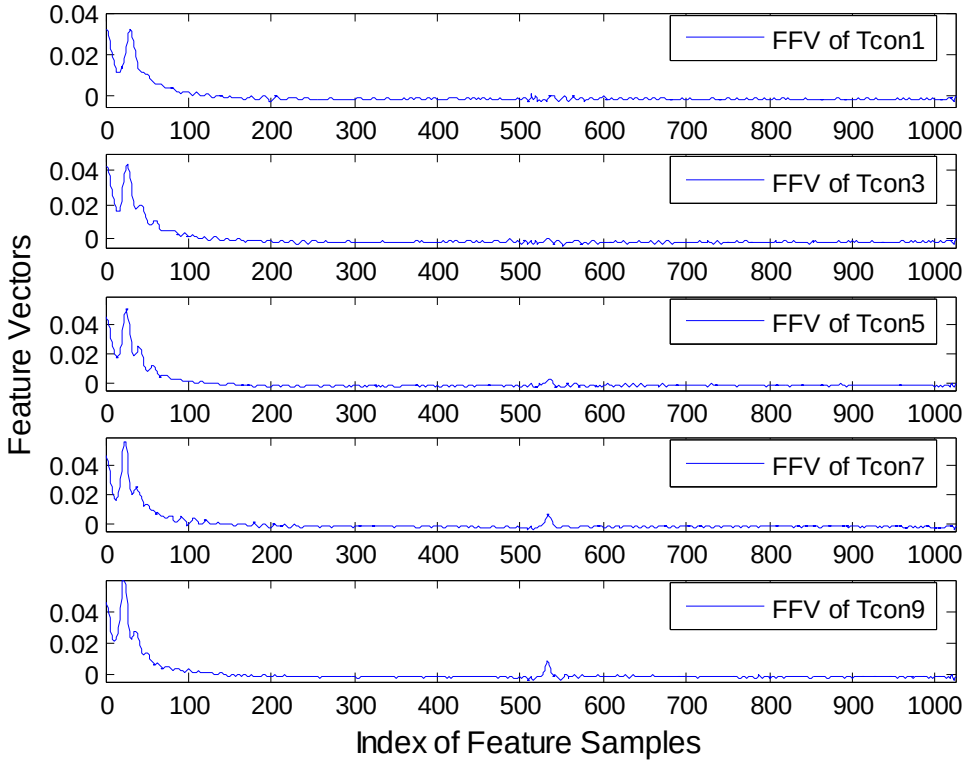

Figure 3.14 FFVs of all targets at 20 dB SNR level

After this classifier is designed as outlined so far, it is tested against the available test data at 12 aspect angles for each one of 5 library targets at the SNR levels of infinity (noise-free case), 40 dB, 20 dB, 15 dB, 10 dB and 5 dB. The correct classification factor values are computed and seen to be decreasing from 80% to 60% as SNR decreases from infinity to 5 dB.

3.2.3 Discussion of Classifier Performance Results for Conducting Spheres

In this subsection, we will compare the performances of target classifiers designed for various target libraries of conducting spheres using noise-free and slightly noisy data (at 20 dB SNR) by means of the MUSIC algorithm based and WD-PCA based classifier design techniques. There are two major

conclusions drawn from the classifier performance results presented so far in section 3.2:

The first conclusion is related to the capability of classifiers to discriminate large number of library targets. The correct decision rates of classifiers, which are designed by both methods using noise free reference data but tested at different SNR levels, for three different target libraries CLCON1, CLCON2 and CLCON3 are listed in Table 3.3. It is concluded based on this table that both classifier design techniques produce very high (close to 100%) accuracy rates in the noise-free design/noise-free test case as we increase the number of perfectly conducting spheres in the target library from 3 to 5 then to 9. The other and the more important conclusion to be drawn is that the classifiers designed for conducting spheres by both methods using noise-free reference data badly fail in tests performed by noisy test data even if the noise is very slight. Their accuracy rates sharply drop from perfect or almost 100% accuracy levels to unacceptably low levels of 40% or below as shown in Figure 3.15. This behavior of the classifiers can be explained by the fact that perfectly conducting spheres are extremely low-Q targets whose natural response signals decay at a very fast rate in late-time region. In other words, the effective SNR level of a given test signal over the optimal late-time interval is much smaller than its overall SNR level. For example, the noisy test signal belonging to the conducting sphere of radius 12 cm (i.e. the target Tcon9) at 165 degrees of aspect and at 10 dB overall SNR level actually has an effective SNR level of -22.7 dB over a late-time interval of [6.70, 8.38] nsec. Obviously, a target classifier that performs perfectly under noise-free conditions but fails in the presence of even a slightly amount of noise is not a useful one. Alternatively, the design of classifiers may be realized by slightly noisy reference data instead of using perfectly noise free data. As shown in Figure 3.15, the MUSIC algorithm based and WD-PCA based classifiers designed for the target library CLCON2 by using slightly noisy data with 20

dB SNR level perform much better when they are tested against noisy data. The accuracy rate of the MUSIC based classifier changes from 80% to 50% as the overall SNR level of the test signals drops from infinity to 5 dB. The accuracy rate of the WD-PCA based classifier is even better, which changes from 80% to 60% as SNR decreases from infinity to 5 dB. These classifiers cannot reach very high accuracy rates close to 100% under noisy testing conditions, the best they can do is about 80%. However, their accuracy rates do not drop to unacceptably low levels such as 20% but stay at acceptable, useful accuracy levels especially for SNR levels at and above 15 dB. As emphasized before, poor noise performance of late-time classifier design techniques should be expected for perfectly conducting spherical targets due to very low-Q nature of these targets.

As mentioned before, results of the WD-PCA classifiers for the target libraries CLCON1 and CLCON3 using noise free design are taken from M. Ayar thesis [35] for comparisons.

Table 3.3 Correct Decision Rates of MUSIC algorithm based and the WD-PCA based classifiers for target libraries CLCON1, CLCON2 and CLCON3 for the noise-free design/noise-free test case.

Target Library	CLCON1 (3 targets)	CLCON2 (5 targets)	CLCON3 (9 targets)
MUSIC method	100	98,3	98,1
WD/PCA method	100	100	97

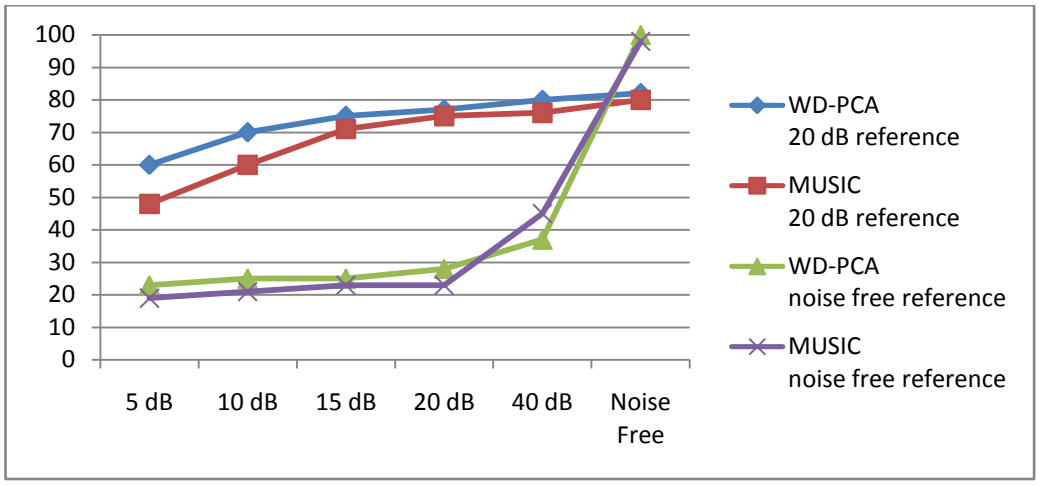

Figure 3.15 Correct classification rates (in percentage) of perfectly conducting sphere classifiers designed for the target library CLCON2 using either noise-free data or 20 dB SNR data.

3.3 Classifier Design for Dielectric Spheres

In this chapter, we have eight dielectric spheres named as Tdie1, Tdie2, Tdie3, Tdie4, Tdie5, Tdie6, Tdie7 and Tdie8 having same radii but slightly different permittivity values ε =3, 3.5, 4, 4.5, 5, 5.5, 6 and 7, respectively. Two different target libraries of dielectric spheres called CLDIE1 and CLDIE2 are shown in Table 3.4. The target library CLDIE1 is used in this section to compare the noise performances of two different electromagnetic target classification techniques.

Table 3.4 Target library descriptions for dielectric spheres.

Target Library	Targets
CLDIE1	Tdie1(ε =3), Tdie3(ε=4), Tdie5(ε=5), Tdie7(ε=6).
CLDIE2	Tdie1(ε=3), Tdie2(ε=3.5), Tdie3(ε=4), Tdie4(ε=4.5), Tdie5(ε=5), Tdie6(ε=5.5), Tdie7(ε=6), Tdie8(ε=7).

3.3.1 Classifier Design Simulations for Dielectric Spheres Using the MUSIC Algorithm Based Method

In this section, MUSIC algorithm based classifiers are designed for target libraries CLDIE1 and CLDIE2 using noise-free reference data and also another classifier is designed for the target library CLDIE1 using a slightly noisy reference data set at 20 dB SNR level.

3.3.1.1 Classifier design with noise-free reference data

As the first step of classifier design, we divide the total time span of noise-free scattered signals into eight overlapping subintervals of length N=256. The other design parameters of the MUSIC algorithm based classifiers for target libraries CLDIE1 and CLDIE2 are chosen as m= 128 and L= 64. Using the same design steps reported in section (3.2.1.1), we search for the optimal late-time interval by the help of the r_{total} values. The r_{total} values computed for each time subinterval during the classifier design for target library CLDIE2 are plotted in Figure 3.16. The maximum value of this bar chart is observed for the seventh late-time index corresponding to the subinterval [15.4, 22.1] nsec. When the same procedure is repeated for the target library CLDIE1, the optimum late-time interval is found to be [18.2, 24.9] nsec for classifier design using noise-free reference data.

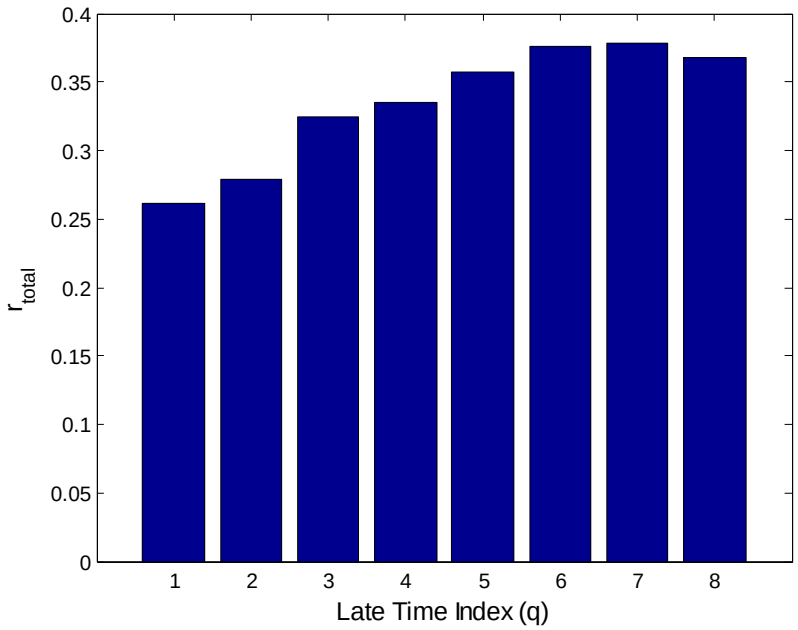

Figure 3.16 The r_{total} values computed during the classifier design for the target library CLDIE2 in the noise-free case.

The FMSMs maps belonging to each of four targets of CLDIE1 library are given in Figure 3.17 together with the MSM map of an unknown test signal which actually belongs to the target under noise-free conditions Tdie1 at θ= 45º aspect angle.

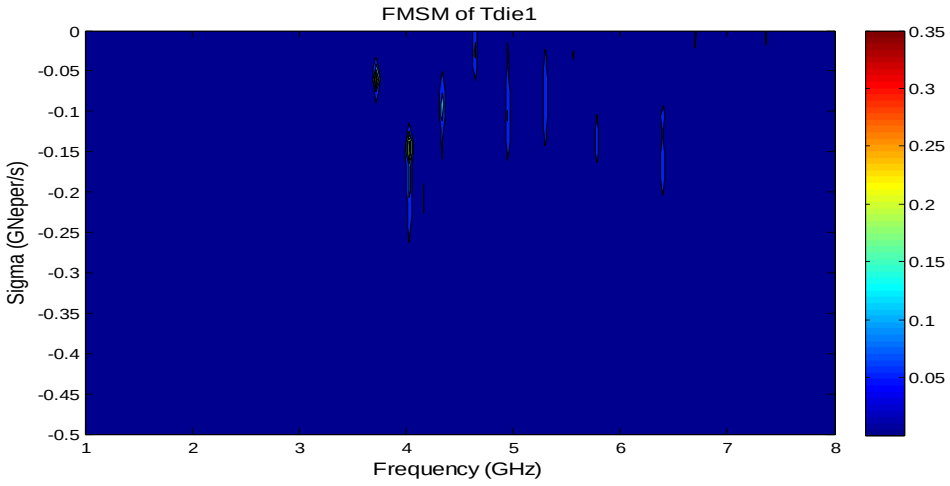
FMSM of Tdie1
Sigma (GNeper/s)
Frequency (GHz)
0
-0.05
-0.1
-0.15
-0.2
-0.25
-0.3
-0.35
-0.4
-0.45
-0.5
1
2
3
4
5
6
7
8
0.35
0.3
0.25
0.2
0.15
0.1
0.05

(a)

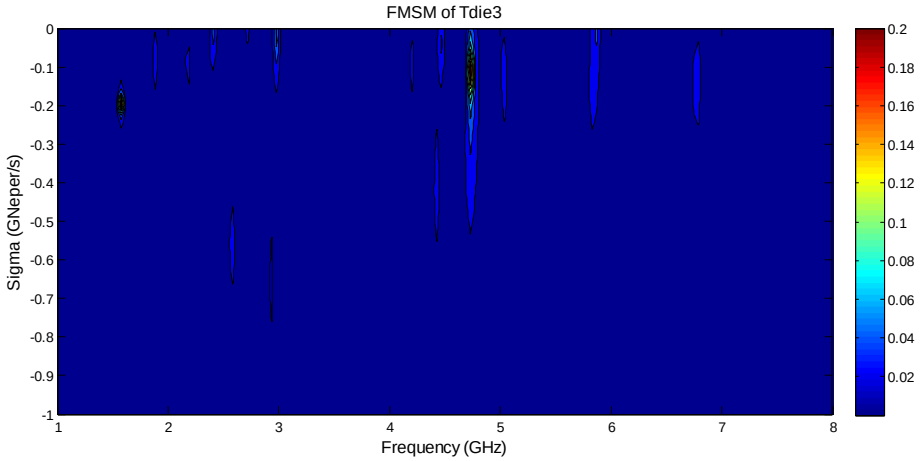
FMSM of Tdie3
Sigma (GNeper/s)
Frequency (GHz)
0
-0.1
-0.2
-0.3
-0.4
-0.5
-0.6
-0.7
-0.8
-0.9
-1
1
2
3
4
5
6
7
8
0.2
0.18
0.16
0.14
0.12
0.1
0.08
0.06
0.04
0.02

(b)

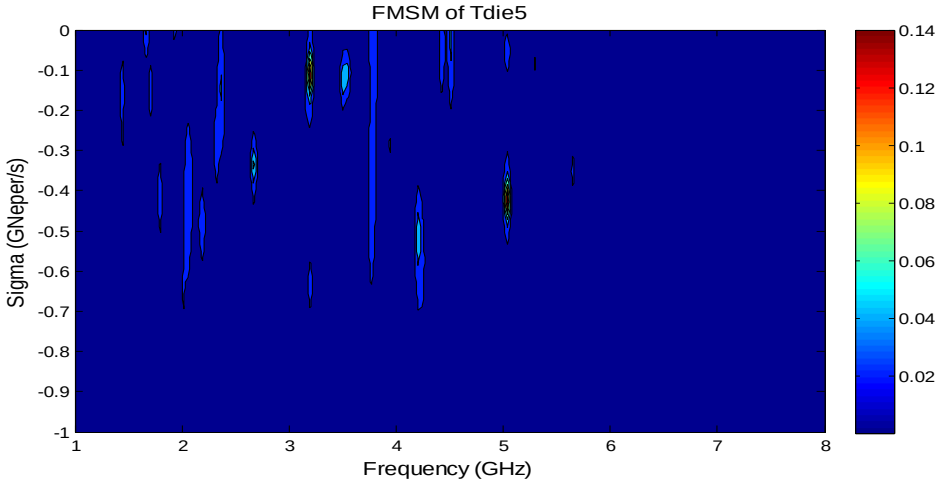
FMSM of Tdie5
Sigma (GNeper/s)
Frequency (GHz)
0
-0.1
-0.2
-0.3
-0.4
-0.5
-0.6
-0.7
-0.8
-0.9
-1
1
2
3
4
5
6
7
8
0.14
0.12
0.1
0.08
0.06
0.04
0.02

(c)

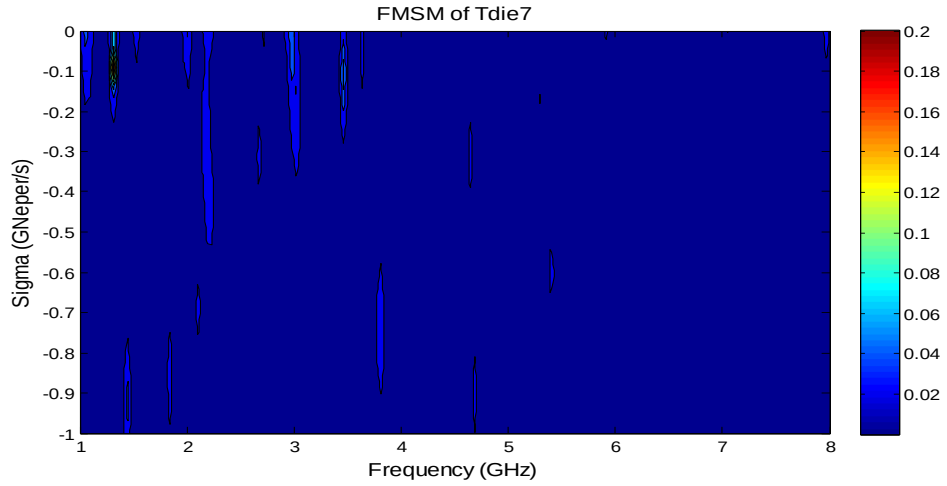

(d)

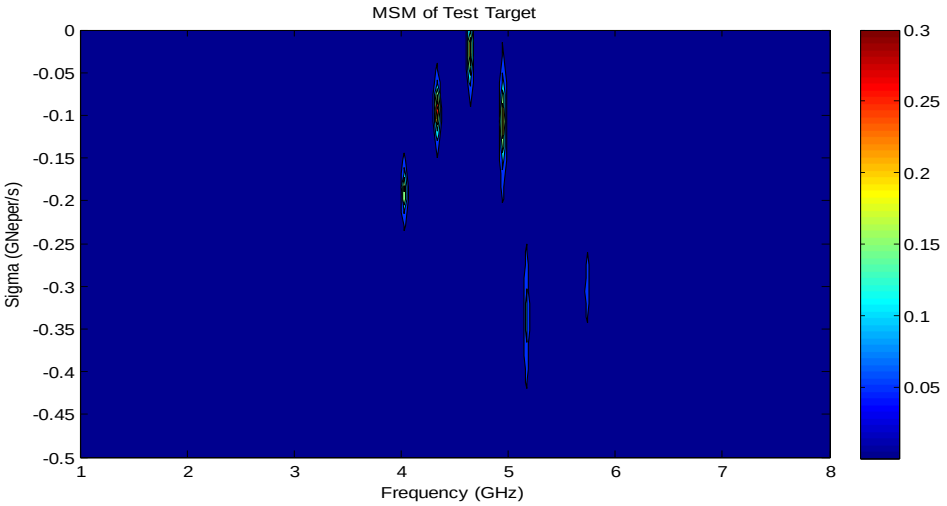

(e)

Figure 3.17 (a)-(d) The FMSM features of the dielectric spheres Tdie1, Tdie3, Tdie5 and Tdie7 of the CLDIE1 library in the noise free case (e) the MSM map of the noise-free test signal belonging to target Tdie1 at θ = 45 degree aspect angle.

Next, correlation coefficients between the FMSMs of all library targets and the MSMs of all available test signals are computed for the classifier designed for the library CLDIE1 in noise free case. These correlation

coefficients are plotted in Figure 3.18 for a total of 48 test signals. The index of test data is defined in exactly the same way as it was defined for Figure 3.4 earlier. We can see in Figure 3.18 that the classifier CLDIE1 makes four mistakes of decision out of 48 trials in this noise-free design/noise-free test case. Therefore, correct classification rate of this MUSIC algorithm based classifier in noise-free case is computed to be 91.2%. Incorrect decisions are basically made while discriminating the targets Tdie5 and Tdie7 with relative permittivity values of 5 and 6, respectively.

This classifier is also tested at the SNR levels of 20 dB, 15 dB, 10 dB and 5 dB. Unfortunately, the accuracy rate of the classifier drops to 35% at the SNR level of 5 dB. These results are given in Table 3.6 of section 3.3.3.

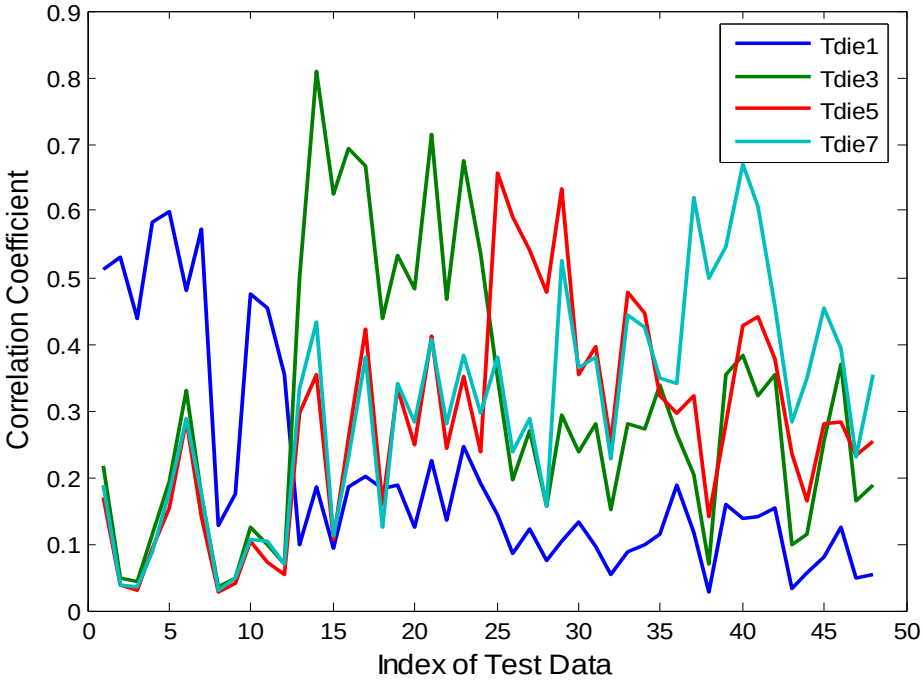

Figure 3.18 Correlation coefficients between the FMSMs of library targets and the MSMs of all available test signals are given for the MUSIC based classifier which is designed for the target library CLDIE1 in the noise-free design/noise-free test case.

3.3.1.2 Classifier design with noisy reference data

In this subsection, a MUSIC algorithm based classifier is designed for the target library CLDIE1 using a set of slightly noisy reference data at 20 dB SNR level. Using the same procedure described in section 3.2.1 with design parameters N= 256, m= 128 and L= 64, we have determined the optimal late-time interval [14.0, 20.7] nsec for this classifier design using noisy reference data at 20 dB SNR level. As expected, this late-time interval is earlier than the optimum late-time interval used for the noise-free classifier design for the same target library. As an example of the noisy scattered signals used in the design, scattered response of the target Tdie3 (ε=4), at θ=75 degrees with 20 dB SNR level is plotted in Figure 3.19.

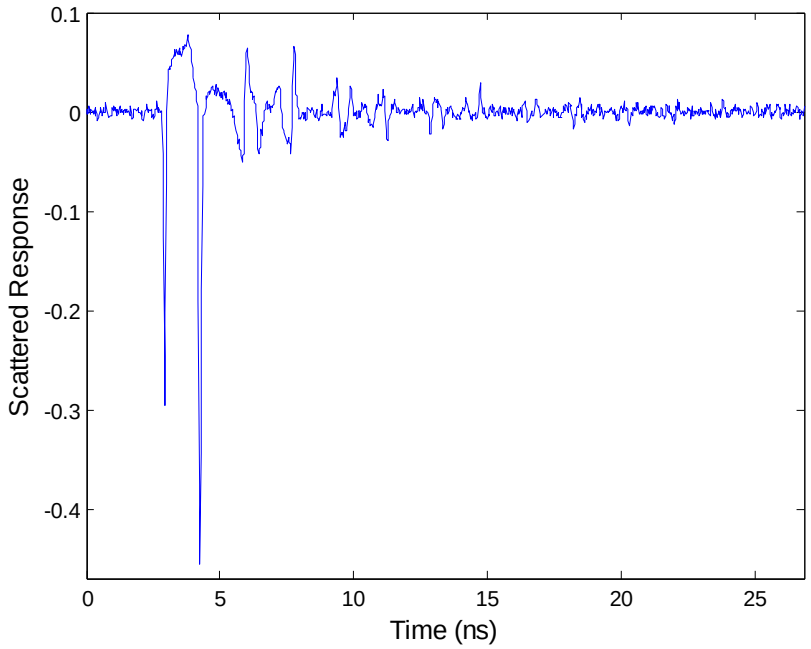

Figure 3.19 Scattered response of the target Tdie3 (ε=4), at θ=75 degrees aspect angle with SNR = 20 dB SNR level.

After determining the optimal design interval, the correct classification rate of the resulting classifier is computed against test data at various SNR levels of

5dB, 10dB, 15dB, 20dB and infinity. Results are given in Table 3.6 of section 3.3.3. The SNR dependent accuracy rates of this classifier is observed to be decaying from 86% to near 50% as the overall SNR level decreases from 20 dB to 5 dB as indicated in this table. Accuracy rate is computed to be 79% when this classifier is tested by noise-free test data. Obviously, this means a degradation of classifier performance at noise-free tests. But, on the other hand, performance of the classifier becomes much better at noisy tests. For example, the accuracy rate is increased from 56% to 81% for performance tests at 15 dB SNR level as a result of designing the classifier by using noisy data at 20 dB SNR instead of using noise-free reference data.

3.3.2 Classifier Design Simulations for Dielectric Spheres Using the WD-PCA Based Method

In this subsection, WD-PCA method based classifiers are designed for the target library CLDIE1, firstly using noise-free reference data and then using slightly noisy reference data at 20 dB SNR level. Earlier, a target classifier was designed for the target library CLDIE2 by M. Ayar [35] using noise free reference data. So, we will not repeat the same classifier design but use his results for comparisons whenever needed.

3.3.2.1 Classifier design with noise-free reference data

In this section, we design a classifier using noise free reference signals for the target library CLDIE1 using the WD-PCA based design technique. The resulting classifier is tested at various SNR levels of 20 dB, 15 dB, 10 dB and 5 dB in addition to infinite SNR level.

As the first step of classifier design, we compute the auto-WD matrices of the scattered signals at reference aspects with N=1024 sample points in time. Some contour plots of the resulting auto-WD matrices for the target Tdie5 at θ=90º and θ=135º degrees aspect angles are given below in Figure 3.20.

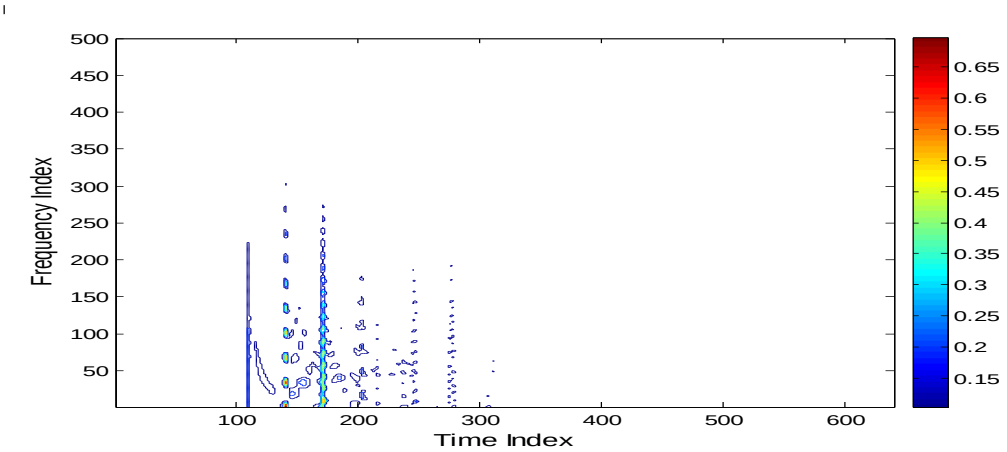

(a)

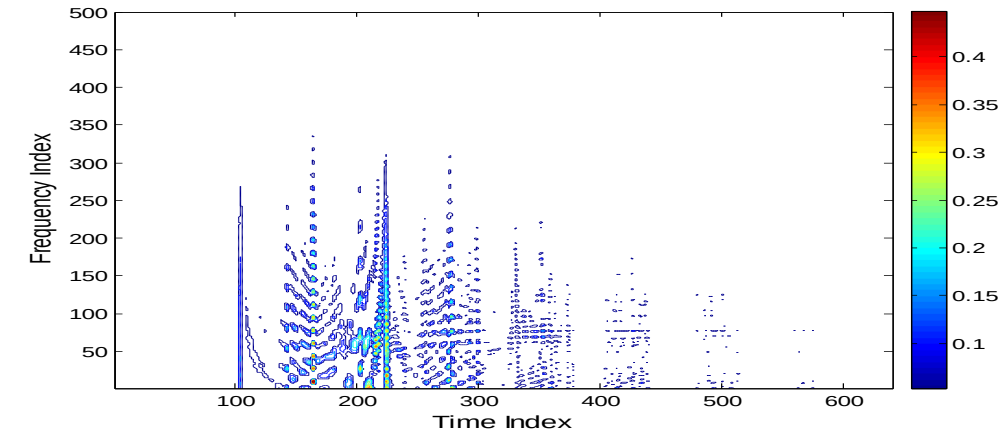

(b)

Figure 3.20 Contour plots of modified auto-Wigner distributions for the target Tdie5 at (a) θ=90º, (b) θ=135º aspect angles.

Afterwards, energy density vectors are computed as described in Section 2.2.1 over Q=16 non-overlapping late-time intervals. Then using these vectors, an optimal late-time interval is determined to construct Late Time Features Vectors (LTFVs) by the help of CCF values. In Figure 3.21, CCF values are plotted against q* for the target set CLDIE1 by using noise-free reference data. It can be seen in this figure that the values of CCF has a maximum at q* = 12, so we choose the combination of time bands q=11 and q=12 as the optimum late-time interval for this WD-PCA based classifier design. This late-time interval corresponds to [16.8, 20.1] nsec in the noise-free design case. The resulting classifier produces a correct decision rate of 100% for testing SNR levels as low as 15 dB, given 90% accuracy for 10 dB SNR level and finally its accuracy drops to 69% at 5 dB SNR. These values are tabulated in Table 3.6.

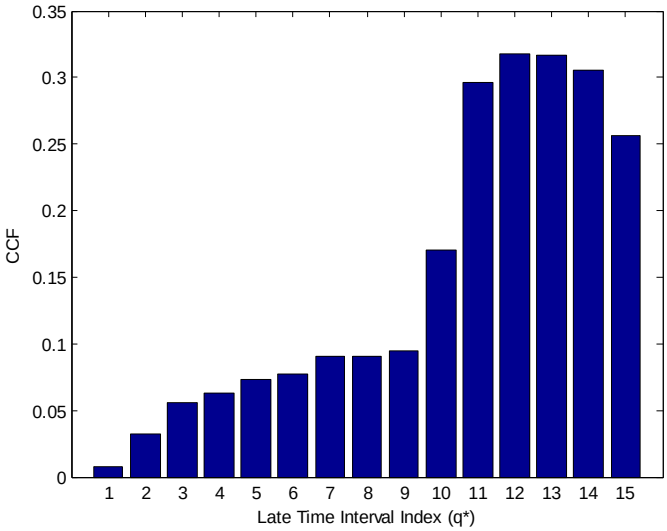

Figure 3.21 CCF values plotted against q* to determine the optimal late-time design interval for the target library CLDIE1 by using noise-free reference data.

3.3.2.2 Classifier design with noisy reference data

In this section, another classifier is designed for the same target library CLDIE1 using the WD-PCA based method, but this time, using reference data at 20 dB SNR level. Also in this classifier, same design steps which are outlined in section 3.2.2.1, are performed. CCF values are plotted in Figure 3.22 against q* to determine the optimal late-time design interval.

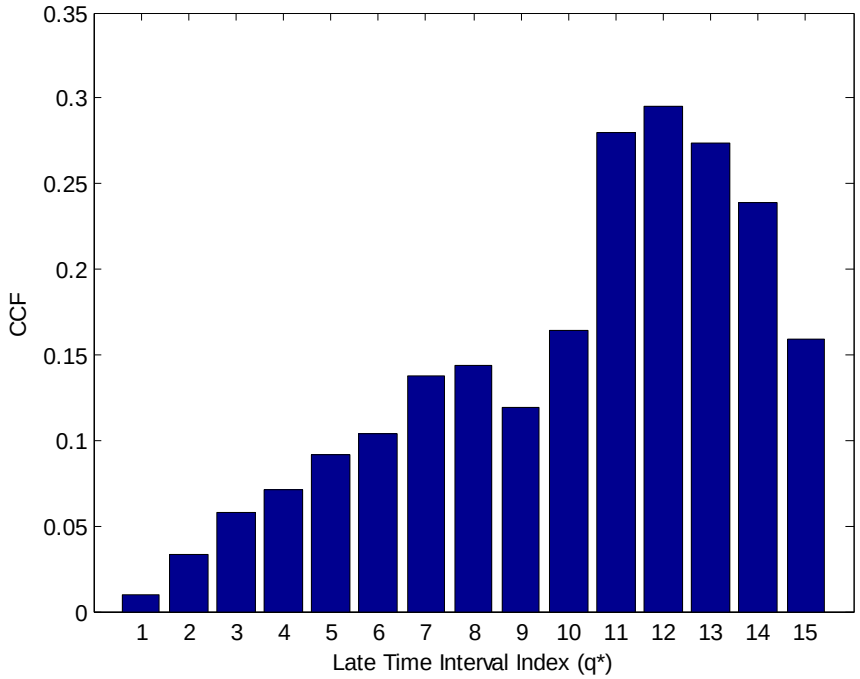

Figure 3.22 CCF values plotted against q* to determine the optimal late-time design interval for the target set of CLDIE1 by using slightly noisy reference data at 20dB SNR level.

For this noisy classifier design, the optimum late-time design interval is chosen to be composed of time bands q=11 and q=12 which corresponds to [16.8, 20.1] nsec. It is the same late-time interval used for the noise-free classifier design. As an example, the extracted late-time feature vectors (LTFV) of the target Tdie3 (ε=4), at the reference aspect angles θ = 15º, 45º,

90º, 135º, 179º for 20 dB SNR level (extracted over this optimum late time interval) are plotted in Figure 3.23.

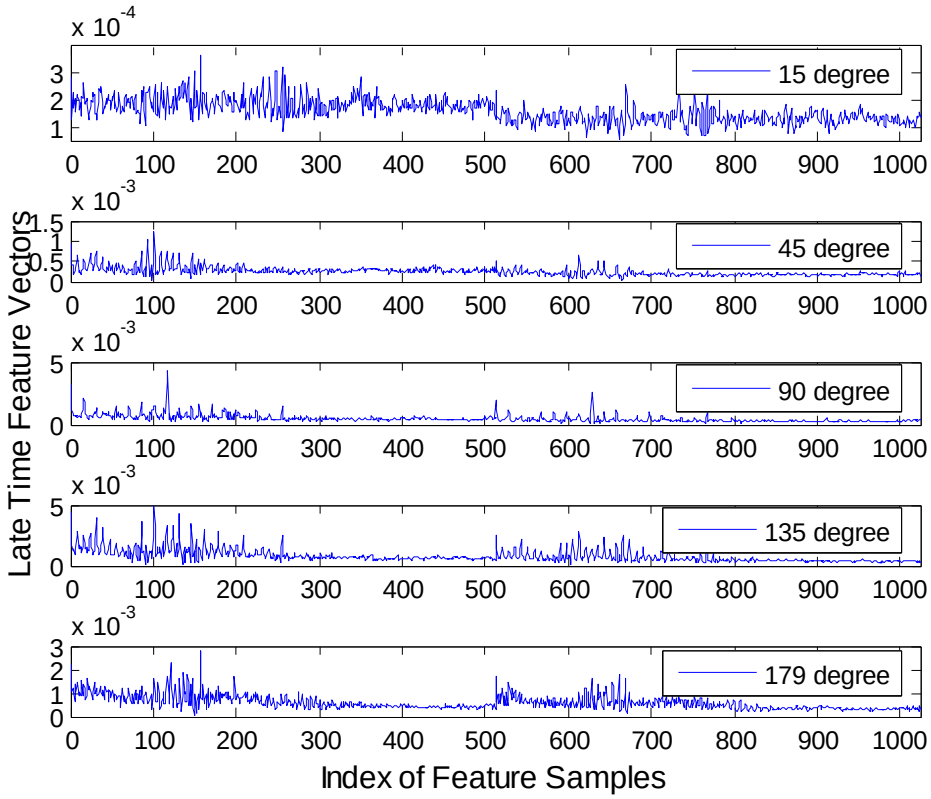

Figure 3.23 LTFVs of target Tdie3(ε=4) at the reference aspect angles θ = 15º, 45º, 90º, 135º, 179º for 20 dB SNR level

For each target, the principal component analysis is applied to obtain its FFV from aspect dependent LTFVs. The eigenvalues obtained during the PCA process are listed in Table 3.5 for each library target. The largest eigenvalue (λ1) is much more dominant than the other eigenvalues λ2 through λ5. So we can use the leading principal component z1 by itself as the FFV of the associated target. The resulting Fused Feature Vectors (FFVs) are plotted in Figure 3.24 together with the LTFV of a test signal belonging to the Tdie1 at θ=105 aspect angle at 20 dB SNR level.

Table 3.5 Eigenvalues computed during the PCA process while designing the WD-PCA based classifier for the target library CLDIE1 at 20 dB SNR level.

	Tdie1(ε=3)	Tdie3(ε=4)	Tdie5(ε=5)	Tdie7(ε=6)
λ1	2,0267e-7	5,3629e-7	1,5129e-6	2,6976e-6
λ2	2,3183e-8	6,1180e-8	2,9106e-7	4,1227e-7
λ3	1,4627e-8	4,6943e-8	7,9363e-8	1,3631e-7
λ4	6,8581e-10	3,4675e-9	1,3265e-8	2,3260e-8
λ5	1,8017e-10	5,9578e-10	2,4507e-9	2,0492e-9

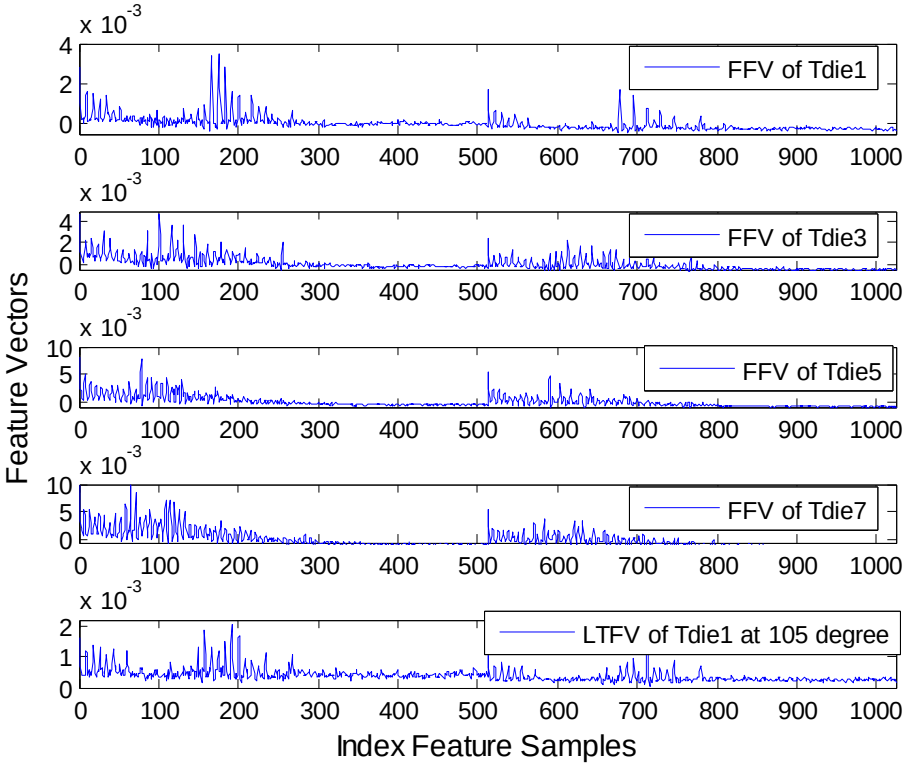

Figure 3.24 FFVs of all targets for the classifier designed at 20 dB using target library CLDIE1 and a LTFV of the test signal belonging to the target Tdie1 (ε=3) at θ=105 aspect angle at 20dB SNR level.

Finally, this classifier is tested against all available test data at the SNR levels of infinity, 20 dB, 15 dB, 10 dB, 5 dB. The correct classification rate turns out to be perfect (100%) for SNR levels as low as 15 dB, it is 92% at 10 dB and decreases to 71% 5 dB SNR level.

3.3.3 Discussion of Classifier Performance Results for Dielectric Spheres

In this subsection, usefulness of target classifiers designed to discriminate dielectric spheres by the MUSIC algorithm based technique and by the WD-PCA based technique will be compared. Our comparisons will be based on the contents of Table 3.6 and Table 3.7.

First of all, in noise-free design case, performance of the WD-PCA based classifier is highly superior to the performance of the MUSIC based classifier. As the SNR level of test signals is reduced from infinity to 5 dB, accuracy rate of the WD-PCA based classifier drops from 100% to 69% while the accuracy rate of the MUSIC based classifier decreases from 92% to 35%.

Secondly, use of slightly noisy reference data in classifier design improves the performances of both classifier design techniques. While the improvement is slight in the WD-PCA classifier, a large improvement is observed in the performance of the MUSIC algorithm based classifier. However, despite this prominent improvement in the MUSIC based technique, performance of the WD-PCA based classifier still looks much better, by about 20% difference in correct decision rates. In both noise-free design and noisy design, the resulting WD-PCA based classifiers give 100% accuracy at overall SNR levels as low as 15 dB. This rate stays around 90% at 10 dB testing SNR and finally drops to about 70% at the very noisy case of 5 dB SNR. Also, performance of the WD-PCA classifier does not get worse

when it is designed at 20 dB SNR level but tested with noise-free data. Performance of the MUSIC based classifier, however, is badly affected under the same conditions. Accuracy rate of the MUSIC based algorithm drops from 92% to 79% at noise-free testing depending upon the SNR level used in the design phase.

Also, we can compare the usefulness of MUSIC based and WD-PCA based classifier design techniques regarding the number of library targets that they can handle. Based on the accuracy rates tabulated in Table 3.7, it can be concluded that the WD-PCA based classifiers designed for the target libraries CLDIE1 and CLDIE2 with 4 and 8 dielectric spheres, respectively, have about 10% better accuracy as compared to the MUSIC based classifiers at this noise-free design/noise-free test case.

Table 3.6 Correct Decision Rates of the classifier designed for the target library CLDIE1 using either noise-free data or 20 dB data.

SNR Levels	5dB	10dB	15dB	20dB	Noise Free
MUSIC method (20dB Ref)	51	69	81	86	79
WD/PCA method (20dB Ref)	71	92	100	100	100
MUSIC method (N. Free Ref)	35	43	56	82	92
WD/PCA method (N. Free Ref)	69	90	100	100	100

Table 3.7 Correct Decision Rates of MUSIC algorithm based and WD-PCA based classifiers for target libraries CLDIE1 and CLDIE2 for the noise-free design/noise-free test case.

Target Library	CLDIE1 (4 targets)	CLDIE2 (8 targets)
MUSIC method	92	89
WD/PCA method	100	100

3.4 Classifier Design for Dielectric Coated Conducting Spheres

In this chapter, we will present design simulations and the results of performance tests for classifiers which have dielectric coated conducting spheres as their library targets. These spheres have exactly the same external size but different values of coating permittivities and different sizes for the inner conducting spheres. All dielectric coated conducting spheres has the same outer radii of r=10 cm. Physical properties of 15 different targets Tcoa1 through Tcoa15 are described in Table 3.8. Also, five different target libraries of dielectric coated conducting spheres called CLCOA1, CLCOA2, CLCOA3, CLCOA4 and CLCOA5 are defined in this table. In this section, classifiers are designed with noise-free reference data for all these target libraries and they are tested under noise-free conditions. Also, four different classifiers will be designed the for target library CLCOA3 to compare the noise performances of MUSIC based and WD-PCA based electromagnetic target classifier design techniques.

Table 3.8 Descriptions of 15 different targets and 5 different target libraries of dielectric coated conducting spheres. In this table, r_{in} is the radius of inner conducting sphere in cm and ε is the relative permittivity of the dielectric coating. All targets have the same outer radius of 10 cm.

Target Library	Targets
CLCOA1	Tcoa1(r_{in}=2 ε =3), Tcoa4(r_{in}=4 ε =3), Tcoa7(r_{in}=7 ε =3), Tcoa10(r_{in}=8 ε =3), Tcoa13(r_{in}=9ε =3).
CLCOA2	Tcoa1(r_{in}=2 ε =5), Tcoa4(r_{in}=4 ε =5), Tcoa7(r_{in}=7 ε =5), Tcoa10(r_{in}=8 ε =5), Tcoa13(r_{in}=9ε =5).
CLCOA3	Tcoa1(r_{in}=2 ε =7), Tcoa4(r_{in}=4 ε =7), Tcoa7(r_{in}=7 ε =7), Tcoa10(r_{in}=8 ε =7), Tcoa13(r_{in}=9ε =7).
CLCOA4	Tcoa1(r_{in}=2 ε =3), Tcoa2(r_{in}=2 ε =5), Tcoa3(r_{in}=2 ε =7), Tcoa4(r_{in}=4 ε =3), Tcoa5(r_{in}=4 ε =5), Tcoa6(r_{in}=4 ε =7),
CLCOA5	Tcoa7(r_{in}=7 ε =3), Tcoa8(r_{in}=7 ε =5), Tcoa9(r_{in}=7 ε =7), Tcoa10(r_{in}=8 ε =3), Tcoa11(r_{in}=8 ε =5), Tcoa12(r_{in}=8 ε =7), Tcoa13(r_{in}=9ε =3), Tcoa14(r_{in}=9 ε =5), Tcoa15(r_{in}=9 ε =7).

3.4.1 Classifier Design Simulations for Dielectric Coated Conducting Spheres Using the MUSIC Algorithm Based Method

In this section, MUSIC algorithm based classifiers are designed for target libraries CLCOA1, CLCOA2, CLCOA3, CLCOA4 and CLCOA5 using noise-free reference data and also another classifier is designed for the target library CLCOA3 using a slightly noisy reference data set at 20 dB SNR level.

3.4.1.1 Classifier design with noise-free reference data

All the design steps used in this simulation are the same as those outlined in section 3.2.1.1. The design parameters of the MUSIC algorithm based classifiers for all target libraries are chosen as N= 128, m= 64 and L= 32. Using these design parameters and noise-free reference data for design, the optimum late-time design intervals for the target libraries CLCOA1, CLCOA2, CLCOA3, CLCOA4 and CLCOA5 are obtained as [16.8, 20.1] nsec, [16.8, 20.1] nsec, [14.2, 17.6] nsec, [19.2, 22.6] nsec and [16.8, 20.1] nsec, respectively. As an example, the r_{total} values computed for each time subinterval for the target library CLCOA5 are shown in Figure 3.25. It can be seen in this figure that r_{total} has a maximum at q=11. So, we choose the corresponding time band [16.8, 20.1] nsec as the optimum late time interval for classifier design for the library CLCOA5.

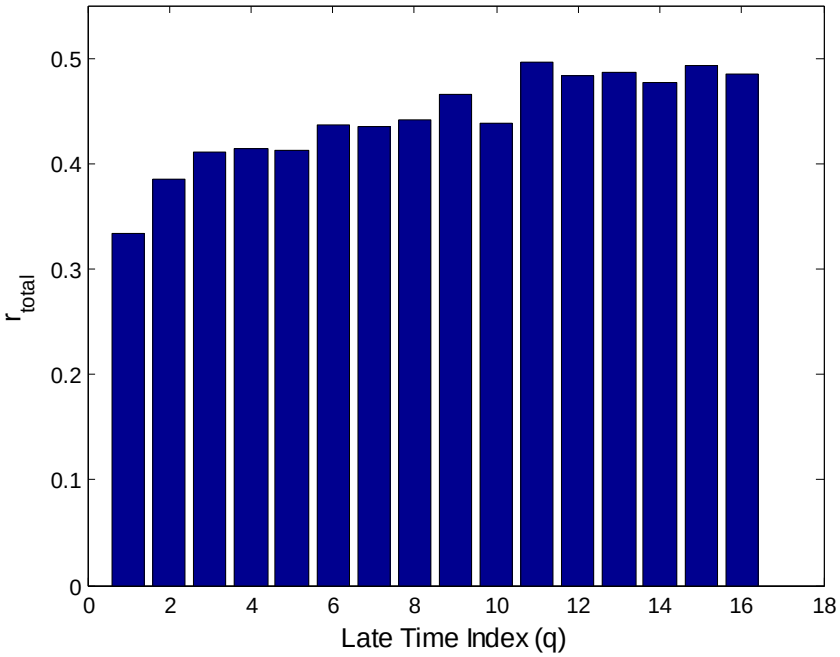

Figure 3.25 The r_{total} values computed for the classifier designs for target libraries CLCOA5 in the noise free case.

After choosing the optimum late-time interval for a given target library, the feature database is formed by the FMSM features of each target in that library. Then, correlation coefficients between the FMSMs of all library targets and the MSMs of all available test signals are computed to obtain the accuracy rate of that specific classifier. These steps are repeated for each target library shown in Table 3.8 to compare the noise-free design/noise-free test simulations. As an example, a plot of matched and mismatched correlation coefficients for the CLCOA3 classifier is plotted in Figure 3.26 for 60 test signals. It can be seen in this figure that MUSIC algorithm based classifier for the target set CLCOA3 makes only two mistakes. Therefore, correct classification rate of this classifier with MUSIC algorithm method at noise-free design/noise-free test case is equal to 96.7%. Both of these mistakes are related to the discrimination of the target Tcoa4 only. Also, based on Figure 3.26, we can say that discrimination of dielectric coated conducting spheres becomes easier as the radius of inner conducting sphere gets larger.

This classifier designed for the target set CLCOA3 (using noise-free reference data) is also tested at the SNR levels of 20 dB, 15 dB, 10 dB and 5 dB. Unfortunately, the accuracy rate of the classifier drops under 30% as the SNR level of test signals decreases to 5 dB. Correct classification rate of this classifier at various SNR levels are given in Table 3.10 and Table 3.11 in section 3.4.3.

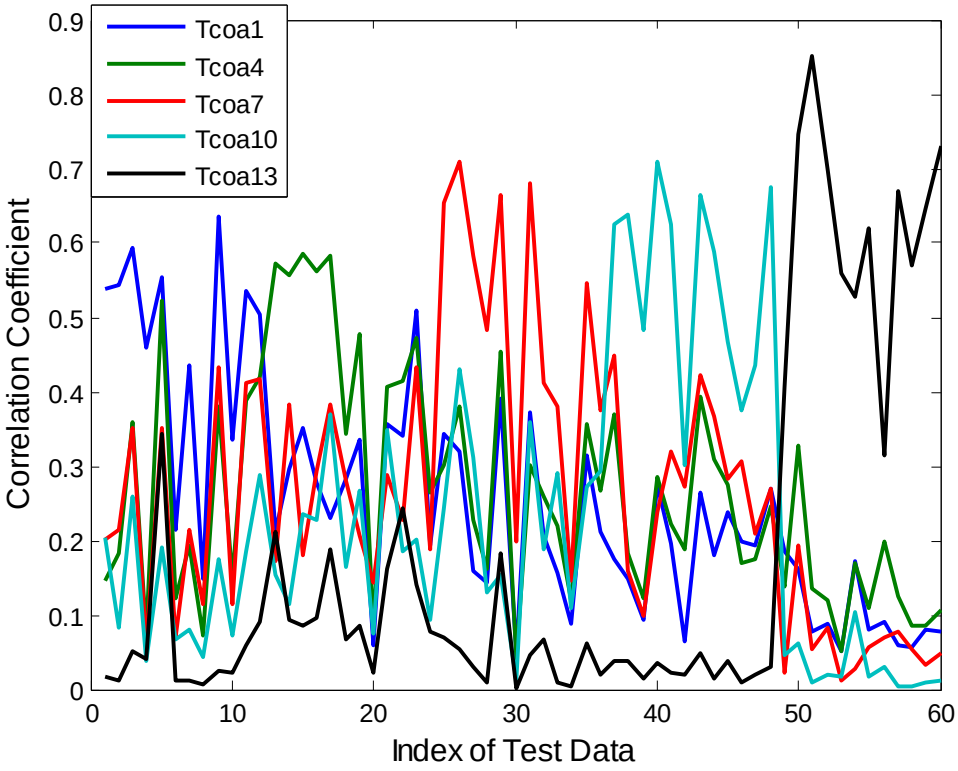

Figure 3.26 Correlation coefficients computed between the FMSMs of all library targets and the MSMs of all test signals for the classifier designed for the library CLCOA3 in noise-free design/noise-free test case.

3.4.1.2 Classifier design with noisy reference data

In this subsection, a MUSIC algorithm based classifier is designed for the target library CLCOA3 using a set of slightly noisy reference data at 20 dB SNR level. Design parameters of this classifier are the same as the design parameters used in section 3.4.1.1 (N= 128, m= 64 and L= 32). The optimum late-time design interval for this classifier is determined to be [6.7, 10.0] nsec which is an earlier interval as compared to one determined for the classifier designed in section 3.4.1.1. As also observed in the design of classifiers for conducting spheres and dielectric spheres in sections 3.2 and 3.3, the

optimal late-time design interval shifts to earlier times when we use noisy reference data instead of noise-free reference data for design. These time shifts becomes more pronounced when the targets are low-Q structures such as conducting spheres or coated conducting spheres with large inner conducting parts. As example to the scattered signal database of the CLCOA3 library, the scattered response of the target Tcoa7 at θ=60 degrees aspect angle with 20 dB SNR level is plotted in Figure 3.27.

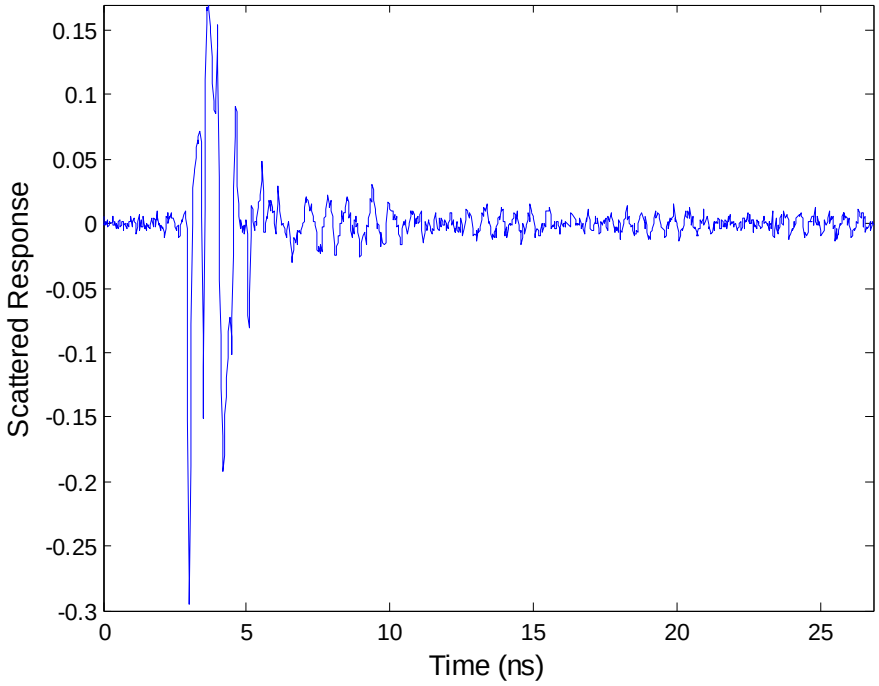

Figure 3.27 Scattered response of the target Tcoa7 observed at θ=60 degrees aspect angle at 20 dB SNR level.

FMSMs for each target of this CLCOA3 library are computed over the optimal late-time interval [6.7, 10.0] nsec and stored in the feature database of the resulting classifier. The FMSMs of library targets and the MSM feature of a

test signal (which belongs to Tcoa10 at θ=135º at 20 dB SNR level) are shown in Figure 3.28. It can be seen in this figure that MSM map of the target Tcoa10 (shown in Figure 3.28 (f)) is highly correlated with its matched FMSM feature(shown in Figure 3.28 (d)), as expected. The accuracy rate computed for this classifier is observed to be decreasing form %82 to %60 as the SNR level of test signals decreases from 20 dB to 5 dB. Therefore, we can conclude that noise performance of the MUSIC algorithm based technique has been highly improved by using slightly noisy data at 20 dB SNR level in the classifier design process.

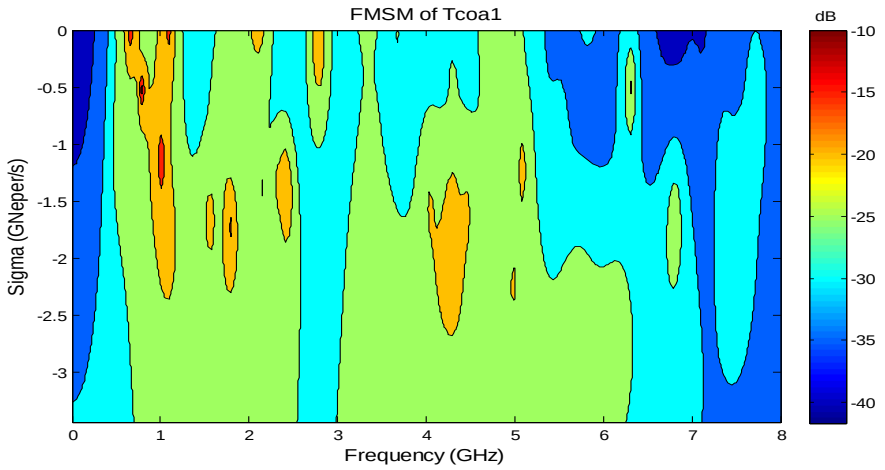

(a)

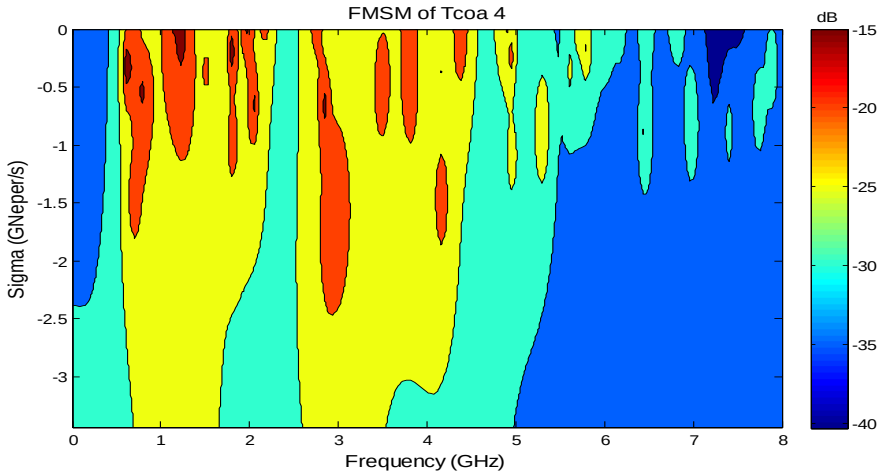

(b)

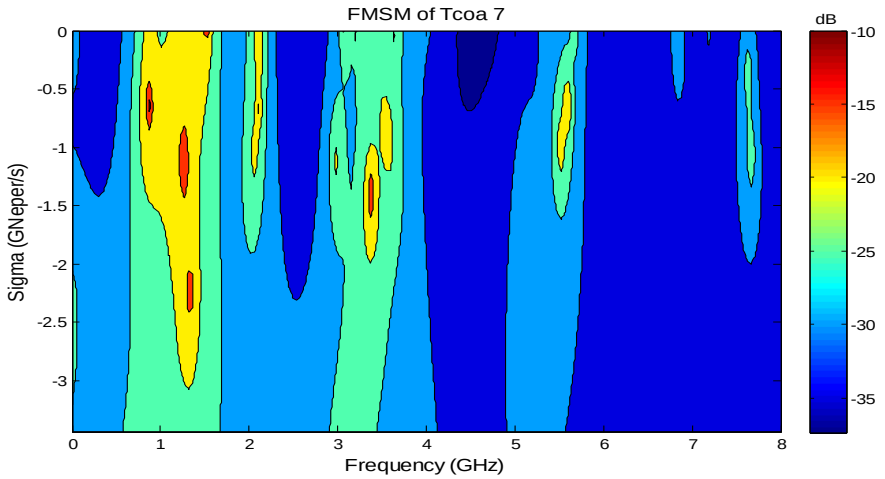
FMSM of Tcoa 7
Sigma (GNeper/s)
Frequency (GHz)
dB

(c)

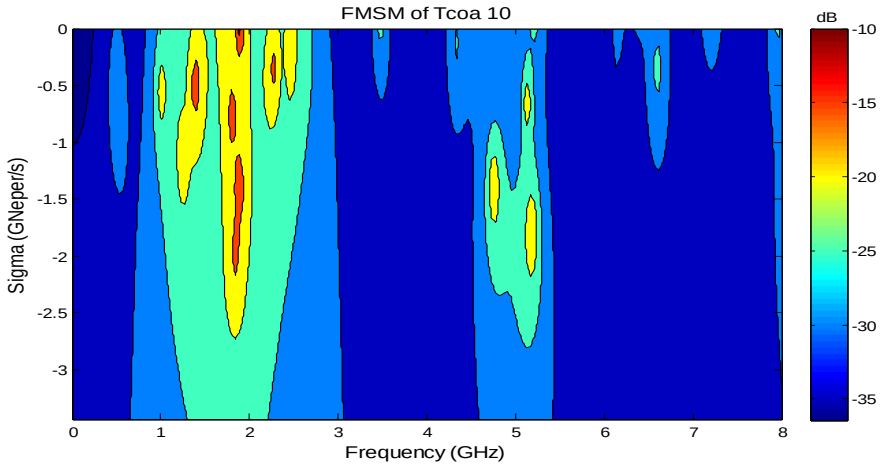
FMSM of Tcoa 10
Sigma (GNeper/s)
Frequency (GHz)
dB

(d)

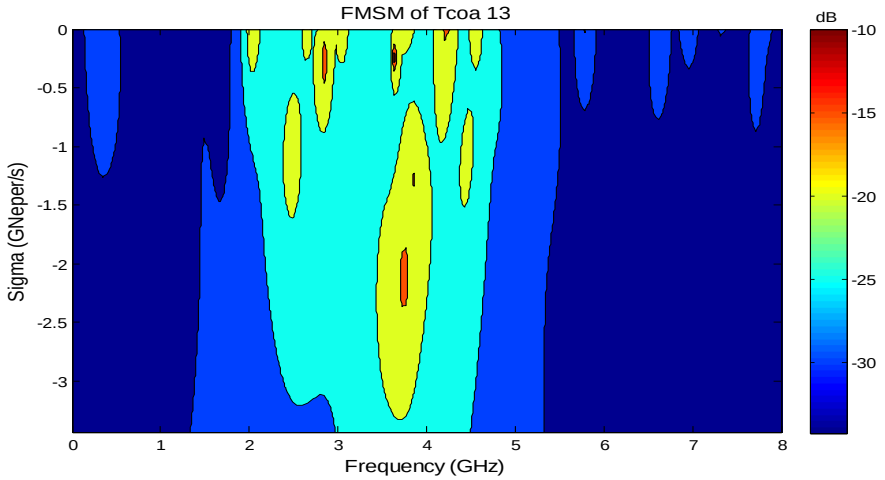
FMSM of Tcoa 13
Sigma (GNeper/s)
Frequency (GHz)
dB

(e)

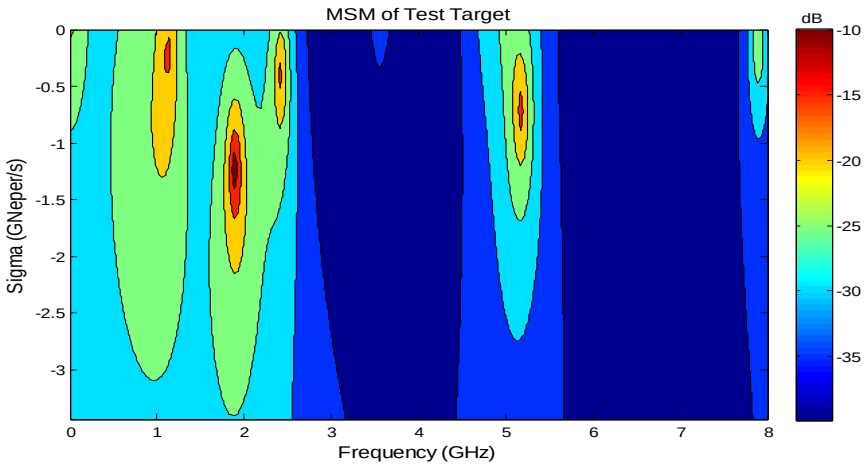

(f)

Figure 3.28 (a)-(e) The FMSM features of the dielectric coated conducting spheres Tcoa1, Tcoa4, Tcoa7, Tcoa10 and Tcoa13 for the classifier designed for the target library CLCOA3 at 20 dB SNR level, (f) the MSM feature of a test signal (belonging to the target Tcoa10 at θ=135 degree aspect angle at 20 dB SNR level)

3.4.2 Classifier Design Simulations for dielectric Coated Conducting Spheres Using the WD-PCA Based Method

In this section, WD-PCA method based classifiers are designed for the target library CLCOA3, firstly using noise-free reference data and then using slightly noisy reference data at 20 dB SNR level. Earlier, WD-PCA based target classifiers were designed for all the target libraries shown in Table 3.8 by M. Ayar [35] using noise-free reference data. So, we will not repeat the same classifier designs for the target libraries CLCOA1, CLCAO2, CLCOA4 and CLCOA5 (i.e. except the CLCOA3 library) but use his results for comparisons whenever needed.

3.4.2.1 Classifier design with noise-free reference data

In this section, we design a WD-PCA based classifier using noise-free reference signals for the target library CLCOA3 and test the resulting classifier at SNR levels of 20 dB, 15 dB, 10 dB, 5 dB and also at infinite SNR level.

The first step of the design was again the computation of the auto-WD matrix of the reference scattered signals at N=1024 sample points. Contour plots of the modified auto-WD matrices obtained for the target Tcoa7 at θ=45º, 105º and 179º degrees are given below in Figure 3.29.

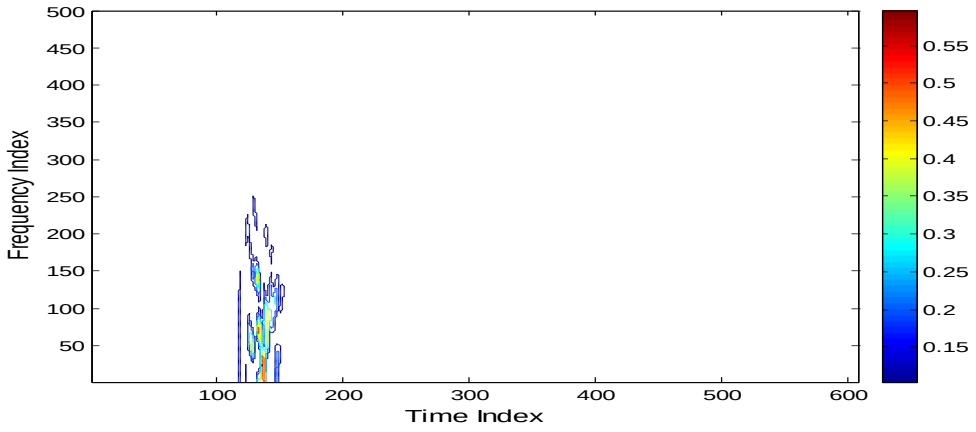

(a)

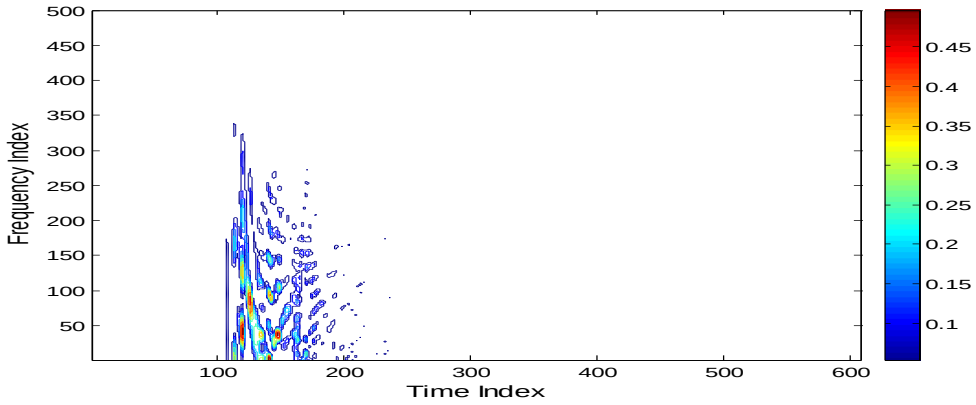

(b)

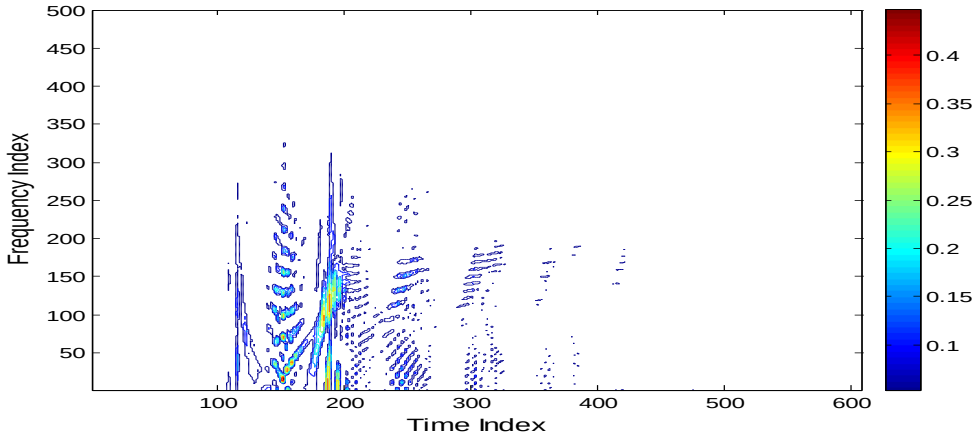

(c)

Figure 3.29 Contour plots of modified auto-Wigner distributions for target responses belonging to Tcoa7 at aspect angles (a) θ=45º (b) θ=105º and (c) θ=179º.

Afterwards, energy density vectors are computed as described in Section 2.2.1 using these auto-Wigner distributions over Q=16 non-overlapping late-time intervals. Then using these vectors, an optimal late-time interval is determined. For this purpose, the CCF values are plotted against q* for q*= 1,2,…,Q-1 for the target library CLCOA3 in this case of noise-free classifier design. By the help of manual fine tuning tests in addition to the computed CCF values, we choose the time bands q=11 and q=12 to construct the optimum late-time interval in this design. The resulting optimal late-time design interval corresponds to [16.8, 20.1] nsec.

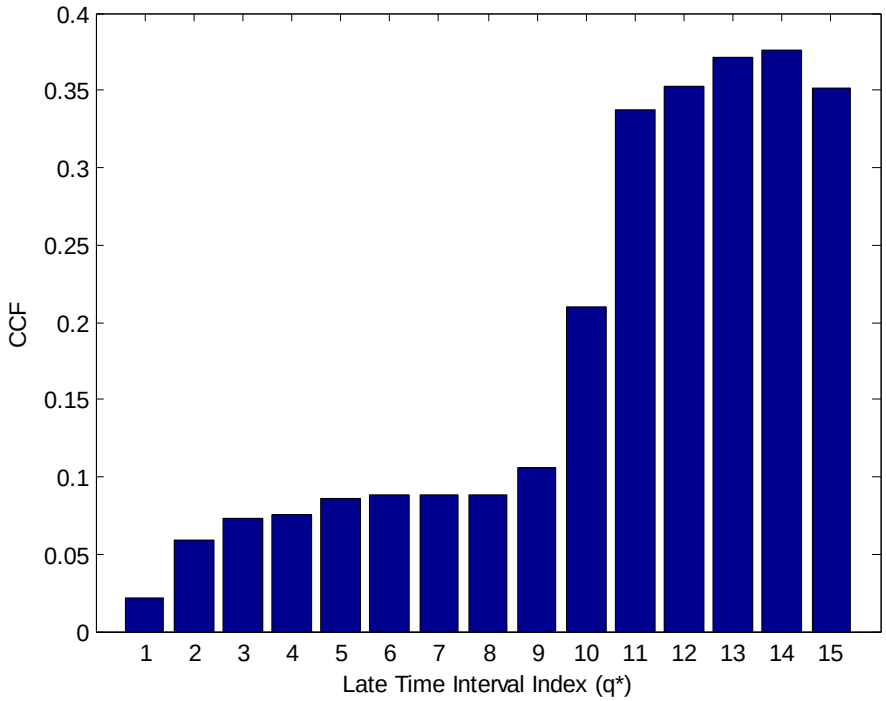

Figure 3.30 CCF values plotted against the late-time index q* to determine the optimal late-time design interval for target library CLCOA3 in the case of noise-free classifier design.

3.4.2.2 Classifier design with noisy reference data

In this section, another classifier is designed for the same target library CLCOA3 using the WD-PCA based method, but this time, using noisy reference data at 20 dB SNR level. Also for this classifier the Q value is selected to be 16. Then, CCF values are plotted in Figure 3.31and are used to determine the optimal late-time design interval which turns out to be [16.8, 20.1] nsec spanning the late-time intervals with indices q=11 and q=12.

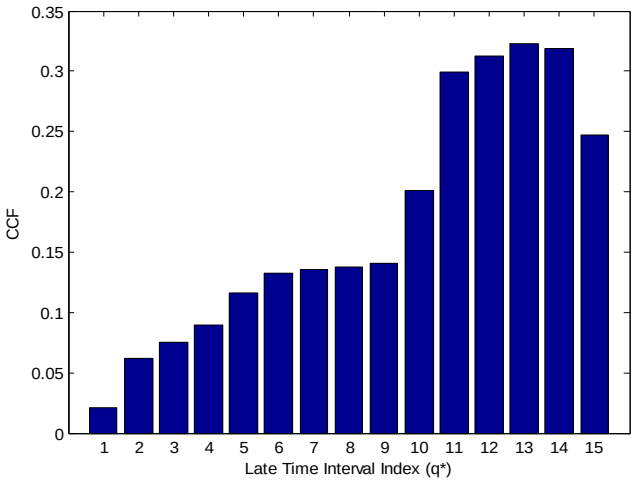

Figure 3.31 CCF values plotted against the late-time index q* to determine the optimal late-time design interval for target library CLCOA3 in the case of classifier design using noisy reference data at 20 dB SNR level.

As an example, extracted late-time feature vectors (LTFV) of the target Tcoa7, at the reference aspect angles θ = 15º, 45º, 90º, 135º, 179º at 20 dB SNR level over this optimum late time window are plotted in Figure 3.32.

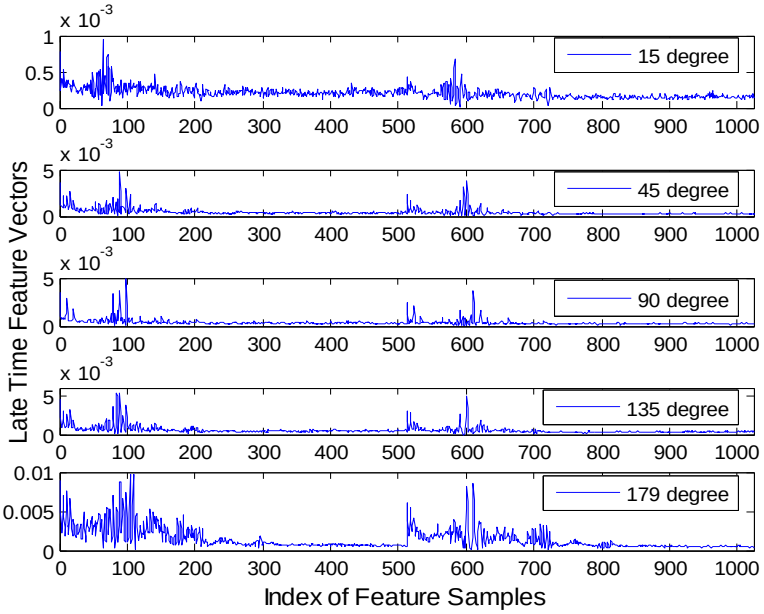

Figure 3.32 LTFVs of target Tcoa7 at the reference aspects θ = 15º, 45º, 90º, 135º, 179º for 20 dB SNR level.

For each target, the principal component analysis is applied to obtain its FFV from aspect dependent LTFVs at reference aspect angles. The eigenvalues obtained during the PCA process are listed in Table 3.9 for each library target. As seen in this table the largest eigenvalue (λ1) is much more dominant than the others. Therefore, the leading principal component z_1 can be used as the FFV of the associated target as mentioned before.

Table 3.9 Eigenvalues computed during the PCA process while designing the WD-PCA based classifier for the target library CLCOA3 at 20 dB SNR level.

	Tcoa1	Tcoa4	Tcoa7	Tcoa10	Tcoa13
λ1	1,5300e-6	3,0928e-6	2,1287e-6	7,9718e-7	4,1854e-7
λ2	2,8152e-7	5,8487e-7	1,7918e-7	2,3495e-8	1,3869e-8
λ3	1,4049e-7	1,6614e-7	6,3879e-8	8,8712e-9	4,7901e-9
λ4	7,2332e-8	9,6526e-8	4,3588e-8	3,4737e-9	1,5289e-9
λ5	6,9499e-9	1,3903e-8	5,6950e-9	1,8870e-9	9,2848e-10

The resulting Fused Feature Vectors (FFVs) of the target library CLCOA3 and LTFV of a test signal which belongs to the target Tcoa7 at θ=165 degree aspect angle at 20dB SNR level, are given altogether in Figure 3.33. It can be seen in this figure that LTFV of the test target Tcoa7 is more closely correlated to its matched FFV, as expected.

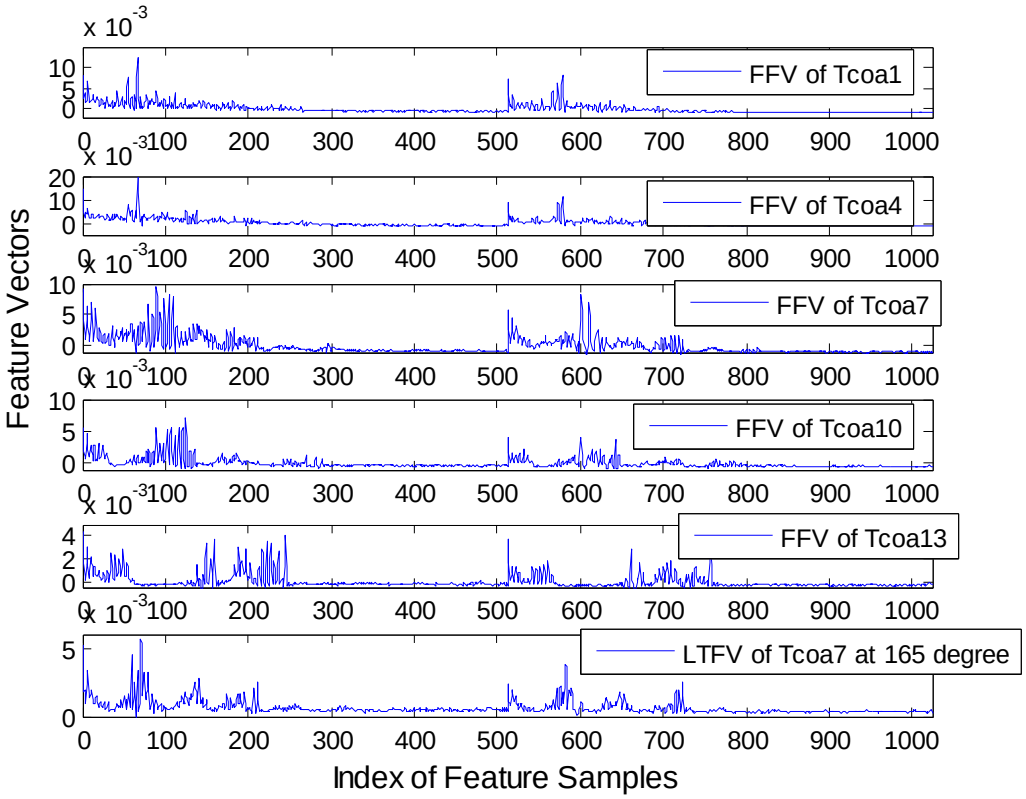

Figure 3.33 FFVs of all targets from the classifier designed at 20 dB using target library CLCOA3 and LTFV of the test target Tcoa7 at θ=165 degree aspect angle at 20dB SNR level.

Finally, this classifier is tested against all available test data at the SNR levels of infinity, 20 dB, 15 dB, 10 dB, 5 dB with accuracy rates changing from 98% to 75%. The results are given in the next section altogether.

3.4.3 Discussion of Classifier Performance Results for Dielectric Coated Conducting Spheres

In this section, performance results of all target classifiers designed for dielectric coated conducting spheres are discussed.

In general, we can see in Table 3.10 that the WD-PCA based classifiers display much better accuracy than the MUSIC algorithm based classifiers in both cases of design with noise-free reference data and design with slightly noisy reference data at 20 dB. Noise performances of both methods, especially the MUSIC algorithm based method, can be improved when the classifiers are designed using a slightly noisy set of reference data. General tendency of the accuracy rates listed in Table 3.10 looks very similar to the one displayed in Table 3.6 of section 3.3.3. Therefore, the conclusions drawn for the noise performance of the MUSIC based and the WD-PCA based classifiers in discriminating dielectric spheres are also valid in the case of classifying the dielectric coated conducting spheres.

Table 3.10 Correct Decision Rates of CLCOA3 target library using either noise-free data or 20 dB data.

SNR Levels	5dB	10dB	15dB	20dB	Noise Free
MUSIC method (20dB Ref)	60	69	77	82	75
WD/PCA method (20dB Ref)	75	85	93	95	98
MUSIC method (N. Free Ref)	27	40	57	72	97
WD/PCA method (N. Free Ref)	73	82	95	95	98

Correct decision rates of classifiers designed for the target libraries CLCOA1, CLCOA2, CLCOA3, CLCOA4 and CLCOA5 by using both the MUSIC based and the WD-PCA based design techniques are listed in Table 3.11 for the noise-free design/noise-free test case. Based on these test results, it can be concluded that better accuracy rates are obtained for larger relative permittivity (ε) values used for coating. When this ε value gets smaller, discrimination of dielectric coated conducting spheres becomes more difficult where the targets are different from each other only in terms of their inner radii. Moreover, most of the wrong decisions made by the classifiers for target libraries CLCOA1, CLCOA2 and CLCOA3 happen for targets with smaller inner radii (r=2 and r=4). We can also confirm these conclusions by comparing the accuracy rate results of the classifiers for target libraries CLCOA4 and CLCOA5. In other words, recognition of targets with smaller radius of conducting inner sphere is much more difficult than the recognition of dielectric coated conducting spheres with larger r_{in} parameters. The WD-PCA based classifier looks more successful than the MUSIC based classifier in this challenging case. The results tabulated in Table 3.11 are not conclusive to make a decision about the usefulness of each design method when the number of targets gets larger.

As mentioned before, results of the WD-PCA classifiers for the target libraries CLCOA1, CLCOA2, CLCOA4 and CLCOA5 using noise free design are taken from M. Ayar thesis [35] for comparisons.

Table 3.11 Correct Decision Rates of MUSIC algorithm based and WD-PCA based classifiers for various target libraries in the noise-free design/noise-free test case.

Target Library	CLCOA1 ε=3 r=2,4,7,8,9 (5 targets)	CLCOA2 ε=5 r=2,4,7,8,9 (5 targets)	CLCOA3 ε=7 r=2,4,7,8,9 (5 targets)	CLCOA4 ε=3,5,7 r=2,4 (6 targets)	CLCOA5 ε=3,5,7 r=7,8,9 (9 targets)
MUSIC based classifier	70	85	97	69	91
WD/PCA based classifier [35]	65	92	98	77	86

3.5 Classifier Design for a Mixed Spherical Target Library

In this section, the MUSIC based and WD-PCA based classifiers are designed for a target library which includes a total of 27 targets; three dielectric spheres, nine conducting spheres and fifteen dielectric coated conducting spheres as described in Table 3.12.

Table 3.12 Description of targets for the library CLMIX.

Target Library	Targets
CLMIX	Tdie1(ε=3), Tdie5(ε=5), Tdie8(ε=7), Tcon1(r=8cm), Tcon2(r=8.5cm), Tcon3(r=9cm), Tcon4(r=9.5cm), Tcon5(r=10cm), Tcon6(r=10.5cm), Tcon7(r=11cm), Tcon8(r=11.5cm), Tcon9(r=12cm), Tcoa1(r_{in}=2cm ε=3), Tcoa2(r_{in}=2cm ε=5), Tcoa3(r_{in}=2cm ε=7), Tcoa4(r_{in}=4cm ε=3), Tcoa5(r_{in}=4cm ε=5), Tcoa6(r_{in}=4cm ε=7), Tcoa7(r_{in}=7cm ε=3), Tcoa8(r_{in}=7cm ε=5), Tcoa9(r_{in}=7cm ε=7), Tcoa10(r_{in}=8cm ε=3), Tcoa11(r_{in}=8cm ε=5), Tcoa12(r_{in}=8cm ε=7), Tcoa13(r_{in}=9cm ε=3), Tcoa14(r_{in}=9cm ε=5), Tcoa15(r_{in}=9cm ε =7).

As mentioned earlier, conducting sphere is a very low-Q target whose natural response decays very quickly with time because of very high real parts of system poles. Therefore, the maximum normalized energy level of unity is attained at much earlier times for a conducting sphere as compared to a dielectric sphere or a dielectric coated conducting sphere of the similar overall size as shown in Figure 3.34. We can easily discriminate conducting spheres within such a mixed target library by using this fact, especially in noise-free tests.

The cumulative normalized energy curve $\bar{e}(t)$ associated with a scattered signal x(t) is defined as

$$\bar{e}_x(t) = \int_0^t \left|\bar{x}(\tau)\right|^2 d\tau \qquad (3.2)$$

where

$$\bar{x}(t) = \frac{x(t)}{\left[\int_0^{\infty} |x(\tau)|^2 \, d\tau\right]^{1/2}} \tag{3.3}$$

is the normalized scattered signal in time domain.

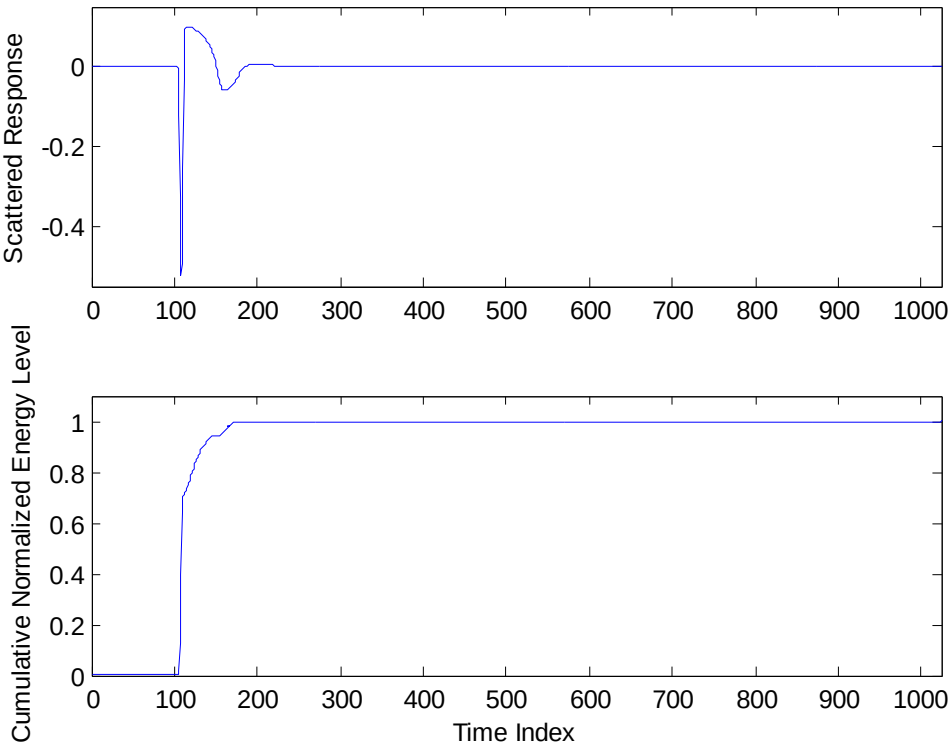

(a)

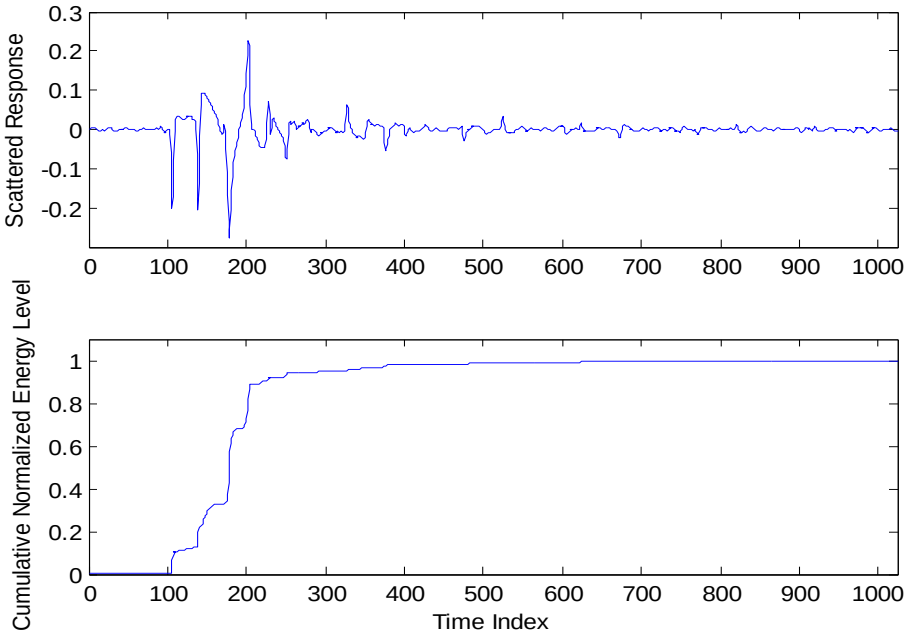

(b)

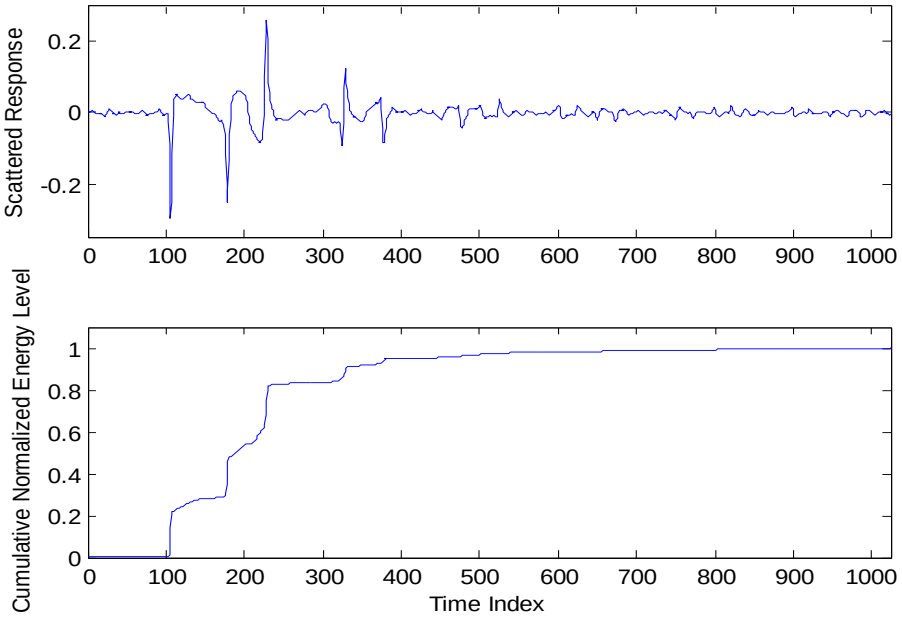

(c)

Figure 3.34 Scattered responses and their cumulative normalized energy curves for (a) Conducting sphere Tcon3 at 120º (b) Dielectric coated conducting sphere Tcoa5 at 120º (c) Dielectric sphere Tdie5 at 120º

To discriminate conducting spheres from the rest, we can determine a threshold value for the time index such that the normalized energy curves of conducting sphere targets of the library reaches to, let say 99% percent, of their maximum value (unity) before that critical time instant. In the classification simulations of this section, the threshold time index is chosen to be 400 out of 1024 time samples. If a given scattered test signal attains the 99.9 percent of its maximum normalized energy level before that threshold time index we can say with confidence that this scattered signal belongs to a conducting sphere. For classifying conducting spheres, we use a classifier which is the same as the classifier designed for the CLCON3 target library. For the other targets, a new classifier whose target library includes 3 dielectric spheres and 15 dielectric coated spheres (a total of 18 targets) is designed. In Figure 3.35, the CCF values are plotted against q* for this target set by using noise-free reference data. We choose the combination of time bands q=11 and q=12 as the optimum late-time interval for this WD-PCA based classifier design and also for WD-PCA based classifier design using noisy reference data. This late-time interval corresponds to [16.8, 20.1] nsec. We choose the optimum late-time intervals correspond to [14.3, 17.6] nsec, [8.6, 11.9] nsec in MUSIC algorithm based classifier design using noise-free reference data and using noisy reference data, respectively.

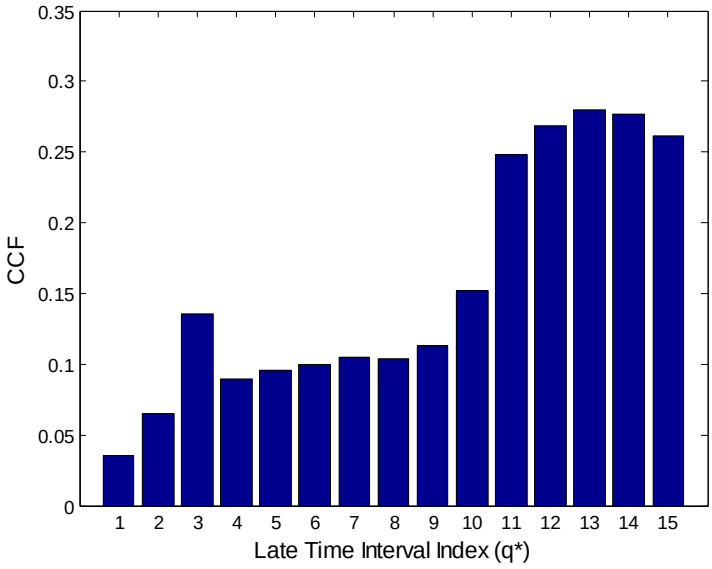

Figure 3.35 CCF values plotted against q* to determine the optimal late-time design interval for the target library CLMIX (excluding the perfectly conducting spheres) by using noise-free reference data

The accuracy rate of the resulting MUSIC based classifier for this CLMIX library is found to be 78% when the classifier is tested against noise-free data. The MATLAB code written to classify a given “unknown test signal” as one of the candidate targets is given in the Appendix. Out of 324 test cases (for 27 targets and 12 aspects we have 27x12=324 test signals), six of them are randomly chosen and the associated test results are given in Figure 3.36. The target indices shown in this figure refer to dielectric spheres and dielectric coated spheres (as the conducting spheres are discriminated at the beginning) of the CLMIX library. Target indices 1 through 18 correspond to targets Tdie1(ε=3), Tdie5(ε=5), Tdie8(ε=7), Tcoa1(r_{in}=2 ε=3), Tcoa2(r_{in}=2 ε=5), Tcoa3(r_{in}=2 ε=7), Tcoa4(r_{in}=4 ε=3), Tcoa5(r_{in}=4 ε=5), Tcoa6(r_{in}=4 ε=7), Tcoa7(r_{in}=7 ε=3), Tcoa8(r_{in}=7 ε=5), Tcoa9(r_{in}=7 ε=7), Tcoa10(r_{in}=8 ε=3), Tcoa11(r_{in}=8 ε=5), Tcoa12(r_{in}=8 ε=7), Tcoa13(r_{in}=9 ε=3), Tcoa14(r_{in}=9 ε=5) and Tcoa15(r_{in}=9 ε =7), respectively.

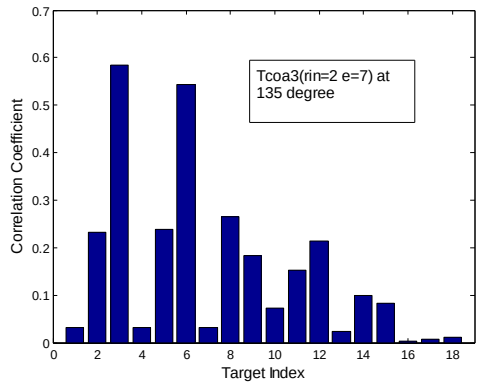

(a)

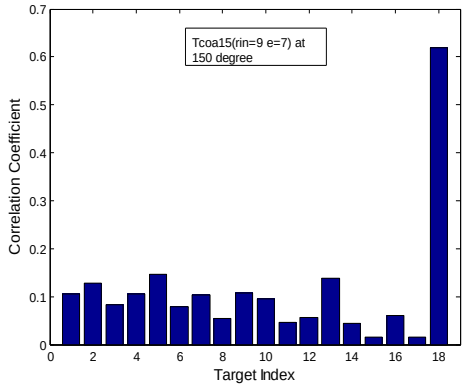

(b)

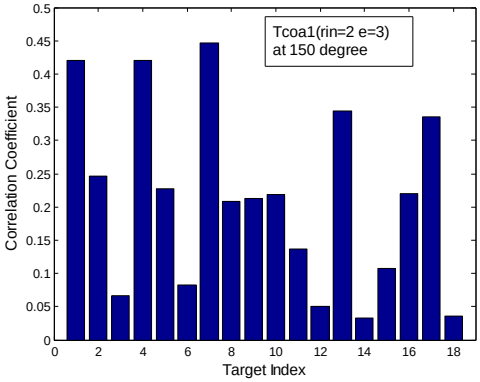

(c)

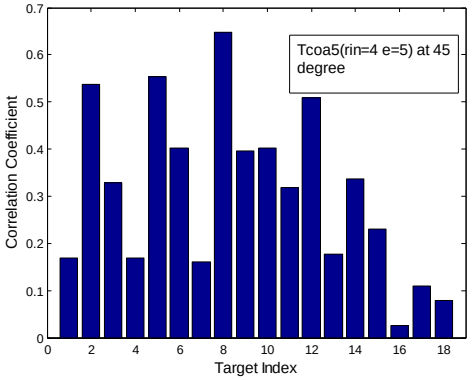

(d)

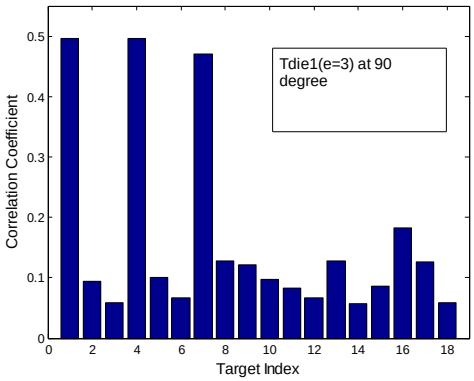

(e)

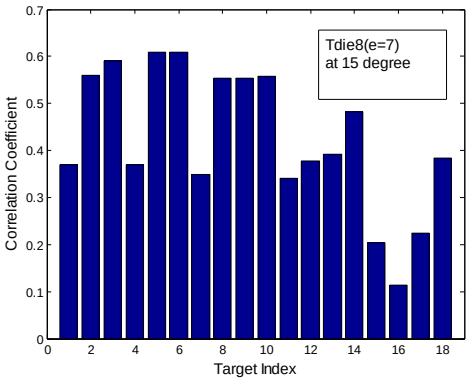

(f)

Figure 3.36 Classification Results for some randomly selected test signals when using the MUSIC algorithm based classifier in the noise-free design/noise-free test case (a) Tcoa3(rin=2cm ε=7) at 135º (b)

Tcoa15(rin=9cm ε=7) at 150º (c) Tcoa1(rin=2cm ε=3) at 150º (d) Tcoa5(rin=4cm ε=5) at 45º (e) Tdie1(ε=3) at 90º (f) Tdie8(ε=7) at 15º

In part (a) of this figure, we see the classification result of the target Tcoa3(r_{in}=2 ε=7) at 135º aspect angle. We expect to see the highest correlation coefficient at the sixth target index. However, classifier makes a mistake and choose the target Tdie8(ε=7) which has the same permittivity value as the test target Tcoa3. Here, the correlation coefficient of the tested MSM and FMSM of Tdie8 is 0.5853, the correlation coefficient of this MSM and the FMSM of the target Tcoa3 is 0.5439. Other correlation coefficients are very small in this simulation example as shown in figure (a).

It can be seen in part (b) that classifier makes correct decision with very large safety margin for the target Tcoa15(r_{in}=9 ε=7) at 150º aspect angle.

In part (c), for the test of target Tcoa1(r_{in}=2 ε=3) at 150º aspect angle, the correlation coefficients between the tested MSM and the FMSMs of the target Tdie1(ε=3), the target Tcoa1(r_{in}=2 ε=3) and the target Tcoa4(r_{in}=4 ε=3) are 0.4208, 0.4206 and 0.4461, respectively. The classifier makes another mistake and chooses the target Tcoa4(r_{in}=4 ε=3) which is very similar to the test target Tcoa1 indeed.

It can be seen in the figure (d) that classifier makes correct decision for the target Tcoa5(r_{in}=4 ε=5) at 45º aspect angle. The target Tcoa2(r_{in}=2 ε=5) has the second highest correlation coefficient, as expected.

Another mistake can be seen in the figure (e) for the target Tdie1(ε=3) at 90º aspect angle. The correlation coefficients computed between the tested MSM and the FMSMs of the targets Tdie1, Tcoa1 and Tcoa4 (which have same ε value) are equal to 0.4966, 0.4967 and 0.4705, respectively. These values are very close to each other, as expected, leading to classification error.

Finally, the classifier confuses the target Tdie8(ε=7) at 15º aspect angle with the target Tcoa3(r_{in}=2 ε=7). Again these targets have the same ε value.

3.5.1 Discussion of Classifier Performance Results for the Mixed Target Library

The correct classification rates (in percentage) of the classifiers designed by both methods (MUSIC based and WD-PCA based), are given in Table 3.13 for CLMIX target library (27 targets). As it can be concluded from these results, both methods lead to classifiers with very similar accuracy values in the noise-free design/noise-free test case.

Table 3.13 Correct Decision Rates of CLMIX target library for noise-free case

Target Library	CLMIX (27 targets)
MUSIC method	78
WD/PCA method	76

Unfortunately, the cumulative normalized energy curves become useless to discriminate conducting spheres when the test data are noisy. Therefore, we could not make tests on the CLMIX target set with noisy data. However, we make such tests on a subgroup of the CLMIX library by excluding the conducting spheres. The results of these tests are presented in Table 3.14 below. We can see in this table that the WD/PCA based classifier shows a better performance as the SNR level of the test data decreases. However, these classifiers (both designed by noise-free reference data) are not good enough for successful target discrimination under noisy test conditions. As it was demonstrated in sections 3.2, 3.3 and 3.4 earlier, slightly noisy reference data must be used in the design of MUSIC based classifier for this subgroup of the CLMIX target library to increase the accuracy rates to acceptable levels.

Table 3.14 Correct Decision Rates of CLMIX target library using 20 dB reference data.

Target Library	CLMIX (18 targets) 20dB	CLMIX (18 targets) 10dB
MUSIC method (20db Ref)	52	26
WD/PCA method (20db Ref)	56	40
MUSIC method (N. Free Ref)	31	15
WD/PCA method (N. Free Ref)	61	45

CHAPTER IV

CLASSIFIER DESIGN APPLICATIONS AND RESULTS FOR SMALL-SCALE AIRCRAFT TARGETS

In this chapter, classifier design applications and their results will be reported for a target library which consists of five small-scale aircraft. The small scale target dimensions are obtained using a factor of 100 and the resulting wire lengths for body, wing and tail are given in Table 4.1 for each target. These aircraft targets are modeled by perfectly conducting, straight, thin wires with length to radius ratio of 2000 for all wire structures.

Table 4.1 The dimensions of the small-scale aircraft targets in the target library used in Chapter 4.

Substructures	Target 1 (Airbus)	Target 2 (Boeing 747)	Target 3 (Caravelle)	Target 4 (P-7)	Target 5 (Tu 154)
Body length (m)	0.5408	0.7066	0.3200	0.3435	0.4790
Wing length (m)	0.4484	0.5964	0.3440	0.3250	0.3755
Tail length (m)	0.1626	0.2217	0.1092	0.1573	0.1340

4.1 Description of Scattered Data Used in Classifier Design and Testing

The scattered responses of aircraft targets were obtained by using a simulation program FEKO, as described in [36] by Mehmet Okan Ersoy. This program is based on the Method of Moments (MoM).

The backscattered responses of the aircraft targets are obtained for Φ-polarized uniform plane wave at a fixed elevation of Θ= 60 degrees over the frequency band from 4 MHz to 1024 MHz with frequency steps of 4 MHz at 12 different aspect angles Φ = 5, 10, 15, 22.5, 30, 37.5, 45, 52.5, 60, 67.5, 75 and 82.5 degrees. Five of them which are equal to Φ = 5, 15, 30, 45 and 75 degrees, are chosen as the reference aspect angles to construct the feature database of the classifiers using noise free reference data and also using noisy data at 10 dB SNR level. The common time span of all scattered responses is 250 nanoseconds with 512 time samples.

As an example, the generated backscattered time domain signal for the target Boeing 747 at 15 degrees aspect angle is given in the noise-free case in Figure 4.1. Also in Figure 4.2 below, problem geometry used to synthesize the electromagnetic signals scatted from small-scale aircraft targets is described.

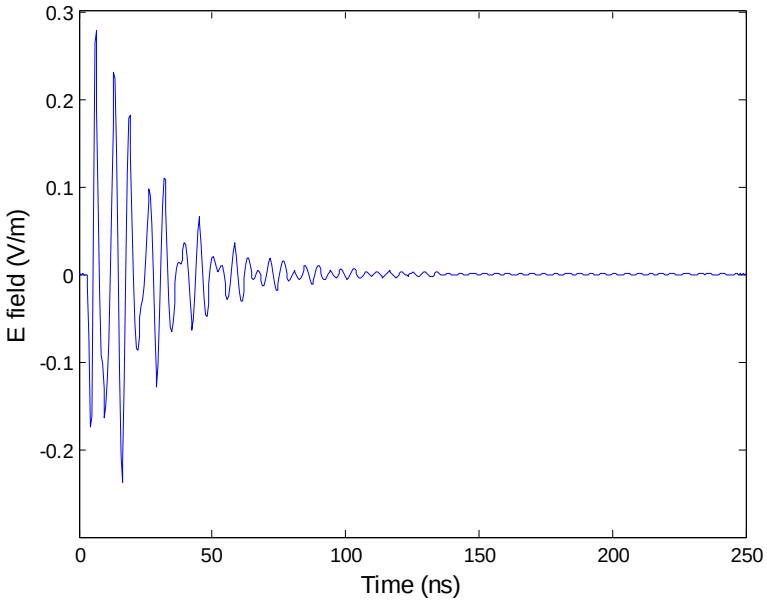

Figure 4.1 Scattered response of the target Boeing 747 at 15 degree aspect angle in the noise free case.

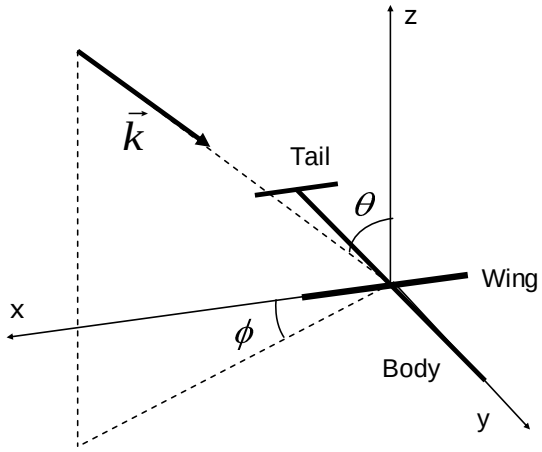

Figure 4.2 Problem geometry for aircraft library where the vector $\vec{k}$ denotes the propagation direction of incident plane wave

4.2 Classifier Design Simulations for Small-Scale Aircraft Using the MUSIC Algorithm Based Method

In this section, two MUSIC algorithm based classifiers are designed for the target library of small-scale aircraft using noise-free reference data and also using noisy reference data set at 10 dB SNR level.

4.2.1 Classifier design with noise-free reference data

First of all, in this MUSIC algorithm based target classifier, the scattered signal is divided into eight overlapping subintervals. For each subinterval, the MUSIC spectrum matrices (MSMs) are computed at each different reference aspect angle of Φ = 5, 15, 30, 45 and 75 degrees. Then, these MSMs are superposed for each given target to obtain the fused MUSIC spectrum matrices (FMSMs) over each subinterval. Using these FMSMs and MSMs, r_{total} values are computed for each subinterval. These r_{total} values (based on noise-free reference data) are shown in Figure 4.3. The design parameters of this MUSIC algorithm based classifier are chosen to be N= 64, m= 32 and L= 16.

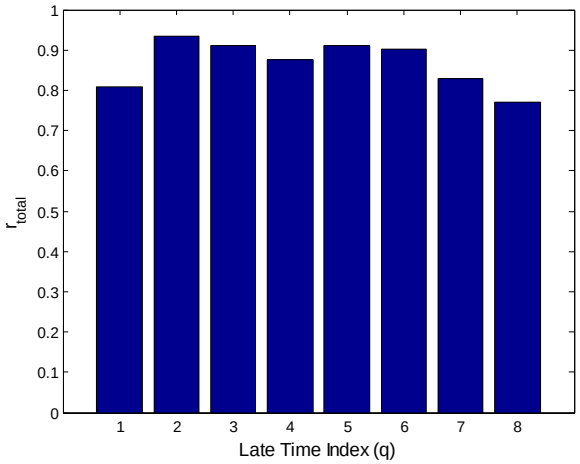

Figure 4.3 The r_{total} values computed for the classifier design for the aircraft target library in the noise-free case.

It can be seen in this figure that the MUSIC algorithm based classifier design using noise free reference data has a maximum r_{total} value at the second subinterval which is the optimal late-time design interval for this classifier. This chosen time interval corresponds to [16, 48] nsec.

After determining the optimum late-time interval for design, we construct the feature database of the classifier as being composed of target FMSMs as described earlier. All FMSMs computed over the optimal late-time interval using noise-free reference data are given in Figure 4.4 together with a MSM feature of a test signal which actually belongs to the target 1 (Airbus) at 45 degree backscattered aspect angle at 20 dB SNR level.

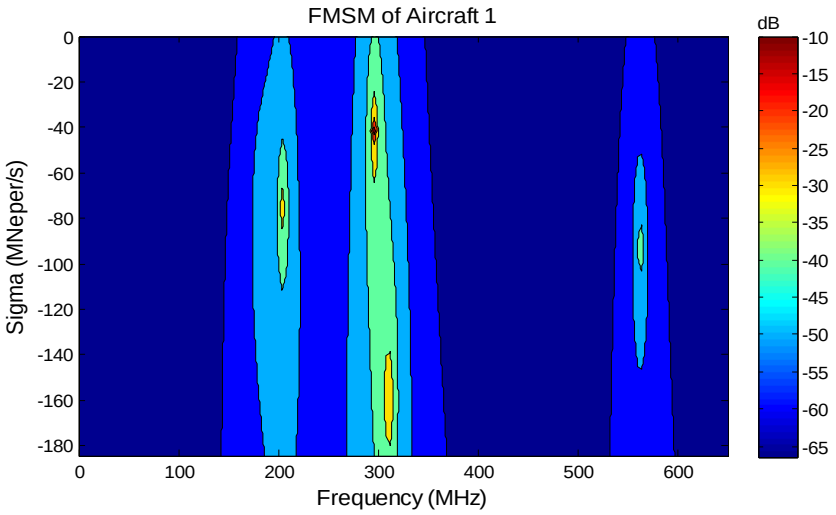

(a)

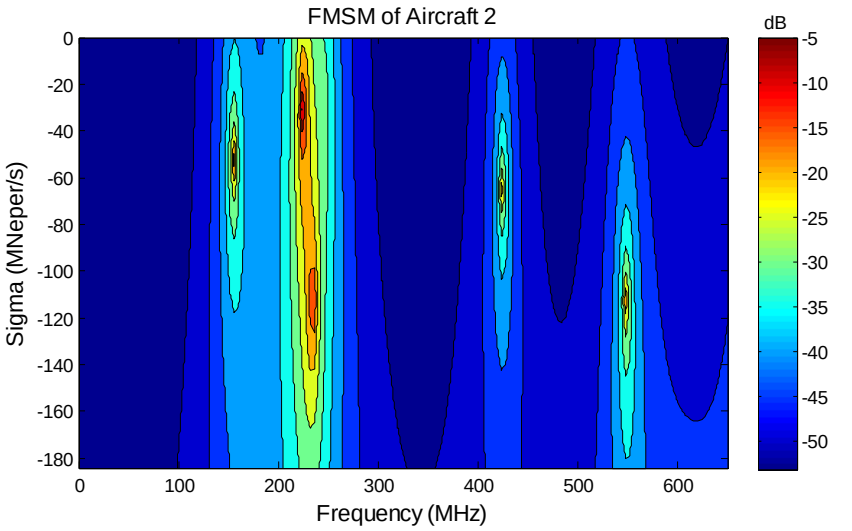
FMSM of Aircraft 2
dB
-5
-10
-15
-20
-25
-30
-35
-40
-45
-50
0
-20
-40
-60
-80
-100
-120
-140
-160
-180
Sigma (MNeper/s)
0
100
200
300
400
500
600
Frequency (MHz)

(b)

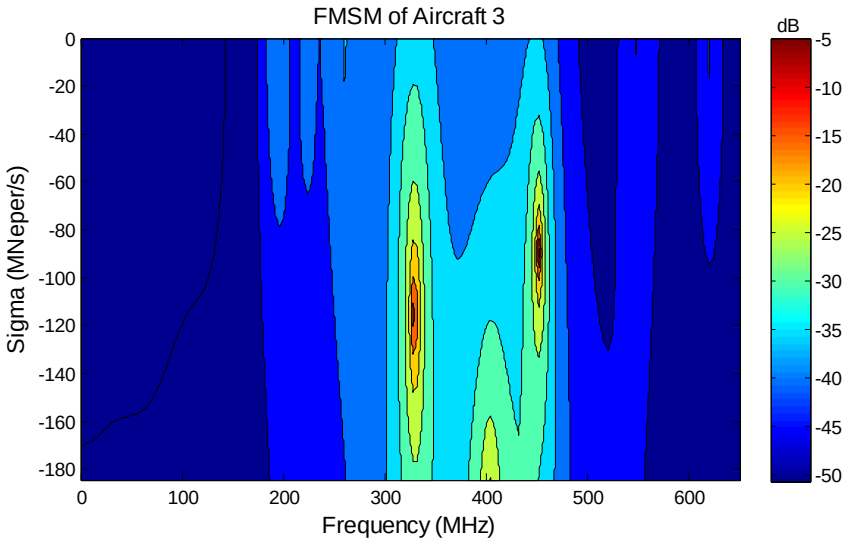
FMSM of Aircraft 3
dB
-5
-10
-15
-20
-25
-30
-35
-40
-45
-50
0
-20
-40
-60
-80
-100
-120
-140
-160
-180
Sigma (MNeper/s)
0
100
200
300
400
500
600
Frequency (MHz)

(c)

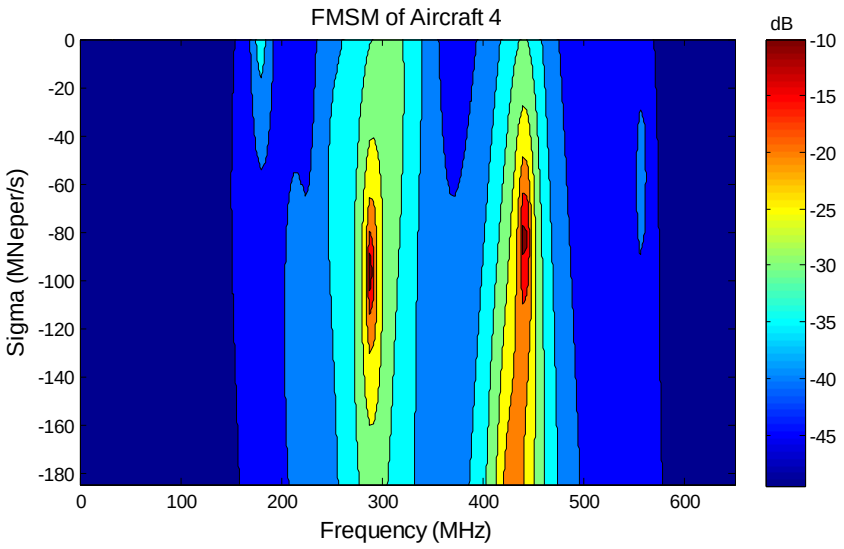
FMSM of Aircraft 4
dB
-10
-15
-20
-25
-30
-35
-40
-45
0
-20
-40
-60
-80
-100
-120
-140
-160
-180
Sigma (MNeper/s)
0
100
200
300
400
500
600
Frequency (MHz)

(d)

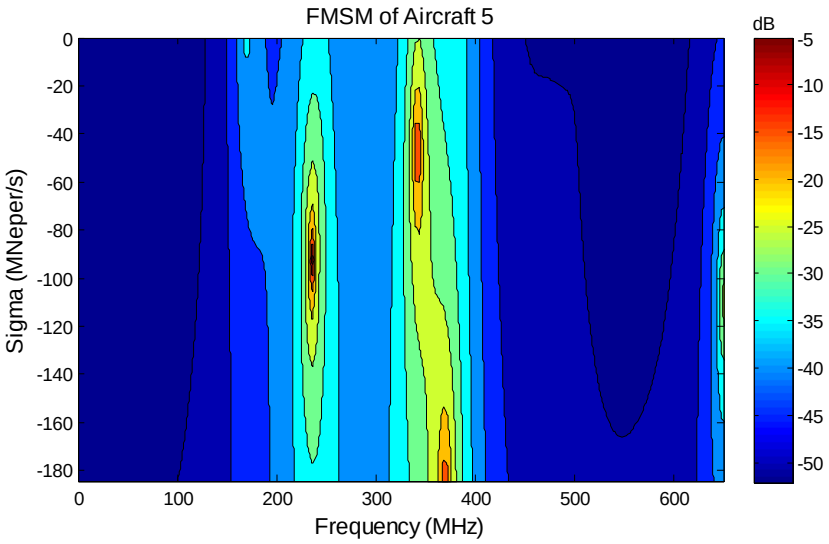
FMSM of Aircraft 5
dB
-5
-10
-15
-20
-25
-30
-35
-40
-45
-50
0
-20
-40
-60
-80
-100
-120
-140
-160
-180
Sigma (MNeper/s)
0
100
200
300
400
500
600
Frequency (MHz)

(e)

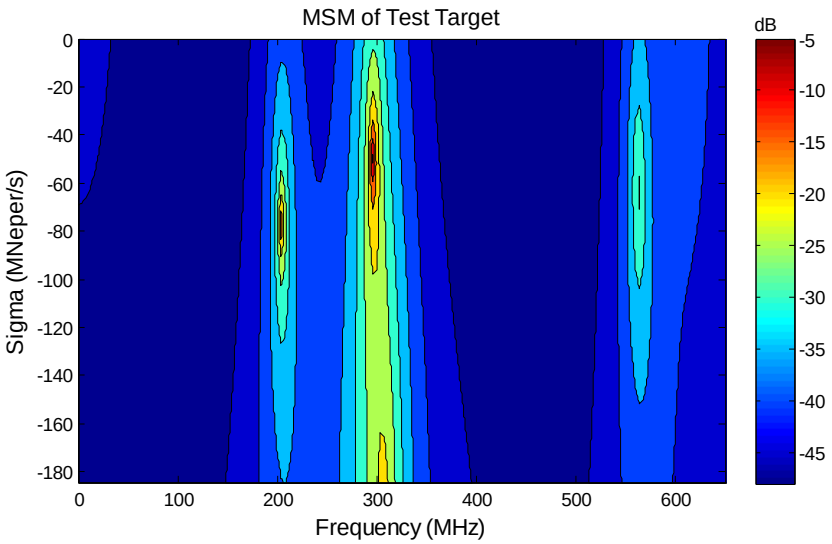

(f)

Figure 4.4 (a)-(e) The FMSM features of the aircraft targets Airbus, Boeing, Caravelle, P-7, Tu 154 in the noise free design case and (f) the MSM feature of the test signal belonging to target Airbus at 45 degree aspect angle at 20 dB SNR level.

Finally, performance tests are done with the whole available data set at SNR levels of 20 dB, 15 dB, 10 dB, 5 dB, 0 dB and -5 dB. All these results are given and discussed in section 4.4. Correlation coefficients between the FMSMs of this MUSIC algorithm based classifier and the MSMs of all available test signals at 20 dB SNR level are plotted in Figure 4.5. It can be seen in this figure that this classifier, makes only one mistake at the target index 11, which is the Airbus target at 75 degree aspect angle, while testing scattered signal at 20 dB SNR level. We can say that Caravelle, P-7 and Tu 154 are the aircraft targets which can be discriminated with much larger safety margins. The accuracy of the classifier is computed to be 98%.

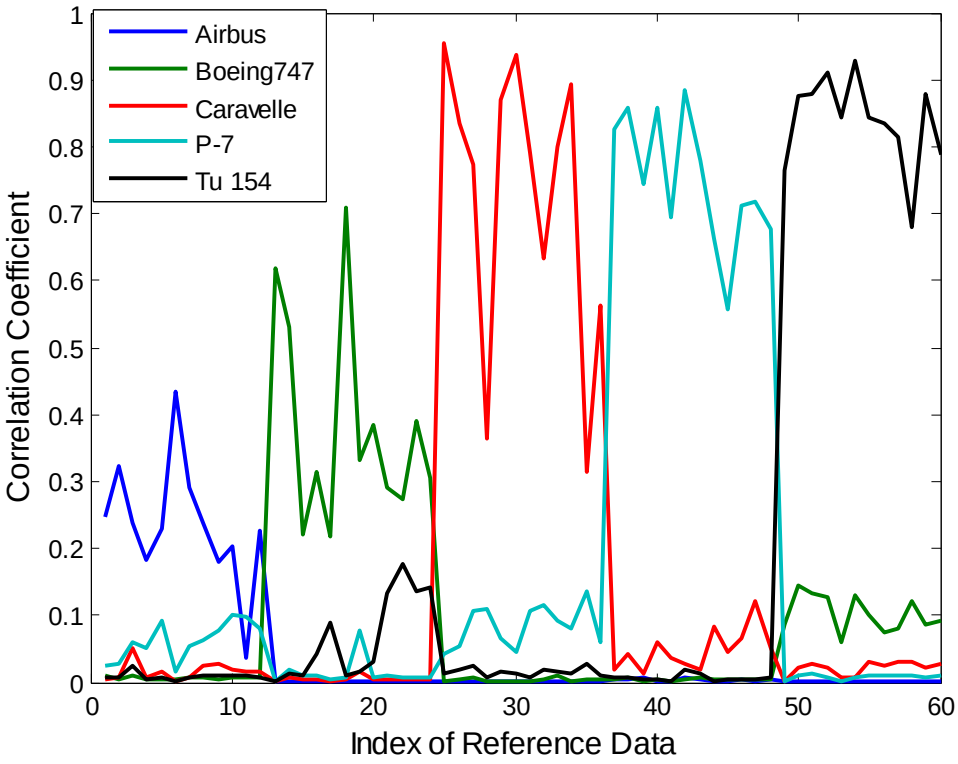

Figure 4.5 Correlation coefficients between the FMSMs of aircraft library targets and the MSMs of all available test signals at 20 dB SNR level. (The classifier is designed using noise-free reference data.)

4.2.2 Classifier design with noisy reference data

In this subsection, a MUSIC algorithm based classifier is designed for the same target library with noisy reference data at 10 dB SNR level, using the same procedures in section 4.2.1 with the same design parameters N= 64, m= 32 and L= 16.

The optimum late-time interval of design is selected by the help of r_{total} values which are plotted in Figure 4.6. The r_{total} value becomes maximum at the late-time index q=2 also for this classifier. Therefore, we again select

the [16, 48] nsec time interval as the optimal design interval for this classifier when noisy reference data at 10 dB SNR level are used. It can be concluded from Figures 4.3 and 4.6 that r_{total} values get smaller in the later time intervals for the 10 dB SNR level design because the effective SNR levels of reference signals become lower with increasing time.

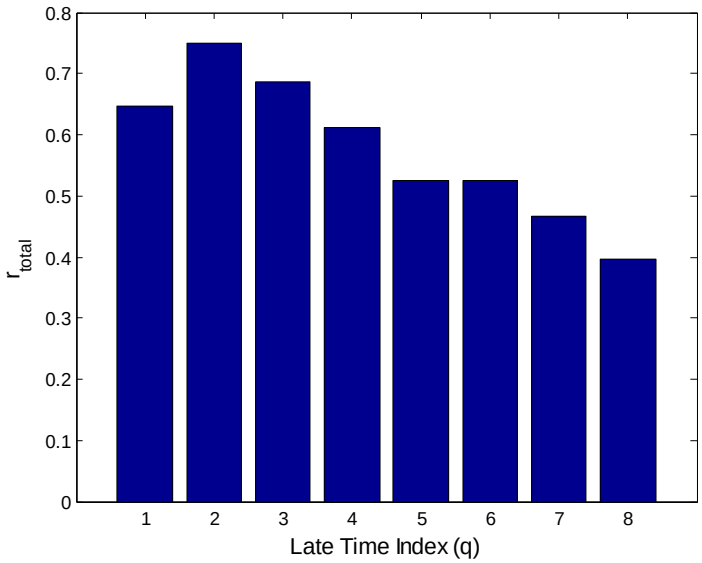

Figure 4.6 The r_{total} values computed for the classifier design for the aircraft target library using noisy reference data with 10 dB SNR level.

After forming the classifier's feature database by using FMSMs computed over the time interval [16, 48] nsec, the correct classification rates of this classifier are computed against test data at various SNR levels (-5 dB, 0 dB, 5dB, 10dB, 15dB and 20dB). Nearly perfect accuracy rates are observed also at SNR levels as low as 5 dB as shown in Table 4.2 of section 4.3. The lowest accuracy rate obtained at -5 dB SNR level is increased from 66% to 87% by training the classifier at 10 dB SNR level instead of training it by noise-free reference data.

4.3 Classifier Design Simulations for Small-Scale Aircraft Using the WD-PCA Based Method

In this section, WD-PCA method based classifiers are designed for the same aircraft target library firstly using noise-free reference data and then using noisy reference data at 10 dB SNR level.

4.3.1 Classifier design with noise-free reference data

In this subsection, we design a classifier using noise free reference signals for the aircraft target library using the WD-PCA based design technique and this classifier is tested at various SNR levels of 20 dB, 15 dB, 10 dB, 5 dB, 0 dB and -5 dB.

As a first step of the WD-PCA based design technique, we compute the auto-WD matrix Wx of the reference scattered signals which are sampled at 512 time points. Some contour plots of the auto-WD matrices for the response signal of the Airbus at 10 and 75 degrees backscattered aspect angles are given below in Figure 4.7 in the noise-free case.

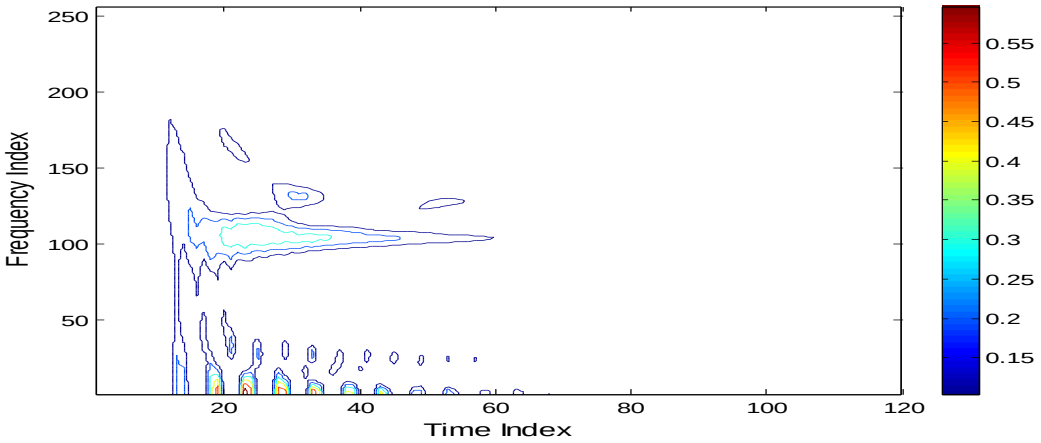

(a)

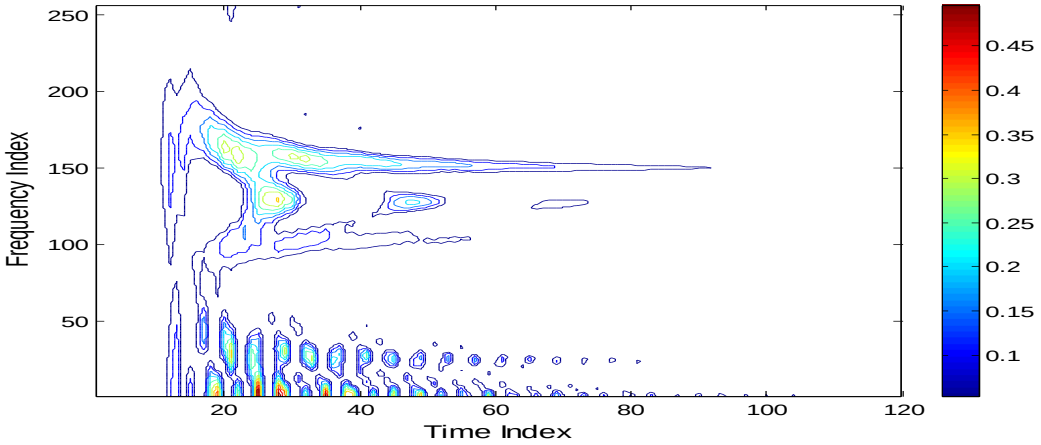

(b)

Figure 4.7 Contour plots of modified auto-Wigner distributions for the target Airbus at (a) 10º and (b) 75º backscattered aspect angles.

Afterwards, energy density vectors are computed as described earlier over Q=16 non-overlapping late-time intervals. Then, by the help of these energy density vectors, we choose the time bands q=2 and q=3, as the optimum late-time interval which corresponds to [15.6, 46.9] nsec. In Figure 4.8, the computed CCF values are plotted against q* for this classifier design.

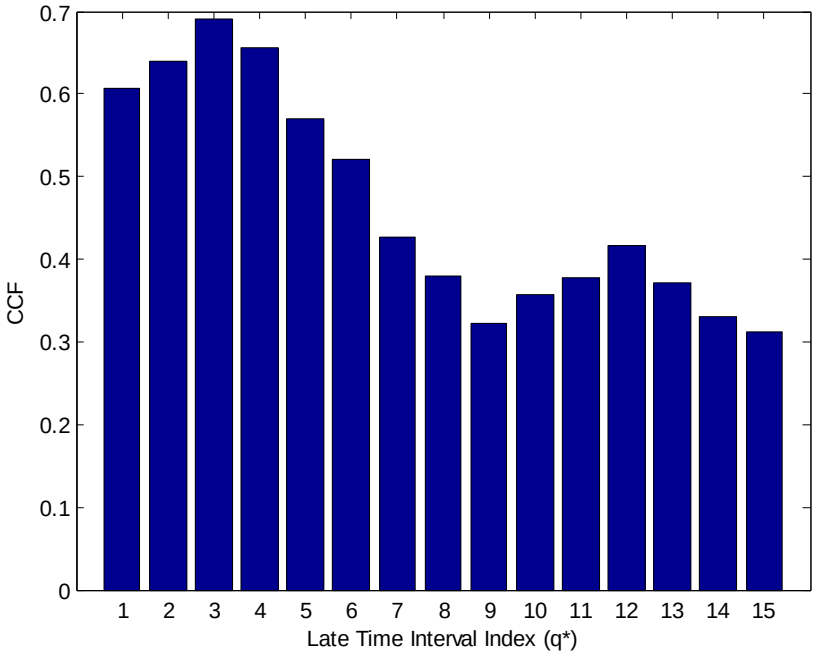

Figure 4.8 CCF values plotted against the late-time index q* to determine the optimal late-time design interval for the aircraft library using noise-free reference data.

Features Vectors (FFVs) of all aircraft targets extracted for noise free design and a test target's LTFV (in noise-free case) are given altogether in Figure 4.9.

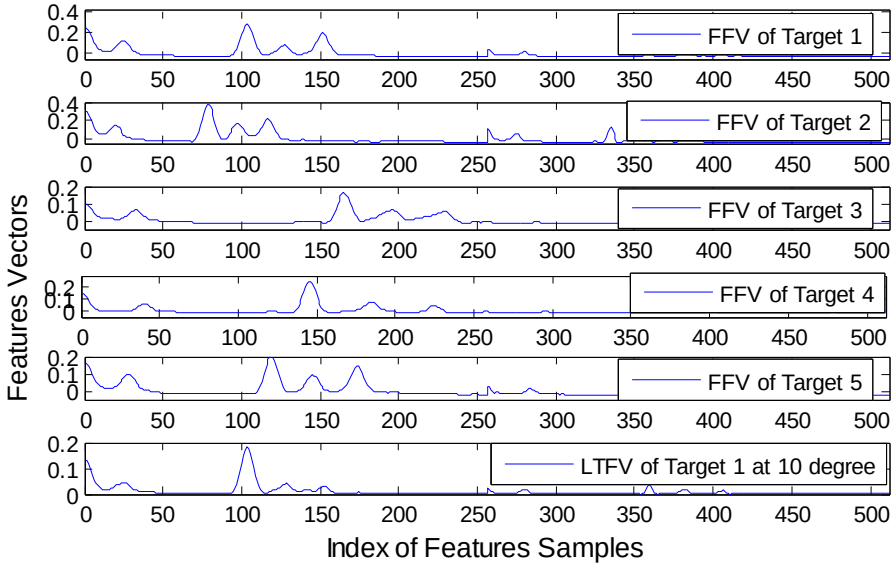

Figure 4.9 The FFVs of library targets for noise-free design and the LTFV of target 1 (Airbus) at the aspect angle 10º in the noise-free case.

Finally, this classifier is tested over this optimal late time interval at the SNR levels of -5 dB, 0 dB, 5 dB, 10 dB, 15 dB and 20 dB. The accuracy rate of the classifier is found to decrease from 98% to 82% as the SNR levels of the test signals decrease from 20 dB to -5 dB.

4.3.2 Classifier design with noisy reference data

In this section, another classifier is designed for the aircraft target library using the WD-PCA based method, but this time, using noisy reference data at 10 dB SNR level. Following the previously described design steps with Q=16 time intervals, the optimal late-time interval of design is determined to be [15.6, 46.9] nsec using the CCF values obtained for noisy reference signal at 10 dB. The CCF versus q* barplot is given in Figure 4.10 where the plot has its maximum for q*=2.

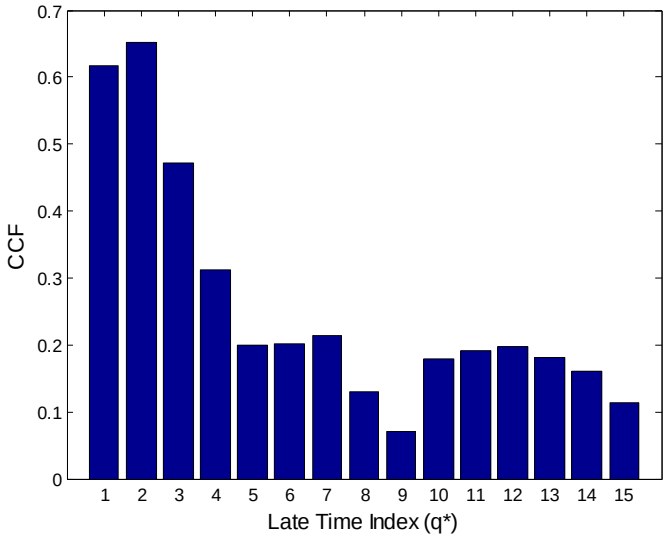

Figure 4.10 The CCF values plotted against the late-time index q* to determine the optimal late-time design interval for the aircraft library using noisy reference data at 10 dB SNR level.

Constructed Fused Features Vectors (FFVs) of all five aircraft targets for this noisy classifier design and a test target's LTFV at 10dB SNR level are shown together in Figure 4.11. FFV of Target 4 and LTFV of the test target look highly correlated with each other as expected because this LTFV feature actually belongs to aircraft P-7 (target 4) at 60 degrees aspect.

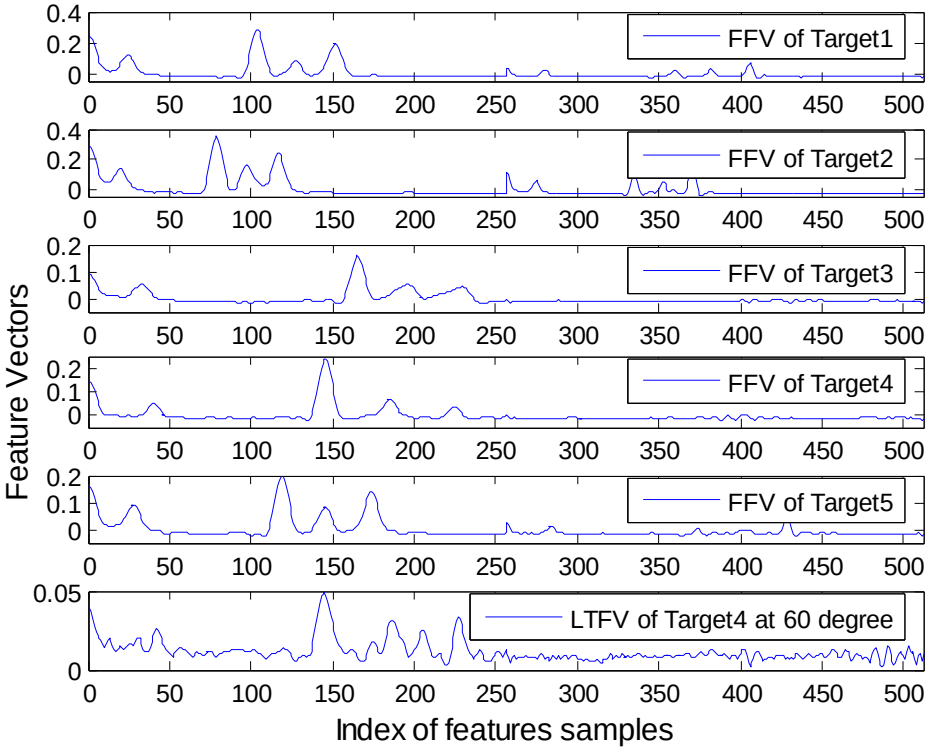

Figure 4.11 FFVs of all targets at 10 dB SNR level and LTFVs of target 4 (P-7) at the aspect angle 60º at 10dB SNR level.

Finally, the performance tests of this classifier are made using test signals at SNR levels -5 dB, 0 dB, 5 dB, 10 dB, 15 dB and 20 dB. The perfect accuracy rate of 100% is obtained at overall SNR levels as low as 10 dB. The lowest accuracy rate of 88% occurred at a very low SNR level of -5 dB.

4.4 Discussion of Classifier Performance Results for Small-Scale Aircraft Targets

The accuracy rates obtained for all four aircraft classifiers (designed for the same target library of five small scale aircraft) of this chapter are computed at various testing SNR levels as shown in Table 4.2.

We can draw the following conclusions based on the information provided by this table. First of all, when the classifiers are designed with noise-free reference data, the WD-PCA based classifier displays a much better performance for testing SNR levels lower than 15 dB. For example, the accuracy rate of the MUSIC based classifier is only 66% at SNR=-5dB while the WD-PCA based classifier has 88% accuracy at the same noise level. However, when the classifiers are designed by using noisy reference data at 10 dB SNR level, performance of the MUSIC based classifier is improved drastically. As a result, for designs with noisy signals, usefulness of both classifier design techniques become quite similar to each other. The second conclusion is that higher rates can be obtained for classifiers designed for the aircraft library as compared to the case of spherical targets. This observation can be explained by the fact that aircraft targets modeled by thin conducting wires are high-Q targets with natural scattered responses having enough signal energy at late times. Consequently, the classifiers designed to discriminate aircraft targets have much better noise performances as compared to those classifiers designed for spherical targets.

Table 4.2 Correct classification rates (in percentage) of all four classifiers designed for the target library of small-scale aircraft targets

SNR Levels	20 dB	15 dB	10 dB	5 dB	0 dB	-5 dB
MUSIC method (10dB Ref)	100	100	100	97	93	87
WD-PCA method (10dB Ref)	100	100	100	98	93	88
MUSIC method (N. Free Ref)	98	94	89	80	75	66
WD/PCA method (N. Free Ref)	98	95	95	95	95	82

CHAPTER V

CONCLUSION

This thesis work has been focused in designing and testing two recently proposed electromagnetic target classifier design techniques, the MUSIC algorithm based technique and the WD-PCA based technique, to compare their noise performances and their capability to handle large number of targets. Target libraries used in design and test simulations have included a variety of classes such as perfectly conducting spheres (example to a class of very low-Q targets), dielectric spheres (example to penetrable targets), dielectric coated conducting spheres (example to targets made of different materials) and small-scaled aircraft modeled by perfectly conducting thin wires (example to relatively high-Q conducting targets with complicated geometries). The MUSIC algorithm based and WD-PCA based target classification techniques are both resonance region techniques, which need extraction of target features from late-time transient scattered data. For such classifiers, effective SNR levels of design and test data over the chosen late-time design intervals are usually much lower than the overall SNR levels of these signals. Therefore, investigation of the noise performances of these two target classification techniques deserves special attention especially in the case of low-Q targets. In this thesis, for each chosen target class, several classifiers are designed by using both design techniques first by using noise-free design data, then by using noisy design data. The simulated classifiers are extensively tested at various overall SNR levels changing from infinity (the noise-free case) to very low levels such as 0 dB or -5 dB. General trends

observed in classifier performances may show variations from one target class to another as summarized below:

I. Comparison of the performances of the MUSIC algorithm based and the WD-PCA based classifier design techniques to handle large number of targets

• First of all, MUSIC based and WD-PCA based classifiers are designed using noise-free reference data for three different libraries of perfectly conducting spheres. The target libraries named CLCON1, CLCON2 and CLCON3 have 3, 5 and 9 conducting spheres, respectively. The smallest of these spheres has a radius of 8 cm and the largest sphere has a radius of 12 cm. The first target library CLCON1 contains 3 spheres with radii of 8, 10 and 12 cm. The second one, CLCON2, has 5 spheres with radii of 8, 9, 10, 11 and 12 cm. Finally, the third library CLCON3 has 9 spheres with radii of 8, 8.5, 9, 9.5, 10, 10.5, 11, 11.5 and 12 cm. Obviously, this last library is the most challenging one not only because it contains a larger number targets but also because these perfectly conducting spheres have very similar sizes. Accuracy rates (i.e., correct classification rates) of the MUSIC based and WD-PCA based classifiers designed for each one of these three libraries are computed and compared under the noise-free design/noise-free test case and they are found to be very close to each other. As shown in Table 3.3, both classifier design techniques lead to classifiers with 100 percent accuracy for the CLCON1 library. The accuracy rates attained by the MUSIC based classifiers drop to 98 percent for the CLCON2 and CLCON3 libraries while the WD-PCA based classifiers display 100 percent accuracy for the CLCON2 library and 97 percent accuracy for the CLCON3 library. In conclusion, both techniques look equally successful as the complexity of the target libraries increases. Even for the most challenging library of 9 targets,

accuracy rates reached by both classifier design techniques for the class of perfectly conducting spheres turns out to be almost perfect.

- Similar effects of library complexity are also investigated for the target class of lossless dielectric spheres using two different libraries, the CLDIE1 library of 4 targets (same size spheres with relative permittivity values of 3, 4, 5 and 6) and the CLDIE2 library of 8 targets (same size spheres of relative permittivity values of 3, 3.5, 4, 4.5, 5, 5.5, 6 and 7). Under the noise-free design/noise-free test conditions, the MUSIC based classifiers reach the accuracy levels of 92 percent for the CLDIE1 library and 89 percent for the more challenging CLDIE2 library. The WD-PCA based classifiers, however, reach the perfect 100 percent accuracy for both libraries. Therefore, the WD-PCA based classifier design technique is shown to be more successful (by about 10 percent accuracy difference) in discriminating these dielectric objects in noise free conditions.

- In the case of dielectric coated conducting spheres, five different target libraries (CLCOA1, CLCOA2, CLCOA3, CLCOA4 and CLCOA5) are used in classifier design and test simulations. Depending upon the size of the inner conducting spheres, behaviors of coated conductors may converge to either those of the conducting spheres or to those of the dielectric spheres. Therefore, for the tested libraries, performance tests of the MUSIC based and the WD-PCA based classifiers are not found to be conclusive to compare them on the basis of their capacity to handle large-size target libraries. For some of these libraries, the MUSIC based classifier performs better. For some others, the WD-PCA based classifier looks more successful. For the library CLCOA3 (contains 5 targets all having the same outer radius, the same relative refractive index of 7 in the dielectric coating but different inner radii of 2, 4, 7, 8 and 9 cm for the conducting sphere part) for instance, both

classifier design techniques are found to be equally useful with accuracy rates around 97-98 percent in the noise-free design/noise-free test case.

• In the meantime, there are two important observations which are made based on the content of Table 3.11 for the classification of dielectric coated conducting spheres: Firstly, classification of coated conducting spheres becomes easier for larger values of the refractive index of coating. According to the results tabulated on the first three columns of this table, the accuracy rates of MUSIC based and WD-PCA based classifiers decreases from 97-98 percent level to 65-70 percent level as relative permittivity decreases from 7 to 3. Secondly, for the same relative permittivity variations, the coated spheres with larger inner conducting parts can be discriminated more easily. Based upon the last two columns of Table 3.11, for example, the targets of the library CLCOA5 with inner radii of 7, 8 and 9 cm can be classified by accuracy rates of 91 percent and 86 percent using the MUSIC based classifier and the WD-PCA based classifier, respectively. In these noise-free design/noise-free test simulations, the CLCOA5 library has 9 targets with coatings at relative permittivity values of 3, 5 and 7 for each inner radius value. When the similar classifier design and test simulations are performed for the library CLCOA4 (that has 6 targets at relative permittivity values of 3, 5 and 7 at each inner radius value of 2 cm and 4 cm), the accuracy rates of the MUSIC based and WD-PCA based classifiers drastically drop to 67 percent and 77 percent, respectively.

• Finally, for a mixed target library CLMIX (containing 9 conducting spheres, 3 dielectric spheres and 15 dielectric coated conducting spheres), the noise-free design/noise-free test simulations are performed. For this large-size library with 27 targets, the MUSIC based classifier displayed 78 percent accuracy while the accuracy rate of the WD-PCA based classifier is found to be 76 percent. In other words, performances of both classifier

design techniques (regarding their library sizes) are found very similar for this specific mixed library.

II. Comparison of the noise performances of the MUSIC algorithm based and the WD-PCA based classifier design techniques

To compare the noise performances of these two classifier design techniques, one target library is chosen for each target class and two different classifiers are designed for the selected library by using each design technique based on noise-free reference data. Then, performances of resulting classifiers are evaluated by test data at various SNR levels decreasing from infinity (the noise-free test data case) to low SNR levels around zero decibels. Next, two more classifiers are designed for the same target library, but this time, using noisy reference data at a given moderate SNR level. Again, performances of resulting noisy classifiers are evaluated by test data at various SNR levels. Results of all these classifier design and test simulations for different target classes can be summarized as follows:

- The target library CLCON2 (containing five conducting spheres of radii 8, 9, 10, 11 and 12 cm) is selected for the class of conducting spheres. A total of four classifiers are designed for this library first by using noise-free reference data and then using noisy (at SNR=20 dB) reference data by each classifier design technique. The accuracy rates obtained for these four classifiers when they are tested at various testing SNR levels are plotted in Figure 3.15. It is seen that classifiers designed by both methods using noise-free reference data fail badly when they are tested by noisy data. When the classifiers are designed by slightly noisy data of 20 dB SNR level, their low SNR performance are improved in a noticeable way, although their accuracy against noise-free test signals decreases from 98 percent (for MUSIC based

classifier) or 100 percent (for WD-PCA based classifier) level to about 80 percent level. The WD-PCA based classifier displays higher accuracy (for example, 60 percent accuracy versus 50 percent accuracy at the testing SNR of 5 dB) at very low SNR tests.

• The target library CLDIE1 (containing four lossless dielectric spheres of the same size, r = 10 cm, but with relative permittivity values of 3, 4, 5 and 6) is selected for the class of dielectric spheres. Again four classifiers are designed and tested for this library as described above. Based on the accuracy results tabulated in Table 3.6, performances of the classifiers designed by both methods using noise-free reference data are found poor when they are tested at low SNR levels. The accuracy rate of the MUSIC based classifier changes from 92 percent to 35 percent as the testing SNR drops from infinity to 5 dB level. The WD-PCA based classifier shows a much better performance as its accuracy rate drops from 100 percent to 69 percent under the same conditions. Use of noisy reference data at 20 dB SNR levels helps improving the performance of the MUSIC classifier. Although its accuracy reduces to 79 percent in noise-free testing, its low SNR testing performance is raised to 51 percent accuracy at 5 dB SNR level. However, despite this improvement, the WD-PCA classifier performs still much better (by about 20 percent difference in accuracy at almost all testing SNR levels) than the MUSIC based classifier.

• The target library CLCOA3 (containing five dielectric coated conducting spheres all having the same relative permittivity value of 7 with internal radii of 2, 4, 7, 8 and 9 cm) is selected for the class of dielectric coated conducting spheres. Again, four classifiers are designed and tested for this library as described earlier. General tendency of the accuracy rates tabulated in Table 3.10 looks very similar to the one displayed in Table 3.6 for the dielectric sphere library CLDIE1. The WD-PCA based classifier

performs much better (by about 15-20 percent accuracy difference) than the MUSIC based classifier for the selected coated conductor library.

• A reduced CLMIX library (containing 3 dielectric spheres and 15 dielectric coated conducting spheres after excluding the perfectly conducting spheres of the original CLMIX library) of 18 targets is used to design classifiers by both design techniques. When the classifiers are designed by noise-free reference data, accuracy rate of the MUSIC classifier is found to be 78 percent at noise-free testing, 31 percent at 20 dB SNR and 15 percent at 10 dB SNR. The accuracy rate of the WD-PCA classifier drops less severely as the testing SNR decreases; it becomes 76 percent at noise-free testing, 61 percent at 20 dB and 45 percent at 10 dB testing. In other words, the noise performance of WD-PCA classifier is much better (by about 30 percent difference in accuracy rates) than the MUSIC based classifier in noise-free design/noisy testing, but in general none of the classifiers can achieve high enough accuracy rates at low testing SNR levels. Designing the classifiers using noisy data at 20 dB helps improving the performance of the MUSIC based classifier slightly but not sufficiently as shown in Table 3.14.

• Finally, an aircraft library (containing five small scale aircraft targets which are modeled by thin conducting wires) is used to design a total of four classifiers by each method first using noise-free design data then by using noisy data at SNR = 10 dB. Based on the accuracy rates listed in Table 4.2, when the classifiers are designed by noise-free reference data, the WD-PCA based classifier performed much better (up to 20 percent accuracy difference) than the MUSIC based classifier at testing SNR levels below 15 dB. When the classifiers are designed by using noisy reference data at 10 dB SNR, however, performances of both classifiers (especially that of the

MUSIC based classifier) are improved and become about the same at all testing SNR levels.

In summary, noise performances of the WD-PCA based classifiers are found distinctively better than that of the MUSIC based classifiers in noise-free design/noisy testing cases. Designing classifiers using slightly or moderately noisy data helps improving the noise performance of classifiers, especially in the case of MUSIC algorithm based design technique. However, despite this improvement, performance of the MUSIC based classifiers either barely catches the performance of the WD-PCA classifiers or remains 10 to 20 percent behind it in terms of accuracy rates. The WD-PCA based design technique is preferable as its accuracy rate is not very sensitive to the SNR level of the design data except for the case of very low-Q library targets such as perfectly conducting spheres. The WD-PCA based classifiers perform better also in handling libraries with large number of targets in the case of dielectric sphere class. Performances of the WD-PCA based and MUSIC algorithm based classifiers are about the same for other target classes.

As a future work, these two target classification techniques can be investigated for the target classes of lossy dielectrics and inhomogeneous dielectrics of varying geometries.

REFERENCES

[1] E.M. Kennaugh and R.L. Cosgriff, “The use of impulse response in electromagnetic scattering problems,” in IRE Nat. Conv. Rec., Part I, pp. 72-77, 1958.

[2] E.M. Kennaugh and D.L. Moffatt, “Transient and impulse response approximations,” Proc. IEEE, Vol.53, pp.893-901, August 1965.

[3] L. Marin, “Natural mode representation of transient scattering from rotationally symmetric bodies,” IEEE Trans. Antennas Propagat., Vol.AP-22, pp. 266-274, March 1974.

[4] C.E.Baum, “Toward an engineering theory of electromagnetic scattering: the singularity and eigenmode expansion methods”, in: P.L.E. Uslenghi (Ed.), Transient Electromagnetic Fields, Academic Press, New York, 1978 (Chapter 15).

[5] D.L.Moffatt and R.K.Mains, “Detection and Discrimination of Radar Targets”, IEEE Transactions on Antennas and Propagation, vol. AP-23, pp. 358-367, May 1975.

[6] C.W.Chuang and D.L.Moffatt, “Natural resonances via Prony’s method and target discrimination”, IEEE Transactions on Aerosp. Electron. Syst., vol. AES-12, 1976.

[7] E.M.Kennaugh, “The K-Pulse Concept”, IEEE Transaction on Antennas and Propagation, vol. AP-29, pp. 327-331, March 1981.

[8] E.M. Kennaugh, D.L. Moffatt and N. Wang,"The K-pulse and response waveforms for non-uniform transmission lines," IEEE Trans. Antennas Propagat., Vol.AP-34, No.1, pp. 78-83, January 1986.

[9] F.Y.S. Fok, D.L. Moffatt and N. Wang, "K-pulse estimation from the impulse response of a target," IEEE Trans. Antennas Propagat., Vol.AP-35, No.8, pp. 926-933, August 1987.

[10] G. Turhan-Sayan and D. L. Moffatt, "K-Pulse Estimation and Target Identification of Low-Q Radar Targets," Wave Motion, No. 11, pp. 453-461, 1989.

[11] G. Turhan-Sayan and D. L. Moffatt, "K-Pulse Estimation Using Legendre Polynomial Expansions and Target Discrimination," Journal of Electromagnetic Waves and Applications, Vol.4, No. 2, pp. 113-128, 1990.

[12] D.P.Nyquist, K.M.Chen, E.Rothwell and B.Drachman, "Radar Target Discrimination using the Extinction-Pulse Technique", IEEE Transaction on Antennas and Propagation, vol. AP-33, pp. 929-937, Sept. 1985.

[13] E. J. Rothwell, K.-M. Chen, D. P. Nyquist, "Extraction of the natural frequencies of a radar target from a measured response using E-pulse techniques," IEEE Trans. Antennas and Propagation, vol. 35, no. 6, pp. 715 720, June 1987.

[14] Baum,C.E. "Signature-based target identification and pattern recognition", Antennas and Propagation Magazine, IEEE ,Volume: 36 , Issue: 3 , Jun 1994 Pages:44 – 51.

[15] K.T.Kim, I.S.Choi, and H.T.Kim, "Efficient radar target classification using adaptive joint time-frequency processing", IEEE Trans. Antennas Propagat., vol. 48, no. 12, pp. 1789-1801, Dec. 2000.

[16] Y. Shi and X.-D. Zhang, "A Gabor atom network for signal classification with application in radar target recognition," IEEE Trans. Signal Processing, vol. 49, no. 12, pp. 2994-3004, Dec. 2001. 23.

[17] G.Turhan-Sayan, "Natural resonance-based feature extraction with reduced aspect sensitivity for electromagnetic target classification," Pattern Recognition, Vol.36, No. 7, pp. 1449-1466, July 2003.

[18] G.Turhan-Sayan, “Real Time Electromagnetic Target Classification Using a Novel Feature Extraction Technique with PCA-Based Fusion” IEEE Transactions On Antennas and Propagation, Vol. 53, No.2, February 2005.

[19] Jouny.I, Garber.F.D, Ahalt,S.C “Classification of radar targets using synthetic neural networks”, Aerospace and Electronic Systems, IEEE Transactions on , Volume: 29 , Issue: 2 , April 1993 Pages:336 – 344.

[20] Azimi-Sadjadi.M.R, De Yao, QiangHuang, Dobeck.G.J, “Underwater target classification using wavelet packets and neural networks”, Neural Networks, IEEE Transactions on , Volume: 11 , Issue: 3 , May 2000 Pages:784 – 794.

[21] G.Turhan-Sayan, K. Leblebicioglu, and T. Ince, “Electromagnetic target classification using time-frequency analysis and neural networks,” Microw. Opt. Technol. Lett., vol. 21, pp. 63–69, 1999

[22] G. Turhan-Sayan, K. Leblebicioğlu and T. İnan, “Input Signal Shaping for Target Identification Using Genetic Algorithms,” Microwave and Optical Technology Letters, Vol.17, No. 2, pp. 128-132, February 1998.

[23] G. Turhan-Sayan and M. Kuzuoglu, "Pole Estimation for Arbitrarily-Shaped Dielectric Targets by a Genetic Algorithm-Based Resonance

Annihilation Technique," IEE Electronics Letters, Vol. 37, No. 6, pp.380-381, March 2001.

[24] Xi Miao; Azimi-Sadjadi, M.R.; Bin Tan; Dubey, A.C.; Witherspoon "Detection of mines and mine-like targets using principal component and neural-network methods", Neural Networks, IEEE Transactions on, Volume: 9, Issue: 3, May 1998 Pages:454 – 463.

[25] M. Secmen and G. Turhan-Sayan, "Radar target classification method with reduced aspect dependency and improved noise performance using multiple signal classification algorithm," IET Radar, Sonar and Navigation, to be published in December 2009 issue.

[26] M. Secmen, "A Novel Music Algorithm Based Electromagnetic Target Recognition Method in Resonance Region for the Classi¯cation of Single And Multiple Targets", Ph.D. Dissertation, METU, Ankara, Turkey, Feb. 2008.

[27] P. Stoica and K. C. Sharman, "Maximum likelihood methods for direction-of-arrival estimation," IEEE Trans. on Acoustics, Speech and Signal Processing, vol. 38, no. 7, pp. 1132-1143, July 1990.

[28] T. T. Georgiou, "Signal estimation via selective harmonic amplification: MUSIC, Redux," IEEE Trans. on Acoustics, Speech and Signal Processing, vol. 48, no. 3, pp. 780-790, Mar. 2000.

[29] M. C. Dogan, J. M. Mendel, "Single sensor detection and classification of multiple sources by higher-order spectra," IEE Proceedings F, Radar and Signal Processing, vol. 140, no. 6, pp. 350-355, Dec. 1993.

[30] P. Stoica, R. Moses, Introduction to Spectral Analysis, Prentice Hall, Englewood Cliffs, New Jersey, 1997.

[31] Y. Li, J. Razavilar and K. J. Ray Liu, "DMUSIC algorithm for 2D NMR Signals," Engineering in Medicine and Biology Society, IEEE 17th Annual Conference, pp. 477 – 478, Sept. 1995.

[32] M. Kerker, The Scattering of Light, and Other Electromagnetic Radiation. New York: Academic Press, 1969.

[33] L. Cohen, Time–Frequency Analysis, Prentice-Hall, Englewood CliBs, NJ, 1995.

[34] J.E.Jackson, A User's Guide to Principal Components, New York: John Wiley & Sons, Inc., 1991.

[35] M. Ayar, “Design of an electromagnetic classifier for spherical targets,” M. Sc. Thesis, Middle East Technical University, April 2005.

[36] M. O. Ersoy, “Application of a natural-resonance based feature extraction technique to small-scale aircraft modeled by conducting wires for electromagnetic target classification,” M. Sc. Thesis, Middle East Technical University, September 2004.

APPENDIX

A SAMPLE PROGRAM CODE WRITTEN IN MATLAB FOR RANDOM TESTING ON CLMIX TARGET SET WITH MUSIC METHOD

```
% An example test code for target library CLMIX
clear
load hdis10_7_15.dat; %loading the time domain response
% Test target is Tdie8(e=7) at 15 degree
testdata=hdis10_7_15;
ENE=[testdata
   ];
ENER=ENE';
tresh=input('Enter treshold value near to 1   = ');
% tresh=0.9999;
for en=1:1;
   yy=ENER(:,en);
   NNN=length(yy);
   ysq=yy.*yy;
   sume=sum(ysq);
   yn=yy/sqrt(sume);
   normen(1)=yn(1)^2;
   for i=2:NNN
      normen(i)=normen(i-1)+yn(i)^2;
   end;
```

```
    for zz=1:1024;
        if normen(1,zz)>tresh;
            if normen(1,(zz-1))<tresh;
                zb=zz;
         %the first point where enegy is over tresh
                energydata(1,en)=zb;
            end;
        end;
    end;
end;

if energydata>400
% test target is not a conducting sphere
load REFmix_nfree_nfreeRef

GG=0;R=0; corrcoef3=0;
    for uo=1:1
        xnorm(uo,:)=testdata(uo,:);
    end

        for kk=1:1
            y=real(xnorm(kk,113+(qstar-1)*72:240+(qstar-1)*72));
            y=y(:);
            N=length(y);                    % data length
            R=zeros(m,m);
            for i = m : N,
                R=R+y(i:-1:i-m+1)*y(i:-1:i-m+1)'/N;
            End
% get the eigendecomposition of R; use svd because it sorts eigenvalues
            [U,D,V]=svd(R);
```

```
        G=U(:,n+1:m);
        GG = G*G'; % find the coefficients of the polynomial
        for u=1:151
            for v=1:437
                alpha(u)=-(u-1)*0.0006;
                w(v)=(v-1)*pi/436;
                s(u,v)=-alpha(u)+j*w(v);
                a=exp(s(u,v)*(0:m-1));
                a=a./norm(a);
                T(u,v,kk)=abs(1./(a*GG*a'));
            end
        end
    end
    for kk=1:1
        T(:,:,kk)=T(:,:,kk)./norm(T(:,:,kk),'fro');
%construct MSMs of test signal
    end

%correlation coefficients between FMSMs and MSMs
    corrcoef3(1,1)=sum(sum(T(:,:,1).*T_2(:,:,qstar)));
    corrcoef3(1,2)=sum(sum(T(:,:,1).*T_3(:,:,qstar)));
    corrcoef3(1,3)=sum(sum(T(:,:,1).*T_4(:,:,qstar)));
    corrcoef3(1,4)=sum(sum(T(:,:,1).*T_5(:,:,qstar)));
    corrcoef3(1,5)=sum(sum(T(:,:,1).*T_6(:,:,qstar)));
    corrcoef3(1,6)=sum(sum(T(:,:,1).*T_7(:,:,qstar)));
    corrcoef3(1,7)=sum(sum(T(:,:,1).*T_8(:,:,qstar)));
    corrcoef3(1,8)=sum(sum(T(:,:,1).*T_9(:,:,qstar)));
    corrcoef3(1,9)=sum(sum(T(:,:,1).*T_10(:,:,qstar)));
    corrcoef3(1,10)=sum(sum(T(:,:,1).*T_11(:,:,qstar)));
    corrcoef3(1,11)=sum(sum(T(:,:,1).*T_12(:,:,qstar)));
```

```
        corrcoef3(1,12)=sum(sum(T(:,:,1).*T_13(:,:,qstar)));
        corrcoef3(1,13)=sum(sum(T(:,:,1).*T_14(:,:,qstar)));
        corrcoef3(1,14)=sum(sum(T(:,:,1).*T_15(:,:,qstar)));
        corrcoef3(1,15)=sum(sum(T(:,:,1).*T_16(:,:,qstar)));
        corrcoef3(1,16)=sum(sum(T(:,:,1).*T_17(:,:,qstar)));
        corrcoef3(1,17)=sum(sum(T(:,:,1).*T_18(:,:,qstar)));
        corrcoef3(1,18)=sum(sum(T(:,:,1).*T_19(:,:,qstar)));

        [ymax,II]=max(corrcoef3(1,:));

       II
       bar(corrcoef3)
else
 % test target is a conducting sphere
load Music_con3
%loading the database of CLCON3 target sets
GG=0;R=0; corrcoef3=0;
   for uo=1:1
       xnorm(uo,:)=testdata(uo,:);
   end

       for kk=1:1
          y=real(xnorm(kk,17+(qstar-1)*32:144+(qstar-1)*32));
          y=y(:);
          N=length(y);                    % data length
          R=zeros(m,m);
          for i = m : N,
             R=R+y(i:-1:i-m+1)*y(i:-1:i-m+1)'/N;
          end
          [U,D,V]=svd(R);
```

```
        G=U(:,n+1:m);
        GG = G*G';
        for u=1:151
            for v=1:437
                alpha(u)=-(u-1)*0.0006;
                w(v)=(v-1)*pi/436;
                s(u,v)=-alpha(u)+j*w(v);
                a=exp(s(u,v)*(0:m-1));
                a=a./norm(a);
                T(u,v,kk)=abs(1./(a*GG*a'));
            end
        end
    end
    for kk=1:1
        T(:,:,kk)=T(:,:,kk)./norm(T(:,:,kk),'fro');
    end
    corrcoef3(1,1)=sum(sum(T(:,:,1).*T_2(:,:,qstar)));
    corrcoef3(1,2)=sum(sum(T(:,:,1).*T_3(:,:,qstar)));
    corrcoef3(1,3)=sum(sum(T(:,:,1).*T_4(:,:,qstar)));
    corrcoef3(1,4)=sum(sum(T(:,:,1).*T_5(:,:,qstar)));
    corrcoef3(1,5)=sum(sum(T(:,:,1).*T_6(:,:,qstar)));
    corrcoef3(1,6)=sum(sum(T(:,:,1).*T_7(:,:,qstar)));
    corrcoef3(1,7)=sum(sum(T(:,:,1).*T_8(:,:,qstar)));
    corrcoef3(1,8)=sum(sum(T(:,:,1).*T_9(:,:,qstar)));
    corrcoef3(1,9)=sum(sum(T(:,:,1).*T_10(:,:,qstar)));

    [ymax,II]=max(corrcoef3(1,:));
    II
    bar(corrcoef3)
end
```